

## Article

# Basal Anseriformes from the Early Paleogene of North America and Europe <sup>†</sup>

Peter Houde <sup>\*</sup>, Meig Dickson  and Dakota Camarena

Department of Biology, New Mexico State University, Box 30001 MSC 3AF, Las Cruces, NM 88003, USA

<sup>\*</sup> Correspondence: phoude@nmsu.edu<sup>†</sup> urn:lsid:zoobank.org:pub:8A63F651-650F-4745-B9E7-9E15B51E5500;  
urn:lsid:zoobank.org:act:033A40C6-2941-4DD4-810F-61971F646EB9;  
urn:lsid:zoobank.org:act:F775D442-1673-44EC-9C69-FE8D556E8B97;  
urn:lsid:zoobank.org:act:D5BAB3AB-203A-4A8C-B9D4-6D27E49423BF;  
urn:lsid:zoobank.org:act:1301901D-F55F-409A-9EE9-F4B9CA9D419D;  
urn:lsid:zoobank.org:act:98FA0546-612B-4C61-9CE0-D1009C9524E4.

**Abstract:** We describe nearly complete skeletons of basal Anseriformes from the Latest Paleocene to the early Eocene of North America and Europe. Collectively, these birds appear to be representative of anseriforms near the divergence of Anhimae and Anseres, but their exact positions relative to these clades remains uncertain. A new family, *Anachronornithidae* nov. fam., is erected on the basis of one of these, *Anachronornis anhimops* nov. gen., nov. gen. et sp., to which the others cannot be confidently assigned. The new fossils augment a growing collection of early Pan-Anseriformes, which in their diversity do not paint an unambiguous picture of phylogeny or character state evolution on the path to or within crown-Anseriformes. *Anachronornis* nov. gen. is similar in some aspects of both cranial and postcranial anatomy to other well-represented early Paleogene Anseriformes and members of Anseres, such as *Presbyornis* Wetmore, 1926. However, it exhibits a more landfowl-like bill, like that of Anhimae and unlike the spatulate bill of Anseres. Additional specimens of similar basal Anseriformes of uncertain affinities from the early Eocene of North America and Europe further complicate interpretation of character state polarity due to the mosaicism of primitive and derived characters they exhibit.



**Citation:** Houde, P.; Dickson, M.; Camarena, D. Basal Anseriformes from the Early Paleogene of North America and Europe. *Diversity* **2023**, *15*, 233. <https://doi.org/10.3390/d15020233>

Academic Editor: Eric Buffetaut

Received: 10 January 2023

Revised: 24 January 2023

Accepted: 26 January 2023

Published: 7 February 2023



**Copyright:** © 2023 by the authors. Licensee MDPI, Basel, Switzerland. This article is an open access article distributed under the terms and conditions of the Creative Commons Attribution (CC BY) license (<https://creativecommons.org/licenses/by/4.0/>).

**Keywords:** Anseriformes; Anseres; Anhimidae; Anachronornithidae; *Presbyornis*; *Anatalavis*; *Netapterornis*; *Anachronornis*; *Danielsavis*

## 1. Introduction

Extant Galloanseres comprises the (land)fowl and waterfowl, orders Galliformes and Anseriformes, respectively. Crown-Anseriformes, in turn, comprise the suborder Anhimae, which includes only the screamers of the family Anhimidae, and the duck-like birds of the suborder Anseres. Anseres typically possess elongate spatulate “duck-like” bills and at least some webbing of the toes. Anseres are further subdivided into Anseranatoidea, currently represented by the monotypic Australian Magpie Goose (*Anseranas semipalmata* Latham, 1798), and the Anatoidea, which include the typical ducks, geese, and swans (family Anatidae, and family Dendrocygnidae of some classifications).

Extant Anhimae are represented solely by three species of screamers, large birds of the South American wetlands. Although renowned for their superficially fowl-like bill, they are perhaps best characterized by their raucous voice, large feet, spurred wings, subcutaneous air sacs, and extremely pneumatized skeleton. Historically, it has been argued that screamers are primitive Anseriformes that unite the waterfowl with the fowl (Galliformes) [1]. The fossil record has served more to confuse than clarify the issue [2], but the sistership of fowl and waterfowl (Galloanseres) is overwhelmingly supported by morphological [3] and phylogenomic analyses [4–7].

Among the new fossils presented in this paper is the three-dimensionally preserved remains, including representative elements of nearly the entire skeleton, of an anseriform from the latest Paleocene of Wyoming. While it is far from being the oldest fossil described as anseriform, it may be the most basal member of stem- or crown-Anseriformes (i.e., the most recent common ancestor of *Anhima cornuta* Linnaeus, 1766 and *Anas platyrhynchos* Linnaeus, 1758 and all their descendants) yet discovered. The fossil is ostensibly that of a “screamer grade” of anseriform evolution because it possesses a fowl-like bill, among other screamer-like characters. Indeed, it has already been referenced as a screamer anecdotally [8–12]. However, the fossil lacks many or all of the synapomorphies of modern screamers, and in many respects the fossil is as much or even more duck-like as it is screamer-like. It is, in fact, so close to the divergence of screamers (suborder Anhimae) and duck-like waterfowl (suborder Anseres) as to preclude truly unqualified assignment to either subordinal clade.

The new fossils have the potential to clarify the polarities of disputed character states in fossil and extant Anseriformes. Many character state transformations in waterfowl have only been inferred by the analysis of extant taxa, with little or even confusing guidance from the few early anseriform fossils yet described. This applies particularly to bill and jaw morphology and the relatively non-pneumatized postcranial skeleton of Anseres, but also the alleged shorebird-like attributes of presbyornithids and “anatalavids”. Characters shared by previously described early Paleogene Anseriformes and new fossils described herein are likely to be typical rather than convergent or aberrant for basal Anseriformes at about the time of divergence of Anhimae and Anseres, because these extinct birds were dissimilar in feeding specialization, and hence in ecology.

It is firmly established that the divergence of Galloanseres from Neoaves occurred in the Cretaceous [4–6]. Fossils of what are believed to be stem representatives of the suborder Anseres near or just prior to the Cretaceous–Paleogene boundary [13–15] imply that the stem lineage of their sister, the Anhimae, was also present at this time [16]. The divergence of Anseres from Anhimae is the most basal among crown-Anseriformes; yet, paradoxically there is to date no documented paleontological record of even stem-Anhimae until the late Oligocene or Miocene. The fossils described herein expose what is in fact a fairly wide representation of Anhimae-like birds in celebrated late Paleocene and early Eocene deposits of North America and Europe. If the new fossils do represent stem-Anhimae, then ironically they were likely relics even in their time. If instead they were stem-Anseriformes, as we believe they may have been, then they were anachronisms all the more. Either way, they may be of limited usefulness for establishing minimum divergence times for timetree calibration. Regardless, they contribute to an ever-increasing known diversity of early Anseriformes that will ultimately establish the polarity of historically disputed characters.

## 2. The Fossil Record of Anseriformes

Both paleontological and molecular studies support the existence of Galloanseres in the Cretaceous [4,5,14,17–20]. This accords well with the observation that the divergence of Galloanseres from Neoaves is among the earliest among Neornithes. *Asteriornis maastrichtensis* is notable as the earliest convincingly diagnosable member of Pan-Galloanseres, although it is possibly sister to Galliformes alone [20].

The pre-Neogene record of Anseriformes is well-documented by only a handful of well-characterized genera. Their fossil record is reviewed by Olson [8], Mlíkovský [21], Ericson [22], Dyke [12], Hope [17], Dyke and Van Tuinen [23], Mayr [24–26], Kurochkin and Dyke [27], Livezey and Zusi [3], Mayr and De Pietri [28], Stidham and Ni [29], De Pietri et al. [30], Worthy and Lee [31], and Zelenkov [32,33], among others. The only described fossil anhimids are *Chaunoides antiquus* Alvarenga, 1999 from either the late Oligocene to early Miocene from the Tremembe Formation of Brazil [34] and an unnamed quadrate from the Early Eocene Tingamarra Local Fauna of Australia [35]. However, *Naranbulagornis khun* Zelenkov, 2019, an anseriform from the Paleocene of Mongolia [36], and *Perplexicervix microcephalon* Mayr, 2010, a fossil of uncertain ordinal affinity from the middle Eocene of Germany [37], have both been described as having potential affinities

with Anhimidae. Modern tribes of Anatidae first appear in the late Oligocene to early Miocene, and anatids are common in Europe, Siberia, New Zealand, and elsewhere by the early to middle Miocene [31,32,38]. The fossil record offers a variety of anseriform taxa of various ranks that are not so readily diagnosed as members of crown clades.

*Vegavis iaai* [39] from Antarctica is significant in being among few fossil Cretaceous birds known from sufficient remains to be widely accepted as representative of Neornithes. *Vegavis* may be the oldest known member of Anseriformes, notwithstanding the somewhat older but questionably diagnosed *Teviornis* (“*Presbyornis*”) *gobiensis* [13,40] and “tentative” anseriform *Kookne yeutensis* [41]. *Vegavis* was first referred to as a Cretaceous *Presbyornis* [39], but later determined to be a distinct form of Anseres [14]. “Because of *Vegavis*’ placement and its unknown skull morphology, advanced filter feeding cannot be assumed to be present in the anseriform lineage by the Maastrichtian. The Anseriformes that can be inferred as present by this point are lineages that today include large-bodied terrestrial browsers and occasional omnivores (that is, screamers, Anhimidae and magpie geese, *Anseranas*) as well as the lineage leading to true ducks and geese [14]”. The inference that *Vegavis* documents and can be used to date [23] the divergence of Anhimae, Anseranatoidea, and stem-Anatoidea is dependent on the veracity of its identification as a member of the latter. The most recent analyses recover *Vegavis* either as sister to crown-Anseriformes (in a clade to include or not include Gastornithidae and Dromornithidae) or to Galloanseres, or even to Neornithes [20,42–45], contra [46]. Thus, it would seem that the only thing so far generally agreed upon is that *Vegavis* was a member of the Neognathae, notwithstanding some dissent [20] (Extended Data figure 9) [45].

Vegaviidae is a family of purported Anseriformes that was erected to include *Vegavis*, the Paleocene *Australornis lovei* Mayr and Scofield 2014, and two more Cretaceous birds, *Polarornis gregorii* Chatterjee 2002 and *Neogaeornis wetzeli* Lambrecht 1929 [42], but their monophyly has been more recently challenged [44]. The latter two had previously been allied with the Gaviidae, and the skull of *Polarornis* has a particularly colorful reputation as having been largely reconstructed from that of a loon [47]. The profound convergence among foot-propelled divers, which is not limited to characters of the pelvic limb, has resulted in a long history of cladistic mishaps involving Hesperornithiformes, Gaviiformes, and Podicipediformes [3,48,49].

*Conflicto antarcticus* Tambussi, Degrange, de Mendoza, Sferco, and Santillana, 2019 is an early Paleocene stem-anseriform from Antarctica [15] that possessed a narrow superficially merganser-like bill and long limbs. In the original description of the species, parsimony analysis recovered *Conflicto* along with “*Anatalavis*” *oxfordi* Olson, 1999 (below) as the earliest diverging clade of Anseriformes, followed by Presbyornithidae and then crown-Anseriformes, including Anhimidae. A similar result was subsequently replicated using constrained parsimony and tip-dating Bayesian analyses of a comparable but different dataset [20]. If correct, then this would imply that the superficially fowl-like bill morphology of extant Anhimidae is homoplasious with the condition found in the sister group of Anseriformes, i.e., Galliformes. However, unconstrained parsimony and node-based Bayesian analyses [20] recovered Anhimidae as sister to both crown-Anseres and another clade consisting of *Conflicto*, “*Anatalavis*”, and Presbyornithidae. Thus, the position of *Conflicto* and other fossils with duck-like spatulate bills relative to Anhimae and Anseres remains unresolved, and consequently so is the character polarity of bill morphology among Anseriformes.

The widespread and long-lived family Presbyornithidae has been said to include *Presbyornis pervetus* Wetmore, 1926, *P. isoni* Olson, 1994, *P. mongoliensis* Kurochkin and Dyke, 2010, *P. recurvirostra* Hardy, 1959, *Bumbalavis anatoides* Zelenkov, 2021, *Teviornis gobiensis* Kurochkin, Dyke, and Karhu, 2002 (but see [40]), *Telmabates antiquus* Howard, 1955, *Wilaru tedfordi* Boles, Finch, Hofheins, Vickers-Rich, Walters, and Rich, 2013, and *W. prideauxi* De Pietri, Scofield, Zelenkov, Boles, and Worthy, 2016 [13,26,30,33]. It has been reported from deposits nearly worldwide ranging in age from latest Cretaceous or early Paleocene until the early Miocene. The type species of the family, *P. pervetus*, was originally described

as close to the Recurvirostridae (Charadriiformes) on the basis of a tarsometatarsus found in the Early Eocene Green River Formation in Wyoming [50]. Great accumulations of its bones eventually found there, however, have documented that *Presbyornis* possessed an unusually deep and recurved (upturned) but indisputably duck-like spatulate bill [2,51]. These authors were so impressed by the long legs and alleged shorebird-like morphology of *Presbyornis* that they retained it within their “Charadriomorphae” [52]. They argued for a primitive position of *Presbyornis* among Anseriformes and suggested that its spatulate bill represented a primitive state of Anseriformes from which the fowl-like bill of screamers was later derived. These authors explicitly rejected the monophyly of Galloanseres, a clade that since has been conclusively shown to be valid [4,6,7] (contra [18]). Subsequent work [1,10] recovered *Presbyornis* as sister to Anatoidea and therefore relatively derived among Anseriformes. If correct, then *Presbyornis* does not provide a wealth of information on basal character state polarities for the order. However, like *Vegavis* and *Conflicto*, *Presbyornis* has since been recovered in alternate positions relative to these suborders and more recently discovered fossil Anseriformes and Galloanseres [15,20,42,43].

Both scanty and abundant remains from other disparate locations and ages have been referred to the Presbyornithidae. *Presbyornis mongoliensis* was described on the basis of a substantial number of mostly partial bones collected in the late Paleocene–early Eocene of Mongolia [27]. The type specimen of *Presbyornis mongoliensis* was later rediagnosed as a member of Juncitarsidae, but other specimens referred to it appear to be correctly identified as presbyornithids [33]. An unassociated partial carpometacarpus and phalanx from the Paleocene Aquia Formation of Maryland–Virginia were described as *Presbyornis isoni* [53], which is likely synonymous with *Headonornis hantoniensis* of the Early Eocene London Clay [12]. However, Olson noted that “the feeding adaptations of *P. isoni* may have been different from those of *P. pervetus*, and that were the entire skeleton available it might be assigned to a different genus”. A variety of other isolated remains have been proffered as presbyornithids of Cretaceous age [17]. The most credible of these is a carpometacarpus and distal humerus, *Tevionis gobiensis*, from Mongolia [13], which currently represents the oldest putative record of the family Presbyornithidae. However, even its assignment to Presbyornithidae has been disputed on the basis of character state polarity [40]. On the other end of the time spectrum are abundant postcrania of the Australian species *Wilaru tedfordi* from the late Oligocene and *W. prideauxi* from the early Miocene [30]. It is notable that, like *Presbyornis*, *Wilaru* had previously been misdiagnosed as a member of Charadriiformes, but in the family Burhinidae [54].

Olson described a half-skeleton that includes a duck-like skull from the Early Eocene London Clay as a new species of *Anatalavis* Olson and Parris, 1987, which he referred to the Anseranatidae [55]. The genus was first described for *Anatalavis rex*, one of three species of *Telmatornis* with similarities to rails but of uncertain affinity, on the basis of isolated fragmentary wing bones from the Early Paleocene, then thought to be Cretaceous, of New Jersey [56]. It was later diagnosed as a new genus of Charadriiformes, “form family” Graculavidae [52]. Olson [55] subsequently inferred that these fragmentary fossils represented duck-like Anseriformes in the Cretaceous based on the London Clay fossil. One might speculate that Olson was motivated to take this action to lend support to his conviction that “Anseriformes . . . evolved from the Charadriiformes” [2]. However, in light of the profoundly longer humeral ventral epicondyle of *Anatalavis rex* than that of its putative Eocene counterpart (Figure S1) [55] (figure 8), Mlíkovský [21] was justified in renaming “*Anatalavis*” *oxfordi* as *Nettapterornis oxfordi* [57]. In a review of his book, Mourer-Chauviré [57] dismissed Mlíkovský’s revision of “*Anatalavis*” as having been preemptively addressed by Olson as “slight differences . . . mainly due to slightly different rotation of the specimens” in the photographed image [55] (figure 8 and caption). However, we (P.H.) confirmed by direct side-by-side comparison of the holotype of “*Anatalavis*” *oxfordi* and a faithful cast of the same specimen of *Anatalavis rex* figured by Olson (i.e., paratype YPM 948) that the differences are both real and profound and cannot be accounted for by any angle of view (Figure S1). Most notably, the ventral condyle of “*Anatalavis*” *oxfordi* is

more pronounced distally than the dorsal condyle, the ventral epicondyle of “*Anatalavis*” *oxfordi* is much shorter distally, but the flexor process associated with it is more pronounced caudally in *Anatalavis rex* (Figure S1). It is impossible to determine from the scant remains of *Anatalavis rex* at what higher taxonomic rank the two may have shared common ancestry. The name *Nettapterornis* is therefore appropriately used henceforth herein to unambiguously distinguish the true Eocene anseriform from the undiagnosable early Paleocene fragments described by Olson and Parris [52] as Charadriiformes. Thus, subsequent reference to the age and distribution of Anseranatidae may be overestimated [58]. Nomenclature notwithstanding, Dyke [12] further disputed Olson’s [55] interpretation of character distributions and moved *Nettapterornis* from the Anseranatoidea to the Anatoidea. However, as noted by Mayr [24], Dyke’s analysis did not include all the characters that Olson used to diagnose *Nettapterornis* as an anseranatid. Like *Presbyornis*, *Conflicto*, and *Vegavis*, *Nettapterornis* has since been recovered in a variety of alternate positions relative to Anhimae and Anseres and more recently discovered fossil Anseriformes and Galloanseres [15,20,42,43].

The fossil record of confidently diagnosed crown-group Anseres begins in the late Eocene or Oligocene. *Eonessa* Wetmore, 1938, from the Late Eocene of Wyoming, was described as an anatid on the basis of a badly crushed, incomplete wing skeleton. It is lacking in sufficient information to justify any placement [2]. The late Eocene *Coosteauvia kustovia*, Zelenkov was described as the oldest diving anseriform, but its familial relationships remain undefined [59]. Worthy and Scanlon [58] described *Eoanseranas* Worthy and Scanlon, 2009 as a late Oligocene/early Miocene species of Anseranatidae from the Riversleigh Formation of Australia. *Anserpica* Mourer-Chauviré, Berthet, and Huguene, 2004 was reported to be an anseranatid from the upper Oligocene of France [60]. Mayr noted similarity to the putative gruoid *Geranopsis*, without indicating whether either the anseranatid or gruoid affinities were more likely [24,26]. Other early candidates more confidently referred to the Anatidae include members of the Romainvilliinae and Oxyurinae. Romainvilliinae includes the genus *Romainvillia* Lebedinsky, 1927 from the upper Eo-Oligocene of France and Kazakhstan. It has also been reported to include *Cygnopterus* Lambrecht, 1931 and indeterminate species (*Paracygnopterus* Harrison and Walker, 1979) from the early Oligocene of Belgium [8,24,61], and *Paracygnopterus scotti* Harrison and Walker, 1979 from the early Oligocene of England [26]. *Saintandrea chenoides* Mayr and De Pietri, 2013 from the late Oligocene of France was the youngest known surviving member of the Romainvilliinae [28]. Species of *Mionetta* Livezey and Martin, 1988 were originally included in the genus *Anas* [62,63], later referred to a new subfamily Dendrocheninae by Livezey and Martin, 1988, and ultimately rediagnosed as early members of the Oxyurinae [31]. Zelenkov [32] provides a more comprehensive review of the fossil record of these and putative members of other subfamilies of crown-Anatidae from the Oligocene and Miocene.

There are three additional clades of fossil birds that are so modified for gigantism, flightlessness, locomotory specialization, and/or feeding specialization that their potential affinities to Anseriformes or Galloanseres had not been fully appreciated until relatively recently. Consequently, these birds also are not particularly useful in comparison in the present context of crown-Anseriformes. These are the Gastornithiformes, Dromornithidae, and Pelagornithidae. Most recently, it has been suggested that cranial characters used to unite these with Galloanseres may be neornithine symplesiomorphies and that any or all of these might represent “early diverging lineages of crown or near-crown stem birds” [64,65].

The rather widespread and speciose Gastornithiformes Stejneger, 1885 were returned to the “Anserimorphae”, i.e., sister to the Anseriformes, after being shuffled back and forth between the Palaeognathae, Psittaciformes, Ciconiiformes, Anseriformes, and Gruiformes by numerous authors [26,45,66]. The massive heads of these large nearly wingless flightless birds led early authors to believe that they were apex predators, but the evidence is equivocal [66,67]. The families Gastornithidae Fürbringer, 1888 and Diatrymidae Matthew and Granger, 1917, have been synonymized, and the genera *Diatryma* Cope, 1876, and *Zhongyuanus* Hou, 1980, are now recognized as synonyms of *Gastornis* Hébert, 1855 [21,68,69]. Collectively, they are known from the middle-Late Paleocene to the middle Eocene from

deposits across the Northern Hemisphere [70]. Andors noted several similarities between *Gastornis* and the Anhimidae. “The parallelisms are problematical . . . but they tend to reinforce the impression that *Diatryma* and anhimids are primitive within the diatrymid-anseriform assemblage [66]”.

Dromornithidae Fürbringer, 1888 was a family of graviportal giants with vestigial-wings endemic to Australia and well-known from complete skeletal remains. Their fossil record is firmly established by the late Oligocene but may extend to the Early Eocene. Although once assumed to be paleognathous “ratites”, the most recent analysis recovers Dromornithidae as sister to Gastornithidae within Gastornithiformes [45]. Their head and feeding apparatus are similar to those of gastornithids, and stable isotope analysis of their eggshell suggests that they were herbivorous [71], lending credibility to the notion that they all were.

The “bony-toothed” seabirds of the family Pelagornithidae may be sister to all other Anseriformes [49], but if so then they are highly diverged. Their skull was superficially pelican-like with rhamphothecal grooves and caudally exaggerated tympanic cavities, but with a deeper bill characterized by tooth-like projections of both the upper and lower tomia. With a wing skeleton like a much-exaggerated version of albatrosses (Diomedidae) and “pelecaniforms” [72,73], they epitomized specialization for pelagic dynamic soaring. They have a nearly cosmopolitan fossil record that extends from the Late Paleocene to the Pliocene [24]. It has been suggested based on the presence of an unfused frontoparietal suture [64,74] and the pterygoid [65] that pelagornithids might have branched early in the evolution of Neornithes and therefore may have no close affinities with Anseriformes.

### 3. Methods

USNM 496700-496702 were found preserved in a small calcareous nodule. Small parts of the fossil and nodule that had broken off the main rock were found and reattached with polyester resin before preparation. The fossil was entirely freed from matrix by dissolving the calcareous rock in a solution of ~7% acetic acid over a period of several years. Polyvinyl acetate was used to protect the fossil from acid, as well as a hardener and preservative. Some fractures were repaired with cyanoacrylate, but most if not all of it was eventually removed and replaced with polyvinyl acetate.

Osteological materials examined (AMNH, American Museum of Natural History; BM, British Museum of Natural History, Tring, Hertfordshire, UK; NMSU, Vertebrate Museum, New Mexico State University; OUV, Ohio University Vertebrate Collections; USNM, National Museum of Natural History, Smithsonian Institution, Washington, DC, USA; YPM ORN, Yale Peabody Museum, New Haven, CT, USA): *Anas platyrhynchos* (USNM 225334 imm.; OUV 10613 imm.), *Anhima cornuta* (USNM 226166, 345208, 345217; YPM ORN 103843, 109922), *Anser caerulescens* (AMNH 11127), *Anseranas semipalmata* (USNM 347638), *Bucephala clangula* (USNM 499411), *Burhinus capensis* (USNM 558484), *Cariama cristata* (NMSU, no number), *Centrocercus urophasianus* (USNM 561361 imm.), *Chauna chavaria* (USNM 18996, 19880, 224836, 226110, 290504, 345216, 346634, 347738), *Chauna torquata* (BM S/1954.5.3 imm., USNM 19942, 19949, 223965, 223968, 225987, 290505, 345218, 345619, 345766, 347352, 430021 imm., 430022, 614547, 614548), *Chloephaga picta* (BM S/1952-1.126-7 imm.), *Crax fasciolata* (USNM 320124 imm., 345793), *Cygnus olor* (NMSU no number), *Dendrocygna arcuata* (USNM 612657 imm.), *Dendrocygna viduata* (USNM 345769, 488133), *Dromaius novaehollandiae* (USNM 614475 imm.), *Megapodius freycinet* (USNM 557005 imm., 560789 imm.), *Melanitta perspicillata* (NMSU no number), *Nettapterornis* (*Anatalavis*) *oxfordi* (BMNH A5922), *Presbyornis* sp. (NMSU, USNM, no numbers), *Pterocnemia pennata* (USNM 227486 imm.), *Rhea americana* (USNM 614472 imm.), *Tachyeres pteneres* (USNM 18553, imm.), and *Tadorna tadorna* (USNM 502548 imm.).

Anatomical terminology and homology: Terminology follows Baumel and Witmer [75], Zusi and Livezey [76], Livezey and Zusi [77], and Elzanowski and Stidham [19], except as noted, but is Anglicized. Reference was made to others [31,33,58,76,78–84] to infer

homology of select characters. Muscle insertions were inferred by dissection of *Chauna torquata* NMSU 4203 and additional references [85–88].

Measurements are millimeters (mm). “>” indicates a precise measurement of a bone that is incomplete. The whole bone would necessarily be larger. “~” indicates an accurate measurement that might be slightly (less than 1 mm) greater or smaller than accurate because a feature is difficult to measure reproducibly or because of mild diagenetic distortion or abrasion. Measurements of paired elements are listed left and right, respectively.

Parsimony analysis was performed using maximum parsimony (MP; PAUP 4a169 [89]) on seven datasets. Dataset 1 consists of eight taxa and 110 parsimony informative (PI) characters defined by parenthetic numbers in the description of *Anachronornis anhimops* nov. gen. et sp. (Supplemental Materials, Supplementary Appendices A1 and A2). It is the only dataset among the six that includes *Danielsavis* nov. gen. Potentially non-independent characters, e.g., pneumatization of different bones, were not coded repeatedly. *Anachronornis* nov. gen. was added to six additional published datasets. Datasets 2 and 3 are based on Ericson [10], including 44 taxa and 71 PI characters and 13 taxa and 51 PI characters, respectively (Supplementary Appendices B1 and C1). The former was originally intended to address the positions of *Presbyornis* and Anseriformes among Aves, whereas the latter was aimed at the position of *Presbyornis* within Anseriformes [10]. Dataset 4 is a modified version of Livezey’s 1986 dataset reduced to six basal taxa and 34 PI characters in which higher taxa were each pooled based on published apomorphies [90] (figure 2) (Supplementary Appendix D1). Dataset 5 is based on Livezey [1,91], consisting of 11 taxa and 123 characters of which 94 are PI and 27 are non-osteological (Supplementary Appendix E1). Datasets 5 and 6 differ from one another only by the addition of *Nettapterornis* and *Vegavis* and the exclusion of non-osteological characters in the latter [12,14] (79 PI characters, Supplementary Appendices F1 and F2). Dataset 7 is that of Field et al. 2020, as modified [20,43,92] (Supplementary Appendix G1). All searches except on Datasets 2 and 7 were performed with exhaustive unweighted parsimony. Datasets 2 and 7 were analyzed with 10 random additions using the TBR heuristic search with 1000 replicates (Supplementary Appendices B1 and G2). Branch support was calculated as bootstrap support (BS) based on one million branch and bound replicates, except Datasets 2 and 7, which used 1000 and 100 TBR heuristic search replicates, respectively. Fully unconstrained Bayesian analysis was also performed on dataset 1 (Supplementary Appendix A2) and on dataset 7 in which *Anachronornis* nov. gen was added to Field et al.’s [20] 39 taxa, 297 (290 PI) character dataset (Supplementary Appendix G3). Both phylogenetically unconstrained and constrained [20] total-evidence (i.e., character data with tip-dating) Bayesian analyses were also performed on dataset 7 (Supplementary Appendices G4 and G5, respectively). We modified the Field et al. dataset by adding new character data for *Vegavis* [92], changing fixed dates to temporal ranges [14,15,30,64,72,73,93–98], relaxing the clock rate prior, deleting one redundant species of Megapodiidae, and correcting the sample probability of neotaxa. Bayesian analyses were performed with MrBayes 3.2 [99] with the following settings: lset rates = gamma, ngammat = 4, coding = variable, clockratepr = exp(1), mcmc temp = 0.1, nchain = 4, samplefreq = 4000, printfr = 1000, nruns = 2, mcmcngen = 60,000,000. Burn-in stationarity and convergence were verified using Tracer 1.7.2 [100]. Branch support is reported as posterior probability (PP).

Parsimony two-tailed and likelihood one-tailed Kishino–Hasegawa (KH) tests were run in PAUP 4.0a169 [89], in which novel fossil taxa were constrained to alternate branches of fixed backbone trees. Interordinal relationships of neotaxa in backbone trees were based on phylogenomic analyses [7,101], with refinement of interfamilial relationships of Charadriiformes [102], or as previously reported for dataset 7 [20]. The positions of previously described paleotaxa in backbone trees were minimally the same as in the papers in which the datasets were originally published, and in some cases also in additional positions. Likelihood scores were calculated using the Akaike Information Criterion (AIC) and Bayesian Information Criterion (BIC) and KH tests were run as normal approximations and RELL BS with 1,000,000 BS replicates. Loosely stated, significance (i.e.,  $p < 0.05$ )

indicates the difference from the “best” tree evaluated, which in most cases was not the same as any predetermined parsimony or Bayesian optimized tree. Inappropriate use of the KH test was selectively avoided in dataset 1 by omitting the parsimony-optimized tree (which was implausible) in datasets 4 and 7 (MP tree only) by doubling parsimony-calculated  $p$  values to convert the two-tailed test to a one-tailed test, and in datasets 2, 3, 5, and 6 by implementing backbone trees based on the current phylogenomic understanding of extant avian relationships that differ from the morphology-based parsimony or Bayesian-optimized trees [103].

In describing the results of our phylogenetic analyses, we define our use of the terms Pan-Anseriformes and Pan-Anseres to include any or all of Presbyornithidae, *Wilaru*, *Nettapterornis*, and *Conflicto* when they are included in the dataset, but neither Pan-Anseriformes nor Pan-Anseres includes *Vegavis*, Vegaviidae, or Pelagornithidae as we define them for the purposes of this paper. We further use the term stem-Anseres to specifically refer to Presbyornithidae, *Nettapterornis*, and *Conflicto* only, whether they are referred to as monophyletic or non-monophyletic sisters to crown-Anseres.

#### 4. Systematic Paleontology

##### 4.1. Class Aves Linnaeus, 1758

##### Order Anseriformes Wagler, 1831

**Diagnosis:** The following combination of characters justify the unambiguous diagnosis of *Anachronornis anhimops* nov. gen. et sp. USNM 496700 as a member of Pan-Anseriformes. The characters described here include only those that are well-preserved in the fossil and are not intended to represent an amended diagnosis of the order.

The zygomatic process, as such, is lacking as it is completely fused with the postorbital process to form a “sphenotemporal process” as described alternatively by Dzerzhinsky [104] (Figure S2). Regardless of interpretation, there is no fossa of origin of the adductor mandibulae externus (AME), pars coronoidea [78], present on the lateral surface of the neurocranium. A fossa faces ventrally instead, flanked laterally by a crest that forms the lateral margin of the neurocranium or “crista muscoli adductoris mandibulae externus pars articularis” of Zusi and Livezey [77] (below and Discussion 6.7). This crest may be formed by any combination of the ventrolateral facies of the squamosal bone, crest of AME articularis, and/or zygomatic crest [77]. The basipterygoid process is elliptical, elevated, and “pedicellate” [91]. The quadrate exhibits both a pronounced subcapitular tubercle of the otic process and pronounced tubercle of the orbital crest. The quadratojugal cotyle of the quadrate is positioned on a distinct “pars quadratojugalis” [19] that is offset caudodorsal to the lateral mandibular condyle of the quadrate (“inflated” [2]). The caudal condyle of the quadrate is absent. A full account of all putative apomorphies summarized and by dataset appear in Supplemental Materials and Supplementary Appendices A3, B2, C2, D2, F3, G6 and G7.

Family Anachronornithidae nov. fam. Houde, Dickson, and Camarena

urn:lsid:zoobank.org:act:033A40C6-2941-4DD4-810F-61971F646EB9

Included genus *Anachronornis* nov. gen.

**Diagnosis:** Anachronornithidae nov. fam. is distinguished from all known Anhimidae and Anseres by a lack of unambiguous synapomorphies diagnosing those respective clades and in many respects is intermediate between the two.

Anachronornithidae nov. fam. exhibits a combination of characters that are present in extant Anhimidae and Anseres (including stem-Anseres) but not shared by both, and by a lack of unambiguous synapomorphies diagnosing those respective clades. These include a fowl-like non-spatulate bill, vacuous tympanic cavity, short postorbital or “sphenotemporal” process, broad palatines lacking an acute caudolateral angle, mandible with narrow and straight dentaries, dorsally pronounced coronoid margin relative to the tomial margin and caudal fossa for the insertion of the depressor mandibulae muscle, presence of the uncinat process of costae, pronounced lateral concavities of the caudal cervical, thoracic, and first presacral vertebrae, a postcranial skeleton that is otherwise inferred to be non-pneumatic



or nearly so based on the slender appendages and absence of conspicuous pneumatic foramina, scapula with acute acromion and large spherical coracoid tubercle, sternum with a shallow carina, costal margin that is less than half the length of the sternal body and deep notches formed between the median and lateral trabeculae, humerus with distally short bicipital crest, broad pelvis with longer preacetabular ilium than postacetabular ilium or ischium, femur that is long and slender and tarsometatarsus with large fossa for metatarsal I, proximally elevated and plantarly deflected trochlea IV, and large neurovascular canal. Autapomorphies that may further diagnose the family include characters 4, 6, 83, 97, 116, and 117 of dataset 1, as well as characters 21, 24, 30, 74, and 77 if *Danielsavis* nov. gen. is also included in it (Description, Supplemental Material).

**Differential Diagnosis:** Anachronornithidae nov. fam. differs from both Anhimidae and Anseres in the following. The quadratojugal process is distinctly caudodorsal to the lateral mandibular condyle but it does not form a submeatic eminence or process. The thoracic vertebrae have an enormous lateral concavity or pleurocoels for pulmonary diverticula [105,106] that replaces the entire vertebral body except for a thin midsagittal septum separating the right and left sides. The circumference of the concavity is sharply defined by the external surface of the vertebral body. Although the concavity is large throughout the caudal cervical and thoracic vertebral column, its aperture diminishes in size in progressively more caudal vertebrae, so by the first presacral vertebra it appears as a large pneumatic foramen like those of extant Anhimidae. At least some thoracic vertebrae bear two additional openings and the anteroventral and ventral surfaces of the transverse processes that closely resemble the lateral openings on the vertebral bodies as well as the verified pneumatic foramina of extant anhimids (see also *Paraortygoides* [81] (figure 3B)), thus calling into question whether they represent openings for pulmonary diverticula, air sacs, or pleurocoels [106]. The costal margin is restricted to the cranial half of the sternal body. The coracoidal sulci are crossed, as known otherwise only in *Presbyornis*.

Anachronornithidae nov. fam. is distinguished from Anseres by the combination of small unfused lacrimals [107], the absence of occipital fontanelles, fowl-like non-spatulate bill, prenasal portion of premaxillae shorter than the osseous nasal aperture, large nasal cavity that is broadly open to the oral cavity, laterosphenoid articulation that extends the full length of the postorbital process, and the absence of the conical recess for the insertion of the depressor mandibulae on the articular. The fossa for the origin of AME articularis is small and located immediately rostral and dorsal to the squamous cotyle of the quadrate. The origin of the depressor mandibulae muscle on the lateral surface of the neurocranium rostral to the nuchal crest is extremely shallow and indistinct. Lateral bodies of caudal cervical, thoracic, and cranial synsacral vertebrae and cranioventral and ventrolateral surfaces of some transverse processes of thoracic vertebrae are perforated by either lateral openings, pleurocoels, pneumatic foramina, or openings for pulmonary diverticula [105,106,108].

Anachronornithidae nov. fam. is further distinguished from all known adult Anseres by a skull with unfused lacrimals (except *Presbyornis*). There is a small notch in the lateral margin of the neurocranium (variously the “zygomatic crest” or “crest of the AME articularis” [76]) caudal to the postorbital process that corresponds in appearance and position to the laterosphenoid-squamosal suture in juvenile anhimids [76] (figure 5A) and resulting in what they describe as a “spurious resemblance to the zygomatic process in direct association with the postorbital process.” However, in ventral view the zygomatic process appears to be present medial to the crest and applied to the postorbital process, as in (at least some) juvenile anatids, and *Nettapterornis* (Figure S2) but not *Presbyornis*. The external spine of the sternal rostrum is present but small. The coracoid has a long flared lateral angle, but has no ridges on the insertion of the sternocoracoideus muscle and no external crest of the sternal articulation.

Anachronornithidae nov. fam. is distinguished from Anhimidae by the following combination of characters. The lateral margin of the neurocranium is nearly horizontally oriented and the fossa for the origin of the AME articularis is particularly small. The

palatine bones are broad, attenuated caudally, and bear a large pit on their dorsolateral surface, rostral to the choana. The capitula of the quadrate are relatively widely spaced, and the body of the quadrate bears a basiorbital pneumatic foramen [19] on its medial surface. The femur is long and slender. The cranial cnemial crest of the tibiotarsus is more pronounced cranially than proximally.

Anachronornithidae nov. fam. differs from Anhimidae by the seemingly complete lack of pneumatization (i.e., lack of pneumatic foramina) of the appendicular skeleton and the following characters. The supraorbital region is narrow as in most Anseres, although it also may be somewhat narrower in juvenile anhimids than in adults, particularly *Anhima* (Figure S3). The lacrimal bone is equilateral triangular with an extended supraorbital process in the lateral aspect, not unlike that of some Anseres, e.g., *Aythya* and *Melanitta*, but without an elongated orbital or ventrocaudal process [107]. The postorbital process is short as in anhimids and *Presbyornis* but directed more rostrally, as in Anseres. The pterygopalatine articulation of the palatine is U-shaped and complex. The mandible exhibits several characters that are somewhat more similar to those of Anseres than seen in extant anhimids. The dentary is thin dorsoventrally and straight rather than decurved. The mandibular angle and coronoid process are elevated dorsally well above the tomial margin of the dentary. It bears a large laterally positioned tubercle of the AME, pars articularis, caput externa muscle. The caudal extremity of the mandible bears a caudal fossa (impression of the depressor mandibulae muscle, but not the deep conical recess of Anatidae), which is circumscribed both dorsally and ventrally by two well-defined crests that extend uninterrupted from the medial process of the mandible to both the dorsal and ventral margins of the dorsoventrally tall but thin retroarticular process. The medial process is offset and directed caudally relative to the mandibular cotyles. Costae bear uncinat processes. The sternal carina is shallow, about one half the width of the sternal body, and the costal margin is less than half the length of the entire lateral margin. The coracoid lacks a pneumatic foramen on the dorsal surface of its sternal end. There are no spurs on the carpometacarpus.

Anachronornithidae nov. fam. differs from Vegaviidae, as described based on a composite of characters represented in *Vegavis*, *Neogaornis*, *Polarornis*, and *Australornis* [42], but see [44]. Most notably, these include a relatively short deltopectoral crest of the humerus, curved scapula, longer slender femur with a deep notch formed proximally between the head and proximally pronounced trochanteric crest, and cranial cnemial crest of the tibiotarsus that is longer cranially than proximally. It further differs from *Vegavis* because the ilioischadic foramen is enclosed and the synsacrum is bilaterally swelled [92], ostensibly to accommodate the glycogen body.

**Anachronornis nov. gen. Houde, Dickson, and Camarena**

urn:lsid:zoobank.org:act:F775D442-1673-44EC-9C69-FE8D556E8B97

**Etymology:** From the Greek ἀναχρονισμός, out of time, and ὄρνις, bird, alluding to the unexpectedly late occurrence of what may be, or may be close to, the most recent common ancestor of the two crown-anseriform lineages, Anhimae and Anseres.

**Type and only known species:** *Anachronornis anhimops* nov. gen. et sp.

**Occurrence:** Late Paleocene of North America.

**Diagnosis:** As for the family, by monotypy. (Full account of all putative apomorphies by dataset in Supplemental Materials and Supplementary Appendices A3, B2, C2, D2, F3, G6 and G7).

**Anachronornis anhimops nov. gen. et sp. Houde, Dickson, and Camarena**

urn:lsid:zoobank.org:act:D5BAB3AB-203A-4A8C-B9D4-6D27E49423BF

Figures 1, 2, 3, S1, S2 and S4–S7



**Figure 1.** Holotype of *Anachronornis anhimops* nov. gen. et sp. (USNM 496700): skull, ventral (A), dorsal (B), right lateral (C), right lateral in matrix (D), caudal (E); mandible with heavy gauge wire glued to medial side of right dentary, right lateral (F), dorsal (G), oblique caudomedial aspect of right side (K), right caudal (O); quadrates, left lateral (H), right lateral (I), left medial (L), right medial (M); basihyal (Q), costal fragment with uncinat process (R), left palatine (S), right thoracic vertebrae (T). Quadrate (USNM 496701; Anseriformes fam. incertae sedis): right lateral (J), right medial (N). Holotype of *Danielsavis nazensis* nov. gen. et sp. (NMS.Z.2021.40.1): right caudal mandible (P). All but (D,P) are coated with ammonium hydroxide. Scale bar 1 cm.



**Figure 2.** Holotype of *Anachronornis anhimops* nov. gen. et sp. (USNM 496700): sternum left ventrolateral (A), inset of caudal margin prior to damage to lateral trabecula (F); coracoids, left dorsal (B), left ventral (C), right dorsal (D), right ventral (E), right lateral clavicle (G); scapulae, left lateral (H), right lateral (I); left carpometacarpus, dorsal (J), ventral (K); left humerus, caudal (L), cranial (M); left radius, cranial (N), caudal (O); left ulna, ventral (P), dorsal (Q). All coated with ammonium hydroxide. Scale bar 1 cm.

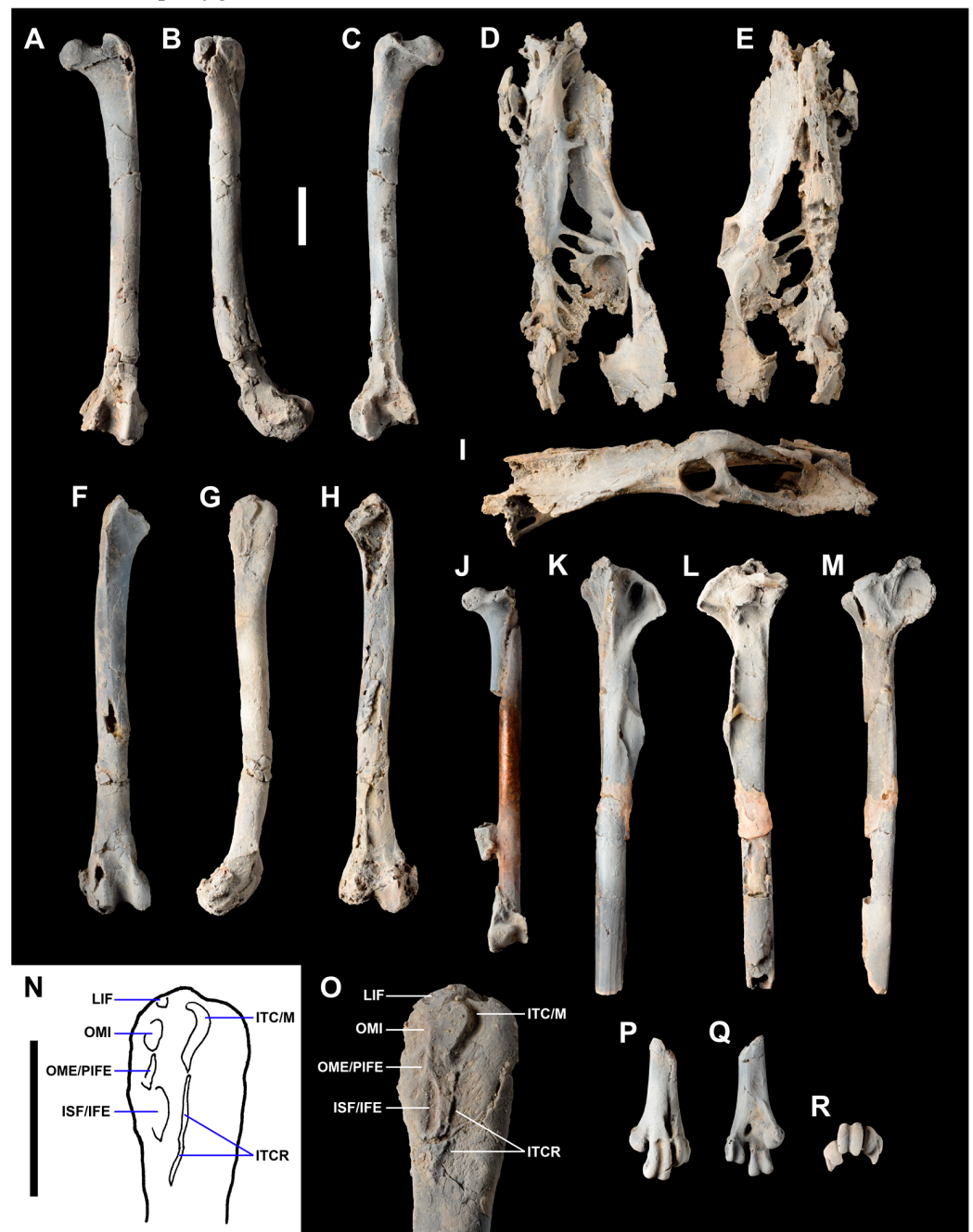


**Figure 3.** Holotype of *Anachronornis anhimops* nov. gen. et sp. (USNM 496700): femora, left cranial (A), lateral (B), caudal (C), right cranial (F), lateral (G), enlarged labeled proximal lateral (N,O), caudal (H); pelvis, ventral (D), dorsal (E), left lateral (I); proximal left tibiotarsus, cranial (K), caudal (L), medial (M); distal left tarsometatarsus, cranial (P), caudal (Q), distal (R). Femur (USNM 496702; Anseriformes fam. incertae sedis) caudal fragmentary right femur with metal bar glued in place prior to removal from matrix to preserve length and midsection of shaft glued randomly to bar (J). Abbreviations of insertions: ISF/IFE, ischiofemoralis/iliofemoralis externus; ITC/M, iliotrochanteris caudalis/medialis; ITCR, iliotrochanteris cranialis; LIF, iliofemoral ligament; OME/PIFE, obturator externus/puboischiofemoralis; OMI, obturator internus. All except (N) coated with ammonium hydroxide. Scale bars 1 cm.

Tables S1 and S2

**Etymology:** From the generic name *Anhima*, a screamer, and *ops* (Greek, face, countenance, appearance of the face). The name is intended to refer to the screamer-like bill and

appearance of the head, particularly like that of *Anhima* in which the supraorbital region may be somewhat narrower than in *Chauna*.

**Holotype:** USNM 496700, skull (pterygoids missing), mandible, partial hyoid apparatus, 18 pre-synsacral vertebrae, 4 caudal vertebrae (pygostyle missing), a few partial ribs, sternum (right half missing), coracoids, humeri, radii, ulnae, left carpometacarpus, pelvis (pubes and the majority of the right coxa missing), femora, proximal end of the left tibiotarsus, proximal end of the left fibula, distal end of the left tarsometatarsus, and a few pedal phalanges.

**Type Locality:** SE 1/4 of NE 1/4 of Sec. 19, T56N R101W, Clark Quadrangle, Park County, Wyoming.

**Horizon:** Latest Paleocene, latest Thanetian, 56.22–55.80 Ma (Cf3, *Copecion* Interval Zone, latest Clarkforkian North American Land Mammal Age, ending at the Carbon Isotope Excursion of the Paleocene-Eocene Thermal Maximum (PETM) measured in the Bighorn Basin [109–111]), Willwood Formation, Clarks Fork Basin.

#### Measurements:

Skull: estimated length, 75–80; length nasofrontal hinge to cerebellar prominence, 44; bizygomatic breadth, 38.8; height of base of skull (paroccipital process to transverse nuchal crest), 19; greatest length of orbit, 19.6; supraorbital width 10.5; length of dorsal margin of lacrimal, 12; length of ventral margin of lacrimal, 7.7; height of lacrimal, 8.7; estimated bilacrima width, 17; estimated height of upper bill (tomium to culmen) at level of rostral margin of osseous nasal aperture, 8; length of osseous nasal aperture (caudal margin unknown), >16; length of rostral tip of premaxillae (damaged) to rostral margin of osseous nasal aperture, >11; maximum width of left palatine (at caudolateral lamina), 7.3.

Quadrate: maximum width of mandibular process, 7.0, 7.2; minimum rostrocaudal length of mandibular process, 2.7, 2.9; length of lateral mandibular condyle to otic process, 12.2, 12.3; length of lateral mandibular condyle to apex of orbital process, >11.9, >11 (damaged); width of otic capitula, 4.3, 4.5.

Mandible: length, 65; depth of dentary, 4.7; depth at level of mandibular angle, 8.2; length of mandibular symphysis, 11.5; width of the caudal extremity (medial to lateral processes), 9.6; length of retroarticular process, 9.9.

Vertebrae: Table S1.

Sternum: length, >64 (damaged); width at craniolateral process, ~50; minimum width of body, ~32; depth of carina, ~20; length of costal margin from craniolateral process, 22; length of craniolateral process from coracoidal sulcus, 9.4; depth of sternal notch (medial incisure of caudal margin), >13.

Coracoid: length, 35.0, 35.7; length of sternal articulation, 15.1, 16.5; height of omal extremity from sternal-most margin of supracoracoid sulcus, 9.6, 9.9; distance of sternal articulation to scapular cotyle, 24.7, 24.3; medial–lateral width of body, 4.0, 4.4; dorsal–ventral width of body, 2.8, 2.8; distance of medial angle to procoracoid process, 25.9 (procoracoid incomplete), 27.2; length of procoracoid (from opposite side of shaft), 7.7, 7.2; width of humeral articular facet, 4.6, 4.6; length of humeral articular facet (“maximum diameter” or “HAF” [112]), 6.2, ≤6.8; width of medial angle to lateral angle (sternal articulation), 15.1, ≥16.5 (minor damage to lateral angle).

Furcula: dorsoventral length, ~29; width (mediolateral) of omal extremity, 1.2; height of omal extremity (craniocaudal), 3.8; minimum diameter at or near symphysis, 1.8; maximum diameter at or near symphysis, 3.1.

Scapula: width of neck, 3.6, 3.5; width of body, 4.1, 4.4; length of humeral articular surface of glenoid process to coracoid tubercle, 7.1, 7.1; width of humeral articular surface, 3.2, 3.3; breadth of head (acromion to glenoid), 7.6, 7.4.

Humerus (left): length, 80.5; length of deltopectoral crest from dorsal tubercle, 22.5; breadth of dorsal tubercle to bicipital crest, 18.8; width of caput, 4.6; length of bicipital crest from caput (longitudinal), ~15.8; distal width (dorsoventral), 13.1; width of dorsal condyle (craniocaudal), 6.8; width of ventral condyle, 4.0; diameter of body at midshaft, 4.5–5.8.

Ulna (left): length, 80.5; proximal width, ventral surface flush with caliper, 8.0; proximal width, dorsal surface flush with caliper, 7.0; diameter of body at midshaft 4.0–4.5; craniocaudal width (length of dorsal cotylar process from opposite side of shaft), 8.8; dorsoventral width (ventral cotyle from opposite side of shaft), 7.9; length of olecranon from ventral cotyle, 3.3; diameter of ventral cotyle, 5.1–6.0; width of distal condyle, craniocaudal axis, 7.5, dorsoventral axis, 5.7.

Radius (left): length, 70.3; minimum diameter of caput (craniocaudal axis), 4.0; maximum diameter of caput (dorsoventral), 5.0; diameter of midshaft 2.3–2.5; distal width, 6.3.

Ulnare (left): height (craniocaudal), 5.9; width (dorsoventral), 6.8; thickness (proximodistal), 3.4.

Carpometacarpus (left): length 41.5; width of carpal trochlea, 5.0; height of carpal trochlea (craniocaudal), measured on dorsal margin, 5.9, measured on ventral margin, 6.4; proximal height (craniocaudal height of extensor process from ventrocaudal margin of carpal trochlea), 10.2; length of alular metacarpal (longitudinal), 6.6; diameter of major metacarpal, 2.4–3.8; distal height, ~7.1; distal width, ~5.8; distal height of major metacarpal, ~4.4; length of proximal synostosis (carpal trochlea to intermetacarpal space), ~13.8; length of distal synostosis, 5.6.

Proximal phalanx of major digit (left): length, 18.3; height (craniocaudal), 5.8; proximal width, 4.4; distal width, 3.1.

Pelvis: estimated length, >64; estimated width at antitrochanters, 35; preacetabular ala of ilium: length (from acetabulum), 32, maximum height (dorsoventral, cranial position), 18.6, minimum height (caudal position), 9.4; height at level of acetabulum, 12.1; diameter of acetabulum, 5.7; ilioischadic foramen: length, 13, height, 5.1; length of ischium (from acetabulum), >>22.4; height of pelvis caudal to ilioischadic foramen, ventral margin of ischium to dorsolateral crest of ilium, 12.1.

Femur: length, 63.8, 65.2; diameter of head (craniocaudal), 5.6, -; length of head from lateral surface of trochanter, 11, -; height of trochanter (craniocaudal), 8.3, ~7.8; mediolateral diameter of body at midshaft, 4.5, ~4.7, craniocaudal diameter of body at midshaft, 4.7, ~4.5; width of distal extremity, 10.6, ~11.7; height of medial condyle, 7.5, -; height of lateral condyle plus tibiofibular crest, 10.0, ~8.5; depth of patellar sulcus, ~2, ~2.1; width of patellar sulcus, 3.5, ~3.7.

Tibiotarsus (left): length of cranial cnemial crest from caudal margin of head (caliper flush with both medial and lateral femoral articulations), 15.1; width of proximal articular facies (mediolateral), 9.9; length of both cnemial crests from medial condyle (caliper flush with both cranial and lateral cnemial crests), 13.6; length of lateral cnemial crest from medial surface of head, 11.4; depth of cranial cnemial crest (proximodistal), 9.7; length of fibular crest (distal extent of articular surface) from proximal extremity (most proximal extent of cranial cnemial crest), 30.6; distance of fibular crest (proximal extent of articular surface) from lateral femoral articulation, 12.5; height of fibular crest (from opposite side of shaft, proximal level of crest), 6.2; height of fibular crest (from opposite side of shaft, distal level of crest), 7.3; diameter of body at midshaft, (craniocaudal), 4.6, (mediolateral), 5.2.

Fibula (left): length of head (craniocaudal), 5.7; width of head, 2.4.

Tarsometatarsus (left): diameter of body at level of fossa for metatarsal I, (mediolateral), 4.5, (craniocaudal), 3.2; width of distal extremity, 10.0; distance from fossa for metatarsal I (i.e., its distal extent) to distal extremity (i.e., of trochlea III), 12.5; interosseous foramen: width, 1.5, length, 2.6, elevation, 7.2.

Pedal phalanges: Table S1.

**Diagnosis:** As for the genus, by monotypy.

**Description:** Numbers in parentheses correspond to character matrix of Dataset 1 (Supplemental Materials).

Skull: The head is relatively small, as in other Anseriformes. The bill is “fowl-like”, not spatulate as in ducks, and is approximately equal in length to the cranium. The nares are holorhinal. Both the osseous nasal aperture and palatine fenestra (1) are large, open, and confluent; the palatine fenestra is expanded rostrally; the osseous nasal aperture occupies

the majority of the length of the bill, but is only about as wide as the dorsal nasal bar. The maxillary rostrum (2) is short, heavy, vaulted, taller than broad, decurved rostrally to the osseous nasal aperture, and possesses only very minute neurovascular foramina (3). The tomial crest is uniformly well-developed throughout its length. The lateral part of the palatine (4) is broad and short; its caudolateral margin curves gently towards the pterygoid process, and is not truncate or pointed. There is a large and conspicuous pit (pneumatic foramen?) (5) on the dorsolateral surface of the palatine, rostral to the choana, that is as wide as the palatine itself. The pterygoid process curves laterally from the parasphenoid rostrum, with which it apparently does not articulate. The pterygoid articulation of the palatine (6) is pedicellate, although not stalk-like. They are expanded ventrolaterally from the narrow neck region, and asymmetrically U-shaped in caudal view, concave dorsomedially with a shallow groove continuing rostrally. They are narrower, longer, and more parallel than in *Anhimae*, decidedly more closely spaced than in *Anhima* and to a lesser extent *Chauna*, but still separated from one another by a midsagittal ridge as in anhimids and *Presbyornis*, and not as closely spaced as in *Dendrocygna*. These complex characteristics suggest that the pterygoid foot was of the “ball and socket” type [1] (character 45, modified), i.e., articulated with the palatines via separate dorsal and ventral rami of the pterygoid foot. The relief of the articulation is, nevertheless, not as exaggerated as in *Anseres*. The pterygoid bone is unknown.

The most conspicuous features of the cranium are the apparent absence of the zygomatic process (although we disagree with this interpretation; Discussion) and short rostrally oriented postorbital process (7), which together result in a nearly horizontal lateral margin of the neurocranium or crest of the AME articularis [76] that extends from the squamosal quadrate cotyle to the apex of the postorbital process. This condition is intermediate between that in *Presbyornis*, *Conflicto*, and extant anhimids. A low crest on the ventral surface of the lateral margin of the neurocranium extends from the fossa of the origin of the AME articularis dorsal to the squamous cotyle of the quadrate rostrally as far as a notch that separates it from the postorbital process. The notch corresponds with the position of the laterosphenoid-squamosal suture in immature modern *Anseriformes* [76] (figure 5A). This crest might be formed by any combination of the zygomatic process, the ventrolateral facies of the squamosal bone, the ossified zygomatic aponeurosis, and/or by the ossified aponeurosis of the AME articularis muscle, all features of the squamosal bone (Figures 1, S2 and S5). The crest defines the lateral margin of a deeply concave ventrally oriented fossa of the laterosphenoid (8) [10] (character 4, modified) occupied by the ophthalmic rete, although it may also serve in part for the origin of the pseudotemporalis superficialis muscle [L. Witmer pers. comm.]. The cranial margin of this fossa is formed by a crest of the laterosphenoid that extends mediolaterally along the caudal margin of the orbit and unites with the postorbital process laterally. The crest exaggerates the concavity of the fossa, similar to the condition in *Dasornis* (“*Odontopteryx*”) [49] (Figure 1). Although there is a faint impression of the AME muscle, the “fossa musculorum temporalium” [76] is obliterated. Outside of *Anseriformes*, this complex of characters is similar only to the condition seen in *Galliformes*, in which only the apices of the postorbital and ossified aponeurosis of the AME may be united.

The neurocranium is fairly well-rounded and is not marked by deep muscular fossae or ridges, except caudodorsally by the transverse nuchal crest. The transverse nuchal crest is rather flat and horizontal (dorsally) and meets the flat and vertical temporal crest (laterally) at caudolateral protuberances (9) that are like the corners of a tall rectangle, as in some anatids (e.g., *Anser*). There are no occipital fontanelles (10). The foramen magnum is positioned centrally in caudal view, and the occipital condyle is small. The supraorbital and nasofrontal regions are quite narrow as in most anatids, and they are shallowly concave. There is no clear impression of nasal glands (11), but beveling of the thin supraorbital margin of the frontal bone preserved on the right side is suggestive that the glands may have been positioned there as they appear to have been in *Conflicto* [15] (figure 4). The interorbital septum (12) is nearly complete. The lacrimal bone (13) is small, unfused, and



generally triangular in the lateral aspect, with the ventral margin (14) forming a straight horizontal line between the orbital process (15) and the rostral apex; the small, rounded supraorbital process forms an acute angle with the much narrower supraorbital margin of the frontal bone. The ectethmoid (16) is extremely low. The infraorbital fossa (17) is very large and deep. The basiptyergoid process (18) is positioned rostrally, low but “pedicellate” (i.e., a lip projecting around its entire circumference), separated from the midsagittal crest of the parasphenoid rostrum by a groove ventrally, and its articular surface is elongate.

Even though the holotype skull shows no overt evidence of incomplete fusion clearly indicative of immaturity, it is possible that the narrow supraorbital region and pronounced (but small) supraorbital process of the lacrimal bone are age-related, as they appear to be in *Anhima* (Figure S3), and not diagnostic of *Anachronornis* nov. gen.

**Quadrate:** The caudal condyle is absent. The medial condyle is continuous in direction with the long axis of the lateral condyle (19). The quadratojugal cotyle (20) is very deep and offset distinctly caudodorsally to the lateral mandibular condyle, producing a distinct but weak submeatic prominence that lacks a submeatic process [19]. The pterygoid condyle is pronounced, but the pterygopalatine articular surface continues broadly into the notch created by the confluence of the orbital and mandibular processes. The otic capitula (21) are neither closely nor widely spaced; the articular facet of the (pro)otic capitulum is round and flat; the articular facet of the squamosal capitulum has two flattened facets, a lateral facet that is widely separated from the otic capitulum by a sulcus and faces caudolaterally, and another that is juxtaposed to the otic capitulum and faces craniodorsally, i.e., the rostral slope of the squamosal capitulum [35], closely resembling that of *Anseranas* in dorsal view and otherwise present only in Anatidae. The otic process is relatively narrow mediolaterally, although not so much as in anhimids. The caudal surface of the otic process (22) is deeply grooved, ending ventrally in a deep pit in the position of the caudomedial pneumatic foramen of Elzanowski and Stidham [19]. A minute caudomedial foramen is present on one quadrate, but is not verifiable on the other. Thus, this condition appears to be similar to that described by Elzanowski and Stidham [19] for a late Cretaceous possible stem-galloanserine, in which they write, “(a) major feature of the caudal aspect is an elongate caudomedial depression (now damaged) that deepens ventrally but does not contain a foramen”. It is noteworthy that the quadrate of *Anachronornis* nov. gen. does not conform to the uniquely derived condition of Anhimidae described for the Early Eocene quadrate from the Tingamurra Formation of Australia in which the tympanic and lateral crests of the otic process are merged as one [35]. Rather, the condition of both the capitula and caudal surface of the otic process in *Anachronornis* nov. gen. is similar to or at least intermediate with that seen in *Anseranas*. There are large tuberosities (23) on the lateral surfaces of both the otic (“subcapitular tubercle”) and orbital processes (“orbital crest” or “quadrate tubercle of the AME”) [19,77]. There is a large foramen on the medial surface of the body of the quadrate (24), immediately caudal to the notch formed by the orbital and mandibular processes, the basiorbital pneumatic foramen as in *Presbyornis* (or possibly the rostromedial pneumatic foramen as in *Megapodius* [19]). The orbital process is deeply concave on its medial surface (25).

**Mandible:** The ramus is straight in lateral aspect as in Anseres, not decurved as in anhimids. The mandibular symphysis is deeply trough-shaped, longer than wide, and rounded rostrally. The rostral mandibular fenestra appears to have been very large and vacuous, but it may have been covered by elements that are not preserved in the fossil. The most striking aspect of the mandible is the long, bilaterally compressed retroarticular process (26) that terminates in a dorsally projecting (27) spur; the process is not smoothly curved, but instead extends nearly straight caudodorsally, at an obtuse angle from the ramus. It is also tapered from its base, which itself forms a low ventrally projecting angle and is the most ventral point of the mandible. In the lateral aspect, the mandibular angle and coronoid process are distinctly elevated dorsally from the tomium of the dentary. There is a large tubercle for the insertion of the AME, pars articularis, caput externa muscle of Livezey and Zusi [77] (28) on the lateral surface of the caudal mandibular ramus, similar

to that in Anseres. There is a slightly concave insertion of the depressor mandibulae (29), absent in anhimids and *Anseranas*, but it is not the cavernous conical recess so characteristic of anatids. In dorsal view, the medial process (30) points slightly rostrally, unlike the slightly caudally pointing medial process of other Anseriformes; together with the caudal margin of the lateral cotyle, the medial process forms an arc that is evenly bisected by the medial cotyle and the retroarticular process. There is a large pneumatic foramen (31) positioned conspicuously on the dorsolateral margin of the medial process.

**Vertebrae:** Apart from the skull and sternum, the vertebrae are the only bones of the skeleton that might have been pneumatized. There is an enormous cavity or pleurocoel in the lateral surface of the body of thoracic vertebrae (33) with a thin midsagittal septum that separates the right and left cavities. In all but the most caudal thoracic vertebrae the opening to the cavity is so large and vacuous that it does not resemble a pneumatic foramen, but instead the impression of pulmonary diverticula [104,105]. The opening is progressively constricted in successively more caudal thoracic vertebrae, so in the most caudal thoracic vertebrae and first presacral vertebra of the synsacrum it resembles a pneumatic foramen. This condition is most similar to that of the modern genus *Puffinus* (Procellariidae) and numerous Mesozoic birds (below).

There are no transverse foramina preserved on the atlas vertebra, but there are fractured surfaces on the vertebral body to suggest that vestiges of them may have existed. There is no notarium (34). The pygostyle is unknown. The synsacrum is described in greater detail below under the heading “pelvis”.

**Ribs:** Uncinate processes are present and fused with the costal body.

**Sternum:** The body appears to have been approximately 50% longer than wide (35), and the depth of the carina is approximately equal to or less than the width of one side of the sternal body. The carina is thin, except for the pila. Its apex is acute but rounded. The caudal margin of the body (36) appears to have been “single-notched” (i.e., only the medial incisure is present), with the median and lateral trabeculae (37) of approximately equal length. The external spine of the rostrum (manubrium) (38) is present and blunt; the internal spine appears to have been absent. Coracoidal sulci are crossed, as in presbyornithids (uniquely, among Pan-Anseriformes), which is independently suggested by the asymmetry of the medial angle of the coracoids. There is a single large pneumatic foramen, as in *Anseranas*. The craniolateral process (39) is low, forming an equilateral triangle whose lateral apex does not point cranially as in other Anseriformes. The internal labrum of the coracoidal sulcus is the most cranial extension of the sternal body (40), unlike anhimids in which the coracoid pila lies prominently craniodorsal to the internal labrum. The six costal processes of the costal margin occupy less than half the length of the sternum (41) and are restricted to the cranial half of the lateral margin of the body. There is no postcarinal plane (42), nor is there a carinal sulcus (43). The dorsolateral intermuscular line (44) appears to continue caudally to the lateral margin of the median trabecula.

**Coracoid:** Nonpneumatic. The acrocoracoid process (46) is large for Anseriformes. It extends far medially from the supracoracoid sulcus, such that there is a substantial fossa beneath the acrocoracoid process. The scapular cotyle (47) is large and very deep. The procoracoid process (48) is also very large for Anseriformes and points cranially, although it is not particularly long. The scapular cotyle and procoracoid process are located between two-thirds and three-quarters of the length of the coracoid from the sternal extremity. The foramen of the supracoracoid nerve (49) is present, but differs in size from very large to very small in the left and right coracoids of the type specimen. The sternal extremity (50) is quite thin, curved, and broad, with an acute medial angle (51) and well-developed lateral angle (52) that is positioned very close to the sternal articulation. There is a thin flange for the attachment of the sternoclavicular membrane (53), concave ventrally, extending cranially from the medial angle. There is a fossa medial to the ventral intermuscular line (54). The cranial margin of the sternal articulation is raised as a ridge on the internal, but not the external, surface. The insertion of the sternocoracoideus muscle (45) is smoothly

concave. Overall, the coracoid is very similar to that of *Nettapterornis*, except that it lacks the pneumatic foramen on the dorsal surface of the sternal extremity.

Furcula: Nonpneumatic. Wide, short, curved, and relatively uniform in diameter throughout (55), the scapus is roughly circular in cross-section sternally but is bilaterally flattened omally. It is not clear whether the clavicular symphysis is preserved, but the hypocleideum appears to have been absent. Although shaped similarly to that of anatids, the omal extremity (56) is neither as long nor as pointed, and the acrocoracoid articulation is not raised as a distinct knoblike tubercle or facet.

Scapula: Nonpneumatic. The neck (57) is narrow, curved, and round in cross-section, while the body (i.e., caudal two thirds) is flat and straight. The coracoid tubercle (58) is large and almost as long as the acromion, from which it is separated by a broad notch. The glenoid process is pronounced from the neck and its humeral articulation (59) is short. Thus, the cranial extremity is similar in proportions to *Nettapterornis*.

Pectoral appendage: Both the medial and lateral angle of the coracoid are flared as they are in *Nettapterornis* and presbyornithids (less so than in the latter), but the sternal articulation is not directed as much in the caudolateral direction relative to the body of the coracoid. Overall, the general proportions of the wing are similar, although perhaps slightly longer and more slender for its size, to those of *Nettapterornis*. The wing is longer and more slender than that of London Clay specimens (below) but not so much as that of presbyornithids. The carpometacarpus is decidedly stouter than as is typical of presbyornithids, anatids, and *Conflicto*, again approaching the condition in *Nettapterornis*.

Humerus: Nonpneumatic. The body (60) is long and gently curved. The head is small, angular, quite pointed proximally, and distinctly set off from the dorsal tubercle and bicipital crest (61), which is itself short, extending distally no further than the middle angle of the deltopectoral crest. The dorsal tubercle (62) is very pronounced, both proximally and caudally. The large, flared, and gently curved deltopectoral crest (63) extends more than a quarter of the length of the humerus. There is no tubercle at the distal end of the crest (64) as there is in anhimids. The coracobrachial impression (65) is broad, shallowly concave, and poorly defined. The ventral tubercle is not preserved in the type specimen. The (pneumo)tricipital fossa (66) is excavated only ventral to the dorsal crus, although the head and dorsal tubercle are raised substantially from the caudal surface of the shaft (67). The head forms a small lip over the capital groove. The brachial fossa is deep, but its margins are poorly defined. The ventral condyle (68) projects further distally than the rather small ventral epicondyle and dorsal condyle, and it forms most of the distal extremity of the humerus (69). The olecranon fossa and humerotricipital groove are deep, but the scapulotricipital groove is indistinct. There is no supracondylar process, but the dorsal epicondyle is raised proximally from the dorsal condyle a distance approximately equal to the size of the condyle itself. In distal view (71), both of the condyles are smaller than is typical of the Anatidae, and the flexor process is not reflected as caudad.

Ulna: Nonpneumatic and about as long as the humerus. The body (71) is slender, not flattened anywhere, and is bowed only in its proximal half. The carpal tubercle (72) is short and not pointed, much like that of *Chauna* and unlike other Anseriformes.

Radius: Nonpneumatic. Unlike any other Anseriformes, the radius has a straight narrow body (73), and a broad, nearly symmetrical distal extremity (74). The humeral cotyle, which is rather oblong in proximal view, is also very broad relative to the shaft.

Radiale: Unknown.

Ulnare: The overall appearance is intermediate between *Anseranas* and Anhimidae. The metacarpal groove is shallow and twice as broad as the dorsal ramus is thick. The body is flat, nonpneumatic, and notched in its caudal margin.

Carpometacarpus: Nonpneumatic. The length is approximately half that of the humerus. The cranial margin of the major metacarpal is slightly bowed, concave cranially. Although the minor metacarpal (75) is preserved incompletely in the type specimen, it is clearly not bowed, nor is there an intermetacarpal process. The intermetacarpal space (76) is wider than in anatids. The distal metacarpal synostosis ("symphysis" [75]) (77) is

shorter than in all Anseriformes. As in anhimids but not other Anseriformes, the extensor process of the alular metacarpal (78) is level (proximodistally) with the distal portion of the ulnocarpal articulation, whereas the large alular articulation extends considerably further distally than the ulnocarpal articulation. Unlike anhimids, the alular process is quite large and distinct, and the extensor process is not elongated into a spur (79). The condition of the pisiform process is unknown, as it is broken in the fossil. The infratrochlear and supratrochlear fossae, as well as both the dorsal and ventral surfaces of the synosteaal region of the alular and major metacarpals, are all quite deeply excavated (80), as are those depressions on the ventral surface of the carpometacarpus of *Anseranas*. In proximal view (81), the dorsal margin of the carpal trochlea is offset more cranially relative to its ventral margin (i.e., the ulnocarpal articulation) as in a parallelogram than it is in other Anseriformes, especially anhimids in which the carpal trochlea more resembles a square. The articular facet of the major digit extends distally beyond the articular facet of the minor digit (82), unlike anhimids and *Anseranas*. In distal view, the cranioventral tuberosity (83) (character 40 of Livezey 1986 [90]) that develops into the distal spur of the carpometacarpus in anhimids appears to be elevated cranially (Figure S6); however, this appearance may be an artifact of the crushing of the cranial surface of the distal extremity between this tuberosity and the articular facet of the major digit in the type specimen.

**Pelvis:** The proportions are short and broad (84), like those of Galliformes and unlike modern Anseriformes. There is an iliosynsacral canal (85) created by the wide lateral displacement of the preacetabular ilia (86). The pectineal process (87) is short, indistinct, and concave ventrally (88). The dorsolateral crest of the ilium (89) is elevated dorsal to the antitrochanter, but it is not as pronounced as in anhimids. The obturator foramen (90) is very long, extending caudally more than half of the length of the ilioischiadic foramen. The body of the ischium immediately dorsal to the obturator foramen (91) is markedly concave laterally. The terminal process of the ischium is damaged in the type specimen, as is the pubis, but the short synsacrum and dorsolateral spine of the ilium suggest that the ischium (92), too, was short. There is a dorsolateral crest of the postacetabular ala of the ilium (93), especially in the region immediately dorsal to the most caudal portion of the ilioischiadic foramen. The ilioischiadic foramen (94) is like that of *Anseranas*, longer than that of anhimids but shorter than that of anatids. There is an infracristal concavity of the ilium, much unlike the condition in anatids. In the ventral aspect, the pudendal part of the renal fossa has both a caudal recess (95) and a much larger and more circumscribed cranial recess (96). This cranial recess is formed dorsally and laterally by the dorsal plate of the ilium and cranially and ventrally by the very long, elevated intermediate iliac crest. The cranial recess is also seen in *Anseranas* and some individuals of *Chauna*. The gracile costal processes of the acetabular vertebrae are also like those of *Anhima*.

Synsacral (transverse and costal) processes can be treated as three separate groups, preacetabular, acetabular, and postacetabular. There are five preacetabular processes (97). The three most cranial of these (apparently transverse processes) (98) project dorsocranio-laterally and meet the ilium halfway between its dorsal and lateral crests, like that in galliform and charadriiform outgroups but unlike modern Anseriformes. The two caudal (apparently costal) processes of the preacetabular group are oriented laterally. The first of the two is robust and articulates directly with the oblique crest, but the second is tenuous and its presence in the fossil is only indicated by spurs on the synsacrum and ilium. There is a long gap between the most caudal of the preacetabular costal processes and the costal processes of the acetabular vertebrae. Thus, there is an extensive hollowed-out portion of the medial surface of the preacetabular ala of the ilium immediately cranial to the acetabulum, and a vacuous cranial renal fossa (99) between it and the synsacrum, much like that of *Crax* but unlike modern Anseriformes. The costal processes of the acetabular group of synsacral vertebrae are extremely long and thin, and project caudolaterally to meet the intermediate iliac crest (100), most similar to *Anhima*. There are two costal processes in the acetabular group and four in the postacetabular group (101). The two groups are distinct as they are separated by a gap. Moreover, the postacetabular processes project more

caudad, are shorter and parallel with one another, and terminate on the medial margin of the postacetabular ala of the ilium. The two groups are not distinct from one another in extant non-anhimid Anseriformes.

**Pelvic appendage:** The lengths of the tibiotarsus and tarsometatarsus are unknown. The femur is quite long and curved, as in presbyornithids, many fowl, herons, and rails. It seems likely that the distal elements of the appendage were longer than London Clay specimens (below) and shorter than presbyornithids. Both the narrow neck and low fibular crest of the tibiotarsus are similar in proportion to many herons and rails. The phalanges are slender and also heron- or ibis-like.

**Femur:** Nonpneumatic (102). The body (103) is long, slender, like those of presbyornithids, *Nettapterornis*, and *Conflictus*, and it is quite curved, like that of Galliformes and very dissimilar to other Anseriformes. In cranial view, the trochanteric crest (104) is long and curved medially as far as the medial margin of the body, producing a deep trochanteric fossa (105). The trochanteric crest is not very broad in lateral profile nor is the crest pronounced cranioproximally. The neck of the femur (106) is long and constricted. In cranial view, the medial condyle is substantially shorter than (i.e., proximal to) the lateral condyle (107). In distal view, the distal extremity is taller and narrower than in other Anseriformes, except *Anseranas*. The medial condyle is narrow (maybe exaggerated by deformation) and the gap between it and the tibiofibular crest is wide (108). The medial crest of the patellar groove rises abruptly from the body (109). The tibiofibular crest (110) is quite long, especially as compared with that of anhimids. There is a shallow cavity (111) on the proximal portion of the fibular trochlea and the lateral surface of the tibiofibular crest that impinges on both of their articular surfaces.

**Tibiotarsus:** Only the proximal half is preserved. As far as is known, the tibiotarsus is similar to primitive Anseres (i.e., *Anseranas* and *Dendrocygna*) except that the cranial cnemial crest (112) is not as long, especially proximally. While the crest is quite large, extending cranially from the shaft a distance approximately equal to the depth of the proximal articular surfaces, it extends proximally only half as far. In proximal view (113), it is positioned relatively medially, as is typical of Galloanseres. The patellar crest (114) is also well-developed, as in *Dendrocygna*, intermediate between those of *Anseranas* and some other anatids. The lateral cnemial crest (115) is broad; its apex forms an angle of approximately 90°. It is strongly curved distally but it has no spine. The distal portion of the caudal surface of the lateral cnemial crest (116) is deeply concave, resulting in a sharp distal margin. There is a large, conspicuous, and deep fovea (117) on the proximal central margin of the cranial surface of the lateral cnemial crest of the type specimen that may be pathological. The flexor fossa (118) is deeply excavated, undercutting the lateral femoral articulation. The tibial incisure (119) is relatively shallow. The fibular crest (120) is pronounced but short (longitudinally), being only as long as the lateral cnemial crest is wide. There is also a pronounced bony spur (part of the fibular articulation?) (121) on the lateral surface of the proximal extremity, just distal to the lateral femoral articulation, in line with the fibular crest but separated from it by the "proximal interosseous foramen".

**Tarsometatarsus:** Only the distal extremity is preserved. There is a large fossa for metatarsal I (122). In plantar aspect (123), trochlea IV is elevated half the length of trochlea III, and trochlea II is elevated the entire length of trochlea III. Each trochlea is fairly broad, particularly as compared with anatids. Trochlea II (124) is also bulbous and deflected strongly plantad. It is only slightly grooved and only distally at that, as in *Anhima*. Its collateral process (125) is knob-shaped, not exaggerated proximally as a ridge. It points plantad (126), not medially as in *Anseranas*. The fovea for the collateral ligament of trochlea II is tiny. Trochlea III (127–129) is deeply grooved and remains broad even proximally on the plantar surface, where it is short rather than tenuous. Its lateral ridge is of larger diameter than its medial ridge. Trochlea IV is closely spaced to trochlea III, such that the intertrochlear notch (130) is quite narrow, unlike other Anseriformes. Furthermore, in distal view (131), it is not displaced dorsally relative to trochlea III, nor in dorsal view is there a groove joining the intertrochlear notch with the distal neurovascular canal, as are both in

most Anseriformes. The distal neurovascular canal (132) is large and the distal interosseous canal (133) is enclosed.

**Remarks:** The holotype has been anecdotally referred to in the literature as a screamer or screamer-like [8–12,26].

All elements were originally articulated or nearly so, and preserved in a small, discrete calcareous nodule, with parts of the skeleton exposed on all sides of the nodule. The neurocranium is uncrushed and undistorted. Prior to the removal of the specimen from the matrix, the bill was preserved in position (Figure 1), but the nasal bones and to a lesser extent the maxillae were so badly fragmented that there was no perfect continuity between the bill and the cranium except via the palatine bones. The rostral tip of the premaxilla is not preserved. The right lacrimal was preserved ventral to the palate, together with several disarticulated rostral cervical vertebrae. The hyoid was preserved in situ, which is remarkable because the left lacrimal and both pterygoids are missing, and the left side of the mandible, quadratojugal, and palatine collapsed medially into the cranium. The left palatine was freed during acid preparation and the right palatine remains applied to the interorbital septum. In general, the left half of the postcranial skeleton is faithfully preserved in three-dimensions, whereas the right pectoral appendage is severely crushed and the right pelvic appendage is missing altogether. The right halves of the sternum and pelvis are also badly damaged. The sternum and pelvis collapsed upon one another, with most of the thoracic vertebrae and a few partial ribs in between. The thoracic vertebrae remained in articulation with one another but not with the synsacrum, and their transverse processes were crushed. The entire pectoral girdle and pectoral appendages were preserved in articulation. The tarsal region, i.e., distal tibiotarsus and proximal tarsometatarsus, of the left pelvic appendage is missing, as are most of the digits.

Associated with the holotype in the nodule were a quadrate bone (USNM 496701) and an extremely fragmentary femur (USNM 496702) that are treated below as familia incertae sedis. Additionally, associated with the holotype in the nodule were numerous articulated and partially articulated bones of two individuals of Sandcoleidae [113], a few appendicular bones of a small unidentified squamate lizard, a single caudal vertebra of an unidentified mammal about the size of a house-cat, and the mandible of a very small unidentified insectivorous mammal.

#### 4.2. *Anseriformes Familia Incertae Sedis*

Basal Anseriformes related or possibly referable to Anachronornithidae nov. fam. are treated as familia incertae sedis in this section. They are arranged below according to the location and horizon from which they were collected. If referable to Anachronornithidae nov. fam., then they could expand the temporal and geographic of the family to span a total of 7–8 m.y. in North America and Europe.

##### 4.2.1. *Anseriformes Familia Incertae Sedis, Willwood Formation*

**Referred Specimens:** USNM 496701 (Figures 1 and S4), right quadrate missing the pterygoid condyle; USNM 496702 (Figure 3), fragmentary right femur consisting of only the proximal and distal ends.

**Occurrence:** SE 1/4 of NE 1/4 of Sec. 19, T56N R101W, Clark Quadrangle, Park County, WY, USA.

**Horizon:** Latest Paleocene, latest Thanetian, 56.22–55.80 Ma (Cf3, *Copecion* Interval Zone, latest Clarkforkian North American Land Mammal Age, ending at the Carbon Isotope Excursion of the Paleocene-Eocene Thermal Maximum (PETM) measured in the Bighorn Basin [109,110]), Willwood Formation, Clarks Fork Basin.

##### **Measurements:**

USNM 496701 (quadrate): maximum width of mandibular process, 5.5; minimum rostrocaudal length of mandibular process, 2.2; length of lateral mandibular condyle to otic process, 11.1; length of lateral mandibular condyle to apex of orbital process, >9.6; width of otic capitula, 3.8.

USNM 496702 (femur): 55.4; diameter of head (craniocaudal) 4.1; length of head from lateral surface of trochanter, >9.2; height of trochanter (craniocaudal), 7.0; craniocaudal diameter of body at midshaft, ~4.5; height of medial condyle, 6.4.

**Remarks:** USNM 496701 and USNM 496702 are presumed to represent a single individual, based solely on size. They are generally similar to *Anachronornis anhimops* nov. gen. et sp. but differ from it in being smaller as well as in the following characteristics in which it is more similar to *Danielsavis nazensis* nov. gen. et sp., described below. The pars quadratojugalis [19] of the quadrate is not as distinctly separated from the lateral mandibular condyle as in *Anachronornis anhimops* nov. gen. et sp. The quadrate lacks the rostral slope of the squamosal capitulum that is present in the holotype of *Anachronornis anhimops* nov. gen. et sp. The squamosal and otic capitula are relatively widely spaced. The otic process is narrower in lateral view and its dorsal margin appears to form a somewhat more acute angle with the orbital process as in *Danielsavis nazensis* nov. gen. et sp., although what would be the deepest part of this region is damaged in USNM 496701. In dorsal view, the dorsal margin uniting the orbital and otic processes is wider and more bulbous, as the lateral surface of the quadrate is not concave as it is in *Anachronornis anhimops* nov. gen. et sp. The femur exhibits a small foramen on the cranial surface of the neck that presumably corresponds to the pneumatic foramen character 192 of Field et al. [20], but which is lacking in *Anachronornis anhimops* nov. gen. et sp. These differences are sufficient to suggest that the smaller quadrate and femur represent a distinct genus, if they can be attributable to Anachronornithidae nov. fam. at all. Nevertheless, they also could represent a smaller congeneric species, or even a smaller individual of the same species since many species of Anseriformes and their sister group Galliformes and galloanserine-sister Palaeognathae are strongly sexually size-dimorphic [114]. Nor can individual variation or ontogenetic differences be excluded, especially as nidifugous Galloanseres may have protracted growth periods related to the greater allocation of limited nutrients to metabolic processes than to growth [115]. Regardless, fossils of unrelated sandcoleids and mammals were also associated in this same small calcareous nodule. The faunas of individual nodules found in this area apparently represent physical traps in which small vertebrate remains were concentrated.

A heavy gauge wire was glued to the proximal and distal ends of the fragmentary femur (USNM 496702) before removing them from matrix to preserve their distance and the original length of the femur as the missing shaft appears to have been originally preserved but eroded away on the surface of the nodule. The orientation of the proximal and distal ends of the femur as well as the relative total length as compared with the femora of USNM 496700 are consistent with the bone having been originally preserved intact; however, seemingly lateral deviation of the distal fragment of the bone from direction of the shaft of its proximal end suggest that the femur may have been distorted or not have been preserved intact.

#### 4.2.2. Anseriformes Familia Incertae Sedis, Green River Formation

##### Figure 4

**Referred Specimen:** Field Museum of Natural History FMNH PA725: essentially complete skeleton preserved flattened on a slab (not examined).

**Occurrence:** Fossil Butte Member of the Green River Formation (GRF) in Lincoln County, Wyoming.

**Horizon:** Ypresian, late Early Eocene to early Middle Eocene, 52.06–51.88 Ma (Wa 7, Lostcabinian substage of the late Wasatchian North American Land Mammal Age (NALMA) [93,116].



**Figure 4.** Screamer-like anseriform (Anseriformes familia incertae sedis, FMNH PA725), essentially complete two-dimensional skeleton on a slab from the Fossil Butte Member of the Green River Formation [117] (figure 120; reproduced courtesy of Lance Grande).

**Remarks:** Grande illustrated this in his book *The Lost World of Fossil Lake* as “an undescribed potential waterfowl” [117] (figure 120). The specimen was not directly examined for this study, but both a few similarities and dissimilarities to *Anachronornis* nov. gen. can be discerned from Grande’s figure. Like *Anachronornis* nov. gen., the GRF specimen is clearly recognizable as an anseriform by its extremely dorsoventrally tall Anseres-like coronoid region of the mandible relative to the tomial margin of the dentary. There also appears to be a pronounced laterally positioned tubercle of the AME, pars articularis, caput externa muscle on the lateral surface of the postdentary mandible, as in Anseres and in *Anachronornis* nov. gen. There is a longitudinal groove in the lateral surface of the dentary that typifies Anseres (character 62 of Field et al. [20]), but that is lacking in *Anachronornis*



nov. gen. Its bill is narrow and not spatulate, although its bilateral width appears to attenuate more continuously and uniformly towards its rostral tip than either in extant Anhimidae or in *Anachronornis* nov. gen. The furcula is broad and gently curved ventrally, with no clear apophysis. Like *Anachronornis* nov. gen., the dorsal tubercle and pectoral crest of the humerus are large and pronounced, its bicipital crest pronounced ventrally but proximodistally short, and the preacetabular ilium appears to be at least as long if not significantly longer than the postacetabular ilium. The preacetabular synsacrum is longer than the postacetabular synsacrum but the preacetabular and postacetabular portions of the pelvis are nearly equal in length. The femur is short, longer than the preacetabular ilium but about equal in length to the coracoid. Trochlea II of the tarsometatarsus is markedly elevated proximally relative to trochlea III (e.g., as in *Anachronornis* nov. gen. and *Presbyornis*; more so than in *Chauna*, but less so than in *Bucephala*), but comparison of trochlea IV cannot be made. Measurements of the Green River specimen are unavailable and severe crushing precludes accurate estimation of even relative bone lengths, but it differs markedly from *Anachronornis* nov. gen. in the proportional length of its femora, and possibly to a lesser extent of other bones, relative to the length of the humerus. In *Anachronornis* nov. gen., the length of the femora is 80% that of the humerus, while those of the Green River specimen are only 60% that of the humerus (Table S2). This profound difference cannot be accounted for by poor preservation. The length of the ulna in the Green River specimen also appears to be slightly shorter relative to the humerus (94% vs. 100% in *Anachronornis* nov. gen.). Apparent differences in the lengths of the coracoids and skull relative to the humerus cannot be confidently distinguished from diagenetic damage and/or incompleteness.

#### 4.2.3. Anseriformes Familia Incertae Sedis, London Clay Formation

There are at least eleven specimens of three-dimensionally preserved screamer-like fossils among the 766 catalogued specimens from the Early Eocene (Ypresian) of the London Clay Formation at The Naze, Essex, England that were originally in the private collection of the late Michael Daniels, which he bequeathed to the National Museums of Scotland in 2021. The National Museums of Scotland specimens and their corresponding original catalog numbers in the Daniels collection, each with the prefix WN for The Naze collecting locality, are NMS.Z.2021.40.1 (WN 80300), NMS.Z.2021.40.2 (WN 85510), NMS.Z.2021.40.3 (WN 84494), NMS.Z.2021.40.4 (WN 89626A), NMS.Z.2021.40.5 (WN 96919 or 86919?), NMS.Z.2021.40.6 (WN 92736A), NMS.Z.2021.40.7 (WN 82405A), NMS.Z.2021.40.8 (WN 86523), NMS.Z.2021.40.9 (WN 87552D), NMS.Z.2021.40.10 (WN 88584), and NMS.Z.2021.40.11 (WN 93768A). The London Clay specimens are similar enough to one another, to the extent that preservation permits comparison, to suggest that they probably represent a monophyletic group that is generally similar to but distinct from Anachronornithidae nov. fam. Unlike *Anachronornis anhimops* nov. gen. et sp., tarsometatarsal trochleae II and IV of all sufficiently known London Clay specimens are nearly equal in distal length to one another and widely spaced from trochlea III. Other differences, particularly of the skull, are insufficiently preserved among specimens to know whether they represent synapomorphies, autapomorphies, ontogenetic differences, or polymorphism. The specimens are arranged below in four groups. NMS.Z.2021.40.1, NMS.Z.2021.40.2, NMS.Z.2021.40.3, and NMS.Z.2021.40.6 may represent a single species (Group A), but they differ from one another in some details and so are described individually in case they are not. These four specimens are about two-thirds the size of USNM 496700 and somewhat more megapode-like in some details but more screamer-like in others than *Anachronornis* nov. gen. NMS.Z.2021.40.4, NMS.Z.2021.40.5, and NMS.Z.2021.40.8 represent one or more similarly sized larger species (Group B). NMS.Z.2021.40.4 is clearly distinct from NMS.Z.2021.40.1 and NMS.Z.2021.40.6 at the generic level. Michael Daniels made note of “barbs on cervical vertebrae” of NMS.Z.2021.40.7, NMS.Z.2021.40.9, and NMS.Z.2021.40.10 (Group C). The last remaining specimen is listed as Group D.

## London Clay Group A

***Danielsavis* nov. gen. Houde, Dickson, and Camarena**

urn:lsid:zoobank.org:act:1301901D-F55F-409A-9EE9-F4B9CA9D419D

**Etymology:** Daniels plus avis, a bird. The genus is named in recognition of Michael C. S. Daniels for his discovery of the rich and remarkably well-preserved avifauna of The Naze locality of the Early Eocene London Clay Formation in Essex, England, and for his lifelong devotion to the collection, preparation, and curation of specimens from that locality.

**Diagnosis:** Identified as Galloanseres on the basis of quadrate with only two mandibular condyles and presence of quadratojugal process. Identified as Anseriformes and distinguished from Galliformes (including Gallinuloididae and Quercymegapodiidae) on the basis of the coracoid with large procoracoid process, foramen of the supracoracoid nerve, broad sternal extremity with flared lateral angle and absence of pneumatic foramen, and sternum without separate intermediate (“lateral” [77]) and lateral (“caudolateral” [77]) trabeculae.

**Differential Diagnosis:** *Danielsavis nazensis* nov. gen. is more consistent with Anachronornithidae nov. fam. than with Anhimidae because the quadrate has a basiorbital pneumatic foramen, the appendicular skeleton excluding the coracoid lacks pneumatization, the sternum lacks prominent coracoid pila, the coracoid has a medially pronounced acrocoracoid and a cranially positioned and directed procoracoid process, the radius has a nearly symmetrical distal extremity, and the carpometacarpus lacks spurs.

*Danielsavis* nov. gen. differs from *Anachronornis anhimops* nov. gen. et sp. in the following characters, and is more screamer-like in many but not all of them. Unlike both extant screamers and USNM 496700, the tomium of the prenasal premaxilla is straight-sided, pointed, and triangular as viewed ventrally, while the dorsal nasal bar is sloped in lateral view (similar to *Asteriornis*) suggesting that the upper bill would have been somewhat wedge-shaped and dorsoventrally tall at its base. The dentary is slightly decurved, in lateral view the postdentary region is dorsoventrally narrow such that the mandibular angle and coronoid process are not pronounced dorsally relative to the mandibular tomium, and the mandible has a less pronounced and less laterally, more dorsally, positioned tubercle of the AME, pars articularis, caput externa muscle. The medial process of the mandible is positioned rostrally and directed medially, dorsoventrally narrow in caudal view, and lacks crests uniting the medial process with the retroarticular process, which itself is narrow and blunt-ended in lateral view. The retroarticular process is narrow, blunt-ended, and oriented more dorsally in lateral view, and its length is less than the rostral–caudal length of the medial mandibular cotyle in dorsal view. The otic process of the quadrate is narrow in lateral view, such that the profiles it creates with the orbital process dorsally and mandibular process caudally are more convex. The pterygoid condyle is small but distinct. The atlas vertebra has well-defined transverse foramina, as in some Anseres. Vertebral ribs are too fragmentary to determine whether there were uncinat processes. The craniolateral process of the sternum is narrow and deeply concave on its cranial margin so it appears strongly hooked cranially (as also in Anatidae). The coracoidal sulci do not meet. The furcula is bowed in cranial view and narrower dorsally than at its widest, but this might have resulted from postmortem warping underwater and/or from healed fractures of both clavicles. In lateral view the furcula has a more dorsally elevated acrocoracoid process and sharply acute and much longer acromial process. The procoracoid process of the coracoid is closer to the acrocoracoid process such that the supracoracoid sulcus between the two is narrow, and the lateral ellipsoid lamina of the acrocoracoid is small, indistinct, and does not extend as far sternad as the articular ellipsoid lamina [77]. The sternal extremity is thicker and on its dorsal side there is a small hole on the right but not the left coracoid that may either be a small pneumatic foramen or simply damage. The acromion of the scapula is long and pointed. Most if not all appendicular elements are stouter (i.e., shaft wider relative to total length). In cranial view, the caput of the humerus is not as pointed, the dorsal tubercle is positioned further proximad, and the distal margin of the bicipital crest is more pronounced ventrally from the diaphysis. In ventral view, the proximal margin of the deltopectoral crest diverges more steeply laterad. The cranial cnemial crest of the tibiotarsus is strongly

deflected laterad in proximal view. Trochleae II and IV of the tarsometatarsus are nearly equal in length distally and more widely spaced from trochlea III in cranial view.

*Danielsavis nazensis* nov. gen. et sp. Houde, Dickson, and Camarena

urn:lsid:zoobank.org:act:98FA0546-612B-4C61-9CE0-D1009C9524E4

Figures 1, 5, 6 and S4



**Figure 5.** Holotype of *Danielsavis nazensis* nov. gen. et sp. (NMS.Z.2021.40.1): premaxilla, dorsal (A), left lateral (B); right side of mandible, caudal (C), dorsolateral (D), dorsal (E); omal extremities of furcula, left (F), right (G); left quadrate, medial aspect (H); right quadrate, medial aspect (I); cranial extremity of sternum (J); dorsal cranial extremity of scapulae, left (K), right (L); coracoids right dorsal (M), left ventral omal extremity and dorsal sternal extremity (T); caudal left humerus (N); left ulna, cranial (O), dorsal (P); radii, left dorsal (Q), right caudal (R); carpometacarpi, right ventral (S), proximal left ventral (U); cranial distal right tibiotarsus (V); tarsometatarsi, right cranial (W), left caudal (X); ventral left proximal major digit (Y); caudal atlas (Z); left lateral pygostyle (AA). Scale bar 1 cm. Images F, G, K–O, and S–X courtesy of Gerald Mayr.

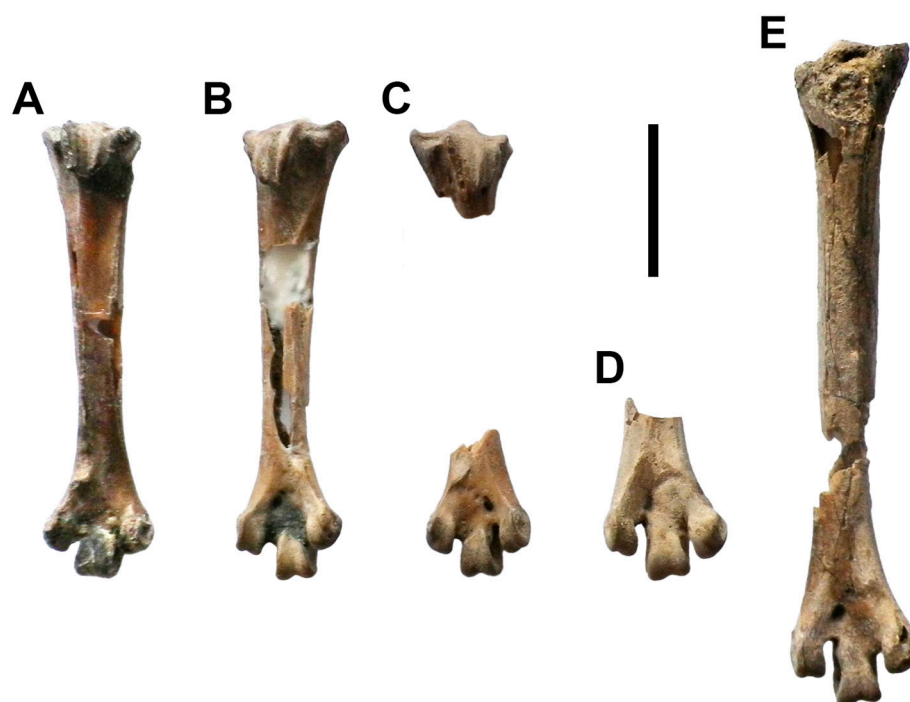


**Figure 6.** Caudal aspect of tarsometatarsi of London Clay screamer-like Anseriformes familia incertae sedis: holotype of *Danielsavis nazensis* nov. gen. et sp. (NMS.Z.2021.40.1) left (A), left (NMS.Z.2021.40.6) (B), proximal and distal extremities of right (NMS.Z.2021.40.3) (C), distal left (NMS.Z.2021.40.5) (D), left (NMS.Z.2021.40.4) (E). Scale bar 1 cm.

Tables S2 and S3

**Etymology:** Named for the type locality, The Naze.

**Holotype:** National Museums of Scotland NMS.Z.2021.40.1: premaxilla, mandible, quadrates, pterygoids, basihyal, ceratobranchial,  $\geq 19$  cervical and thoracic vertebrae, sternal and fragmentary vertebral ribs, cranial margin of sternum, partial furcula, right and damaged left coracoids, cranial ends of scapulae, left and distal end of right humeri, radii, left ulna, radiales, ulnares, right and proximal left carpometacarpi, proximal and distal fragments of right and left femora, right fibula, proximal fragment of left and distal right tibiotarsus, right and distal left tarsometatarsi, alar and pedal phalanges, sclerotic plates, and tracheal rings.

**Type Locality:** The Naze, Essex, England. Daniels' note on stratigraphy, "Lower foreshore, about 'C'" (i.e., just north of Naze Tower).

**Horizon:** Early Eocene (Ypresian 54.6–55.0 Ma), Walton Member (Division A2, European Mammal Paleogene zone MP 8 + 9), London Clay Formation [96].

**Measurements:**

Premaxilla: premaxillary length, 8.0.

Quadrate (right): lateral otic capitulum to medial mandibular condyle, 8.8.

Vertebrae: Table S3.

Coracoid: length, -, 35.5; height of omal extremity from sternal-most margin of supra-coracoid sulcus, 7.6, 7.2; width from medial angle to lateral process, -, 17.2; width of medial angle to lateral angle (sternal articulation), 40.0, 40.0.

Scapula: breadth of head (acromion to glenoid), 7.3, 7.3; width of neck, 3.5, 3.5.

Humerus (left): length, 59.1; distal width (dorsoventral), 15.9; dorsoventral diameter of shaft, 4.9; craniocaudal diameter of shaft, 4.4; width of dorsal condyle (craniocaudal), 5.0.

Radius (dorsoventral): proximal width, 3.5, -; distal width, -, 5.1; diameter of shaft, 2.5, 2.5.

Ulna (left): length, 61.0.

Carpometacarpus: length, -, 33.5; proximal height (craniocaudal height of extensor process from ventrocaudal margin of carpal trochlea), 9.1, -; craniocaudal diameter of major metacarpal, -, 3.0.

Alar phalanges: alular digit, length, 11.4, -; proximal major digit, length, 15.8, 15.8; craniocaudal depth, 6.0, 6.0; distal major digit, length, 11.0, 11.0; minor digit, 8.0, 8.0.

Femur (right): distal width, 9.0; height medial condyle, 6.1; height of lateral condyle plus tibiofibular crest, 6.5.

Tibiotarsus: width of proximal articular facies (mediolateral), 6.8, -; distal width, -, 6.8; craniocaudal length of lateral condyle, -, 5.8; craniocaudal length of medial condyle, -, 6.5.

Fibula (right): length of head (craniocaudal), 4.1.

Tarsometatarsus (right): length, 33.1; proximal width, 7.5; proximal depth (cotyles plus hypotarsus), 6.5; distal width, 7.9; diameter of shaft (craniocaudal), 2.8; diameter of shaft (mediolateral), 3.7; craniocaudal height of lateral cotyle, 4.0; craniocaudal height of trochlea II, 4.0; craniocaudal height of trochlea III, 4.2; craniocaudal height of trochlea IV, 4.5.

Metatarsal I: length, 5.8, 5.8.

Pedal phalanges: Table S3.

**Diagnosis:** As for the genus, by monotypy.

**Description:** Premaxilla: the prenarial region is nearly as wide as it is long, wider than tall, and its tomial margin is only slightly curved ventrally. The ventral surface is flat, not grooved, and extends caudally to separate the rostral portions of the right and left sides of the ventromedial fenestra. The dorsal nasal bar is straight and rises at a distinct angle from the prenarial premaxilla.

Quadrate: The basiorbital pneumatic foramen is present. There is no foramen on the caudal side of the otic process.

Mandible: The mandible is long and narrow in lateral view. The mandibular rostrum is short. There is a well-defined tubercle for the insertion of AME, pars articularis, caput externa muscle on the dorsolateral surface of the coronoid region in addition to the coronoid process. The mandibular angle is poorly defined such that the dorsal margin of the coronoid region is smoothly continuous with the tomial margin of the dentary. The aperture of the mandibular canal is small and there are no mandibular fenestrae. The length of the retroarticular process (right side broken) is less than the rostral-caudal length of the medial mandibular cotyle. The medial process bears a pneumatic foramen. Unlike *Anachronornis* nov. gen., the medial process arises directly medially from the mandibular cotyles, points medially, is dorsoventrally narrow, and it is not united by a crest either dorsally or ventrally to the retroarticular process. There is no fossa for the insertion of the depressor mandibulae.

Vertebrae: The atlas bears transverse foramina. Most cervical vertebrae are approximately as wide as their bodies long. Thoracic vertebrae bear a large conspicuous lateral opening, similar to that of *Anachronornis* nov. gen. There is no notarium.

Sternum: The external manubrial spine is small and the internal spine is altogether lacking. Coracoidal sulci are uncrossed and clearly separated from one another by a depression.

Furcula: The bodies of the clavicles are narrow and bilaterally compressed at their omal extremities, but not flat. In lateral view, the acrocoracoid process is dorsally elevated, forming a nearly right angle with the acromial process, which is much longer and acutely pointed.

Coracoid: The scapular cotyle is large, deep, and well-defined. The procoracoid process is large and omally directed with a foramen of the supracoracoid nerve. The acrocoracoid and clavicular articulation projects medially over the supracoracoid sulcus, but its sternal-facing surface is not concave, nor does it bear foramina. The supracoracoid sulcus is narrower than the mediolateral width of the midshaft. Ridges on the dorsal surface are evident on the dorsal surface from the sternal articulation nearly to the foramen of the supracoracoid nerve. There is what may be a small pneumatic foramen in the sternomedial region of the impression of the sternocoracoideus muscle immediately above the medial angle of the left but not the right coracoid. The lateral process is close to and extends considerably further laterad to the sternal articulation. The internal labrum of the sternal

articulation is prominent medially, while the external labrum is present but much narrower and indistinct. A pronounced medial process exists adjacent to the medial angle. The intermuscular line is positioned far laterad, and there is a very shallow depression medial to it.

**Scapula:** The acromion is straight and long. The body is narrow and straight.

**Humerus:** The dorsal tubercle is pronounced. The coracobrachial fossa is shallow. The pectoral crest, although damaged dorsally and distally, is thin and flared, and extends distally approximately 32% the length of the humerus. The bicipital crest is pronounced, projecting ventrally from the shaft approximately as it is long proximodistally. There is no pneumatic foramen in the pneumotricipital fossa. The ventral condyle projects distal from the dorsal condyle and more so beyond the ventral epicondyle. The dorsal supracondylar process is lacking as such. There is no scapulotricipital sulcus to speak of. The brachial fossa is very well-defined but small and limited to the ventral half of the distal extremity.

**Ulna:** Slightly longer than the humerus, slightly less than twice the length of the carpometacarpus, and nearly four times the length of the proximal phalanx of the major metacarpal. The olecranon is short, and the insertion of the brachialis is well-defined along its caudal margin. The shaft is not flattened and does not bear raised papillae of remiges.

**Radius:** The distal extremity approaches symmetry in cranial view.

**Carpometacarpus:** Stout, approximately 3.5 times as long as the craniocaudal height of the ventral margin of the carpal trochlea to the extensor process, and 6 times as long as the craniocaudal width of the major and minor metacarpals. The intermetacarpal space is only slightly narrower than the craniocaudal diameter of the major metacarpal. The alular metacarpal is shorter than the craniocaudal height of the ventral carpal trochlea, and slightly longer than the proximodistal and craniocaudal measurements of the proximal synostosis.

**Tibiotarsus:** The condyles are proximodistally subequal in size, neither narrowly nor widely spaced, and the medial condyle is not significantly offset from the shaft in cranial view. The supratendinal bridge is proximodistally unremarkably narrow.

**Tarsometatarsus:** Short. The lateral cotyle is offset distally to the medial cotyle, and the intercondylar eminence projects further proximally than the medial and lateral margins of both cotyles. The hypotarsus is unperforated. The medial hypotarsal crest is the most pronounced part of it, and there is a single deep sulcus juxtaposed lateral to the medial crest, and a single much less conspicuous sulcus lateral to that. Parahypotarsal fossae exist both medially and laterally. The medioplantar crest extends less than half the length of the shaft but the flexor sulcus is indistinct. The fossa of metatarsal I is large and positioned medially. The trochleae are widely divergent and subequally elevated. The distal vascular foramen is large and continuous with the distal interosseous canal.

**Pedal phalanges:** One pedal ungual is considerably longer and less curved than the others, consistent with the straight and elongate ungual of digit I in extant Anhimidae.

**Remarks:** *Danielsavis nazensis* nov. gen. et sp. was illustrated and briefly described by Mayr [26] (pp. 60–61, figure 4.10f).

**London Clay Group A referred specimens:** NMS.Z.2021.40.2, NMS.Z.2021.40.3, and NMS.Z.2021.40.6.

**Remarks:** NMS.Z.2021.40.2, NMS.Z.2021.40.3, and NMS.Z.2021.40.6, each described in turn in the following paragraphs, were collected at the type locality and are possibly conspecific with *Danielsavis nazensis* nov. gen. et sp. They were used for scoring characters that were not preserved in the holotype of *Danielsavis nazensis* nov. gen. et sp., NMS.Z.2021.40.1 for phylogenetic analysis.

**NMS.Z.2021.40.2**

Figures 7 and S4, Table S4

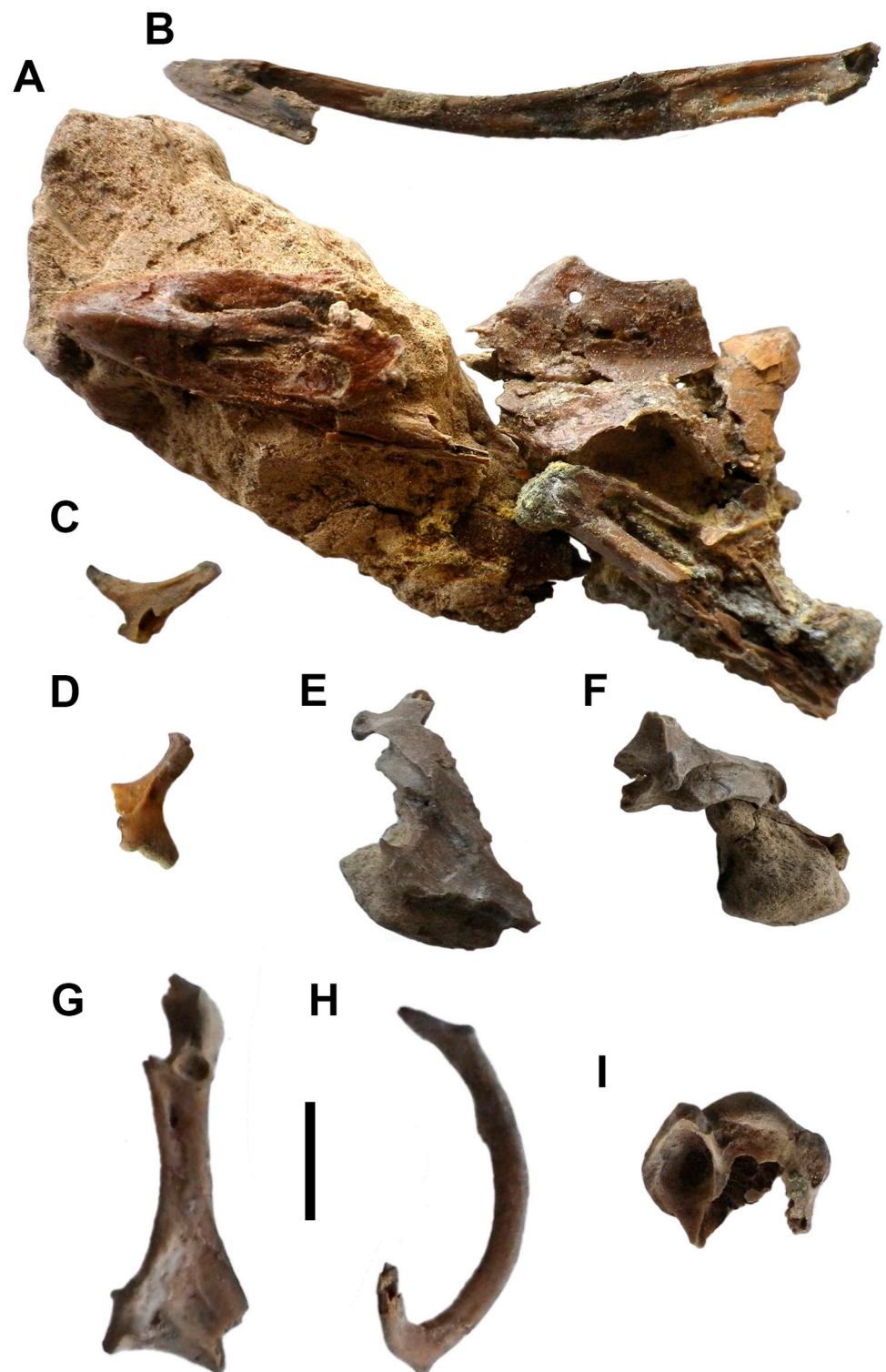


**Figure 7.** Screamer-like anseriform from the London Clay Formation (NMS.Z.2021.40.2, Anseriformes familia incertae sedis): dorsal aspect of skull in two unattached pieces of matrix (A), right ventrolateral mandible (B); quadrates, left lateral (C), right medial (D); cranial portion of sternum, right ventrolateral (E), cranial (F); right coracoid, dorsal (G); furcula, right craniolateral aspect (H); proximal right humerus, caudal (I). Scale bar 1 cm.

**Material:** skull including supraorbital region and complete upper bill, left side of mandible including the rostrum, quadrates, five cervical vertebrae, cranial portion of

sternum, incomplete furcula and right coracoid, cranial extremity of scapula, proximal end of right humerus, distal left carpometacarpus, and alar and pedal phalanges.

**Locality:** The Naze, Essex, England. Daniels' note on precise location "(illegible) . . . foreshore about E" (i.e., about north–south midpoint of the Naze).

**Horizon:** Early Eocene (Ypresian 54.6–55.0 Ma), Walton Member (Division A2, European Mammal Paleogene zone MP 8 + 9), London Clay Formation [96].

**Measurements:**

Skull (incomplete): >55.

Prenarial premaxilla, 10.0.

Quadrate (right): lateral otic capitulum to medial mandibular condyle, 9.4.

Mandible (incomplete): >46.

Vertebrae: Table S4.

Coracoid (incomplete): >33.

Alar phalanx, major digit, proximal: length, 14.8, craniocaudal depth, 6.0.

Pedal phalanges: Table S4.

**Differential Diagnosis:** NMS.Z.2021.40.2 differs from *Anachronornis anhimops* nov. gen. et sp. and *Danielsavis nazensis* nov. gen. et sp. because in lateral view the orbital process of the quadrate is narrower and the dorsal margin of the quadrate between it and the otic process is more uniformly curved. The premaxilla is slightly longer and narrower than that of *Danielsavis nazensis* nov. gen. et sp. The tubercle of the external head of the AME, pars articularis is positioned closer to the dorsal margin of the coronoid region.

**Description:** All features are as described for *Danielsavis nazensis* nov. gen. et sp. to the extent that they are known or differentiated in the differential diagnosis. The supraorbital region of NMS.Z.2021.40.2 is broader than USNM 496700, and within the range of individual variation of extant *Anhima* and markedly immature specimens of *Chauna*. However, the lacrimal, unknown in *Danielsavis nazensis* nov. gen. et sp., is fused to the frontals, unlike both *Anachronornis* nov. gen. and extant anhimids. The mandible is dorsoventrally narrow throughout its length in lateral view, the dentary decurved relative to the postdentary, and tubercles of the AME are positioned close to or on the dorsal margin of the coronoid region. The ventral portion of the furcula exhibits details not preserved in *Danielsavis nazensis* nov. gen. et sp., to which the omal extremity is otherwise similar. The furcula is widely curved ventrally as viewed dorsally, but not notably wide overall relative to the length of the clavicles. The shaft becomes dorsoventrally rather than mediolaterally compressed. It bears a small but distinct clavicular synostosis and apophysis. The sternum is as described for *Danielsavis nazensis* nov. gen. et sp., but also preserves a well-defined but short, bilaterally compressed external manubrial spine. The cranial margin of the craniolateral process is deeply concave, and terminates laterally in well-defined cranially directed spurs (Figure 7). The coracoid is also similar to that of *Danielsavis nazensis* nov. gen. et sp., but to the extent that it is preserved it appears that the supracoracoid sulcus may have been wider, the shaft slightly narrower mediolaterally and slightly more robust, the foramen of the supracoracoid nerve larger, and ridges on the dorsal surface restricted to the sternal extremity associated with the insertion of the sternocoracoideus muscle. There is what may be a pneumatic foramen in the sternomedial region of the insertion of the sternocoracoideus muscle near the medial angle and sternal articulation, but it is difficult to ascertain whether this is a natural feature of the bone because it is partly covered with glue. The single known pedal ungual is fairly straight and long.

**Remarks:** NMS.Z.2021.40.2 was illustrated and briefly described by Mayr [26] (pp. 60–61, figure 4.10g).

**NMS.Z.2021.40.3**

Figures 6 and 8, Table S5



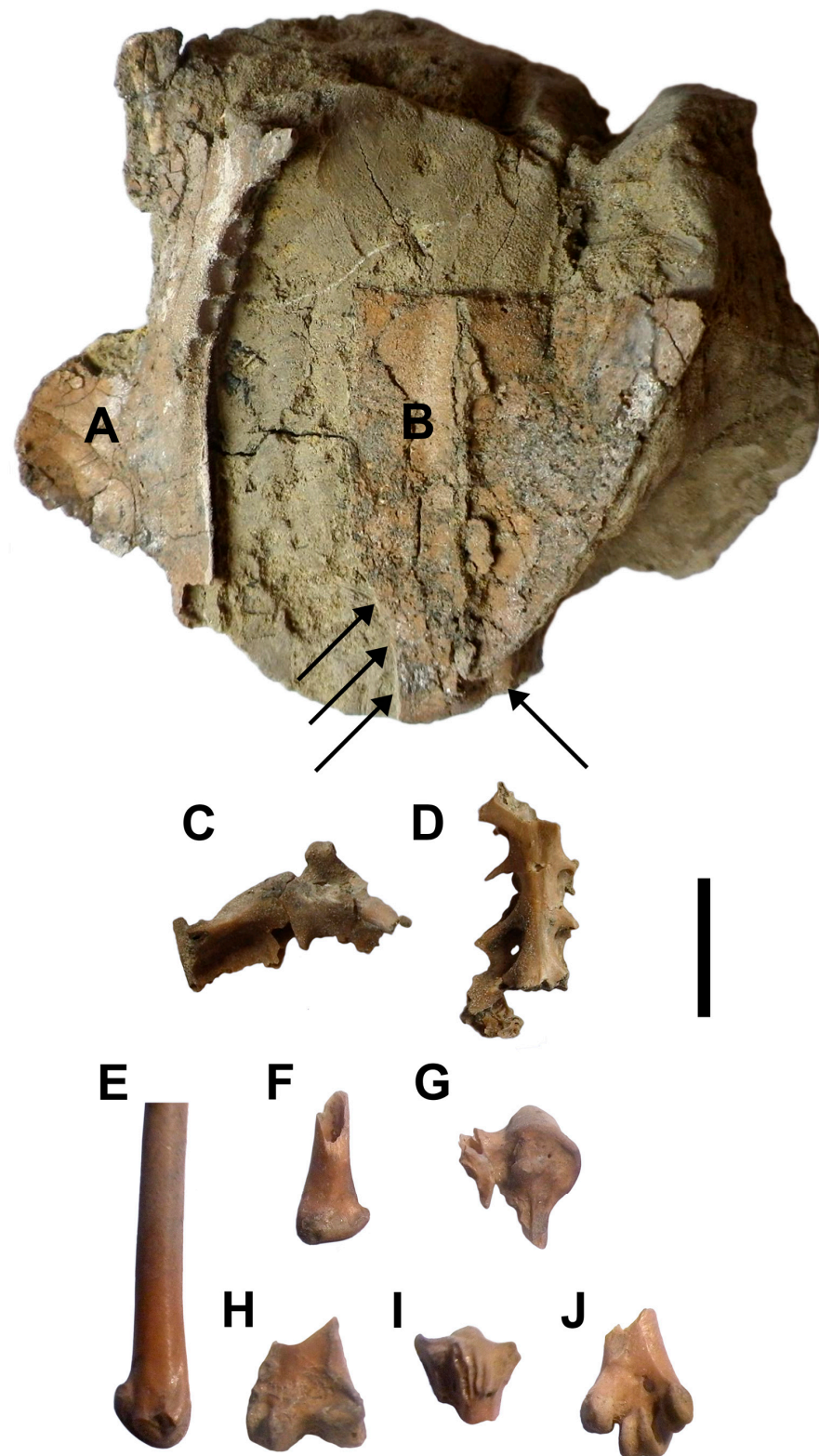


**Figure 8.** Screamer-like anseriform from the London Clay Formation (NMS.Z.2021.40.3 Anseriformes familia incertae sedis): sternum in matrix, right costal margin and lateral cardiac plate, dorsal aspect (A), right ventrolateral aspect, union of right medial abdominal plate and caudal carina marked by label (B), arrows denote lateral margins of median trabecula of sternum, cranial extremity, dorsal (C); caudal fragment of synsacrum, ventral (D); distal left ulna, ventral (E); distal right radius, caudal (F); proximal right carpometacarpus, ventral (G); distal left femur, caudal (H); right tarsometatarsus, proximal caudal (I), distal caudal (J). Scale bar 1 cm.

**Material:** Two cervical, two thoracic, and two caudal vertebrae, fragments of ribs, representative portions of most of the sternum in three pieces, distal left ulna, distal radii, distal right carpometacarpus, distal left femur, and proximal and distal ends of right tarsometatarsus, proximal left alar and pedal phalanges.

**Locality:** The Naze, Essex, England. Daniels' note on precise location "Cliff base-H, say 75 ft. up from base of formation" (i.e., northernmost extent of the Naze).

**Horizon:** Early Eocene (Ypresian 54.6–55.0 Ma), Walton Member (Division A2, European Mammal Paleogene zone MP 8 + 9), London Clay Formation [96].

**Measurements:**

Vertebrae: Table S5.

Radius: length, 56, -; distal width, 5.7, 5.7.

Ulna(left): distal width, craniocaudal, 6.0; dorsoventral, 5.0.

Femur(left): distal width 8.8; height of lateral condyle plus tibiofibular crest, 7.5.

Tarsometatarsus (right): proximal width, 7.5; proximal depth (cotyles plus hypotarsus), 5.5; distal width, 7.8; craniocaudal height of lateral cotyle, 4.2; craniocaudal height of trochlea II, 4.2; craniocaudal height of trochlea III, 4.2; craniocaudal height of trochlea IV, 4.7.

Metatarsal I: length, 6.1.

Pedal phalanges: Table S5.

**Differential Diagnosis:** The sternum differs from that of *Anachronornithidae* nov. fam. because the carina is deep (dorsoventrally) and the hepatic or abdominal plate [90] extends an unknown distance caudal to the carina.

**Description:** The sternum is as described for *Danielsavis* nov. gen., but also preserves a deep carina, 5–6 costal tubercles, deeply incised caudal margin, and an abdominal plate that extends an unknown distance caudal to the carina, as is the case in extant anhimids. The alular metacarpal of the carpometacarpus is extremely short proximodistally and positioned proximally, such that the distal limits of the alular process and the pisiform process are approximately equal, unlike the holotype of *Danielsavis nazensis* nov. gen. et sp. NMS.Z.2021.40.1. The supratrochlear and infratrochlear fossae and synostosis of alular and major metacarpals are not deeply excavated. A short segment of the postacetabular synsacrum is preserved. The first costal process is clearly acetabular as it is thick and ventrally oriented. The second differs significantly as it is very thin and caudodorsally oriented, the third slightly thicker, and the fourth thicker still while expanding fairly smoothly onto the transverse lamina, which itself is sufficiently preserved to indicate that there was at least one more vertebra. The body of the synsacrum narrows markedly from cranial to caudal, and curves ventrally at the last preserved vertebra. Based solely on these characteristics, it appears that the postacetabular pelvis was probably short. The tarsometatarsus is as described for *Danielsavis nazensis* nov. gen. et sp.

**NMS.Z.2021.40.6**

Figure 6

**Material:** left tarsometatarsus, pedal phalanges.

**Locality:** The Naze, Essex, England. Daniels' note on precise location "Cliff base—H, say 75 ft. up from base of formation" (i.e., northernmost extent of the Naze).

**Horizon:** Early Eocene (Ypresian; 54.6–55.0 Ma), Walton Member (Division A2, European Mammal Paleogene zone MP 8 + 9), London Clay Formation [96], London Clay Formation.

**Diagnosis and Description:** Known from only the tarsometatarsus, NMS.Z.2021.40.6 does not differ from *Danielsavis nazensis* nov. gen. et sp., to which it is possibly referable.

London Clay Group B Referred Specimens

**Locality and Horizon:** all Group B specimens same as London Clay Group A.

**NMS.Z.2021.40.4**

Figure 6

**Material:** premaxilla, mandible, pterygoid, vertebrae, costae, sternum, coracoid, humerus, radius, ulna, carpals, carpometacarpus, femur, fibula, left tarsometatarsus, alar

and pedal phalanges. Remarks: NMS.Z.2021.40.4 is distinct from *Danielsavis* nov. gen. at the generic level because its tarsometatarsus is considerably more elongate.

**NMS.Z.2021.40.5**

Figure 6

**Material:** premaxilla, mandible, hyoid, vertebrae.

**Remarks:** The specimen is problematic as it was recorded by Michael Daniels as catalog number WN 96919 but elsewhere as WN 86919. He considered it to be screamer-like and it compares well with NMS.Z.2021.40.4 and NMS.Z.2021.40.8 (P.H., pers. obs.). However, the associated quadrate has three mandibular condyles and therefore is not referable to Galloanseres. It is possible that the quadrate is incorrectly associated.

**NMS.Z.2021.40.8**

**Material:** proximal and distal left tarsometatarsus, pedal phalanges.

London Clay Group C Referred Specimens

**Locality and Horizon:** all Group C specimens same as London Clay Group A.

**NMS.Z.2021.40.7**

**Material:** premaxilla, mandible, hyoid, vertebrae, pygostyle (not examined).

**NMS.Z.2021.40.9**

**Material:** mandible, vertebrae, pygostyle (not examined).

**NMS.Z.2021.40.10**

**Material:** cranial fragment of vertebra (not examined).

Remarks: Michael Daniels made note of “barbs” on the cervical vertebrae of these three specimens. The barbs may be homologous to the cervical tubercles of *Perplexicervix microcephalon*, a species from the Middle Eocene of Messel, Germany with otherwise anhimid-like characteristics, as described by Mayr [37].

London Clay Group D Referred Specimen

**Locality and Horizon:** same as London Clay Group A.

**NMS.Z.2021.40.11**

**Material:** tarsometatarsus (not examined).

## 5. Results of Phylogenetic Analyses

### 5.1. Dataset 1

Neither *Anachronornis* nov. gen. nor *Danielsavis* nov. gen. was recovered by dataset 1 within crown-Galloanseres in the single MP and Bayesian trees when both were included in the search simultaneously and *Burhinus* was designated as an outgroup (BS = 69%, PP = 65%, PI consistency index (CI) = 0.67, retention index (RI) = 0.50; Figure S8; Supplementary Appendix A4). When treated individually, *Anachronornis* nov. gen. was excluded from crown-Galloanseres (BS = 81%) and *Danielsavis* nov. gen. was excluded from crown-Anseriformes (BS = 69%). Neither parsimony nor likelihood KH tests detected a significant difference between all parsimony trees within five steps of optimal ( $p > 0.05$ ), or among trees in which either *Anachronornis* nov. gen. or *Danielsavis* nov. gen. was constrained as sister to all Anseriformes (length 300), to Anseres (length 302), or to Anhimidae (length 304), or among 42 trees (out of all possible 10,395 trees) in which either *Anachronornis* nov. gen. or *Danielsavis* nov. gen. or both were sister to all Anseriformes, to Anseres, or to Anhimidae (Supplementary Appendices A5–A11).

### 5.2. Dataset 2

Dataset 2 recovered *Anachronornis* nov. gen. as sister to Pan-Anseriformes in all 216 optimal maximum parsimony (MP) trees (Figure S9; BS < 50%, CI = 0.33, RI = 0.69; Supplementary Appendix B3). This position was not significantly better than any constraint tree in which *Anachronornis* nov. gen. was sister to Galloanseres, Galliformes, Anseriformes, Anhimidae, Anseres, Anatidae, or *Presbyornis*, regardless of the position of *Presbyornis* relative to *Anseranas* and/or Anatidae (parsimony KH test  $p > 0.05$ ; Supplementary Appendix B4).

When BS analysis was repeated with paleognath and galliform outgroups included and all 34 neoavian outgroups omitted, *Anachronornis* nov. gen. was recovered as sister to all Anseriformes (BS = 99%; not shown).

### 5.3. Dataset 3

Dataset 3 recovered *Anachronornis* nov. gen. as sister to Anhimidae alone (BS = 64%; CI = 0.62, RI = 0.80, Figure S9, Supplementary Appendix C3). This position was not significantly better than any constraint tree in which *Anachronornis* nov. gen. was sister to crown- or Pan-Anseres, Pan-Anatidae, or *Presbyornis* (parsimony KH test  $p > 0.05$ ; Supplementary Appendix C4; Discussion) or these and Pan-Anseriformes by likelihood KH test.

### 5.4. Dataset 4

Dataset 4 recovered *Anachronornis* nov. gen. in a monophyletic Anseres (BS = 92%, CI = 0.95, RI = 0.95) as sister to Anatidae including *Dendrocygna* to the exclusion of *Anseranas* (BS = 78%; Figure S10; Supplementary Appendix D3). It was not possible to exclude the parsimony-optimized tree for the KH test because there were too few taxa to construct constraint trees that differed from it. Therefore,  $p$  values should be doubled in the parsimony KH test, in which the “best” tree was the MP tree, to make it a one-tailed test [103]. There was no significant difference between “best” trees calculated using either parsimony or likelihood and any tree in which *Anachronornis* nov. gen. was constrained as sister to all Anseriformes, Anhimidae, Anseres, *Anseranas*, or Anatidae ( $p > 0.05$ ; Supplementary Appendix D4).

### 5.5. Dataset 5

Dataset 5 recovered *Anachronornis* nov. gen. as sister to Pan-Anseres (BS = 87%, CI = 0.64, RI = 0.75; Figure S10; Supplementary Appendix E2). However, trees in which *Anachronornis* nov. gen. was constrained as sister to Anhimidae or to all Anseriformes were not significantly different from the optimal tree by the parsimony KH test ( $p > 0.05$ ; Supplementary Appendix E3). Likelihood KH tests did not exclude many other positions as significantly different, including those in which *Anachronornis* nov. gen. was sister to *Presbyornis*, crown-Anatidae, and some outgroups of Anseriformes.

### 5.6. Dataset 6

There were no topological differences among Anseriformes in analyses of dataset 6 run with or without *Vegavis*, which itself was scored for only 10 characters, except that the position of *Anachronornis* nov. gen. was less resolved in the bootstrap tree that included *Vegavis*. In optimal MP trees (CI = 0.64, RI = 0.76 with or without *Vegavis*), *Anachronornis* nov. gen. was recovered within Pan-Anseriformes (BS = 94%), as sister to Pan-Anseres (BS = 78%; Figure S11; Supplementary Appendices F4 and F5). *Vegavis* was sister to flamingos within Neoaves when it was included. The addition of *Nettapterornis* to dataset 6 resulted in little difference in KH test results from those of dataset 5 (Supplementary Appendices F6 and F7). Trees in which *Anachronornis* nov. gen. was sister to Pan-Anseriformes (“best”) were not significantly better than those in which it was sister to either Pan-Anseres or Anhimidae. Pan-Anseriformes and *Vegavis* was reduced to a polytomy in the only three constraint trees in which *Vegavis* was included, because the paucity of characters on which *Vegavis* could be scored might result in spurious results for the multitude of positions in which it could be placed. With *Vegavis* included, trees in which *Anachronornis* nov. gen. was sister to either crown- or Pan-Anseriformes were not significantly different from that in which *Anachronornis* nov. gen. was sister to Anhimidae (parsimony KH  $p > 0.05$ ) or to crown-Anseres (likelihood KH  $p > 0.05$ ). Accordingly, the only BS support *Anachronornis* nov. gen. received was for inclusion in Pan-Anseriformes, excluding *Vegavis*. With *Vegavis* excluded, trees in which *Anachronornis* nov. gen. was sister to Anhimidae or Pan-Anseriformes were

not significantly different than its position in the MP tree, in which *Anachronornis* nov. gen. was sister to Pan-Anseres (but excluded from it, BS = 91%).

5.7. Dataset 7

One parsimony and three Bayesian analyses were performed on dataset 7 in which *Anachronornis* nov. gen. was added to Field et al.'s 39 taxon, 297 (290 PI) character dataset as modified [20,43,92], with *Ichthyornis* designated as an outgroup.

5.7.1. Phylogenetically Constrained Parsimony Tree

Parsimony analysis in which neotaxa were phylogenetically constrained produced three optimal trees that differed from one another only in the positions of *Asteriornis*, *Gallinuloides*, and crown-Galliformes relative to one another. In the strict consensus tree, *Anachronornis* nov. gen. was recovered as monophyletic with *Vegavis* and sister to Pan-Anseriformes (CI = 0.2624, RI = 0.5839, Figure 9, Supplementary Appendix G8). Anhimidae was sister to a monophyletic stem-Anseres and crown-Anseres. Pelagornithids were recovered as sister to all Neognathae. None of these relationships except the grouping of pelagornithids with Neognathae received BS ≥ 50%.

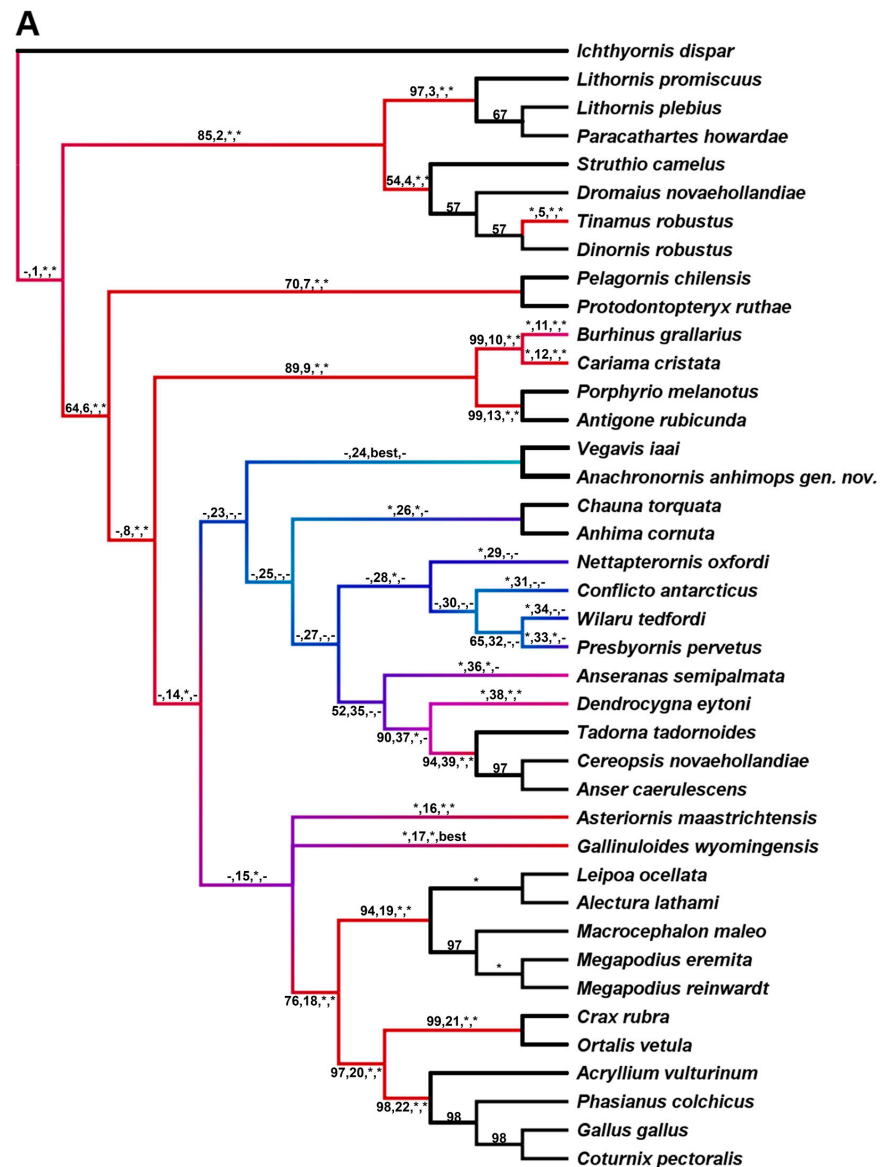
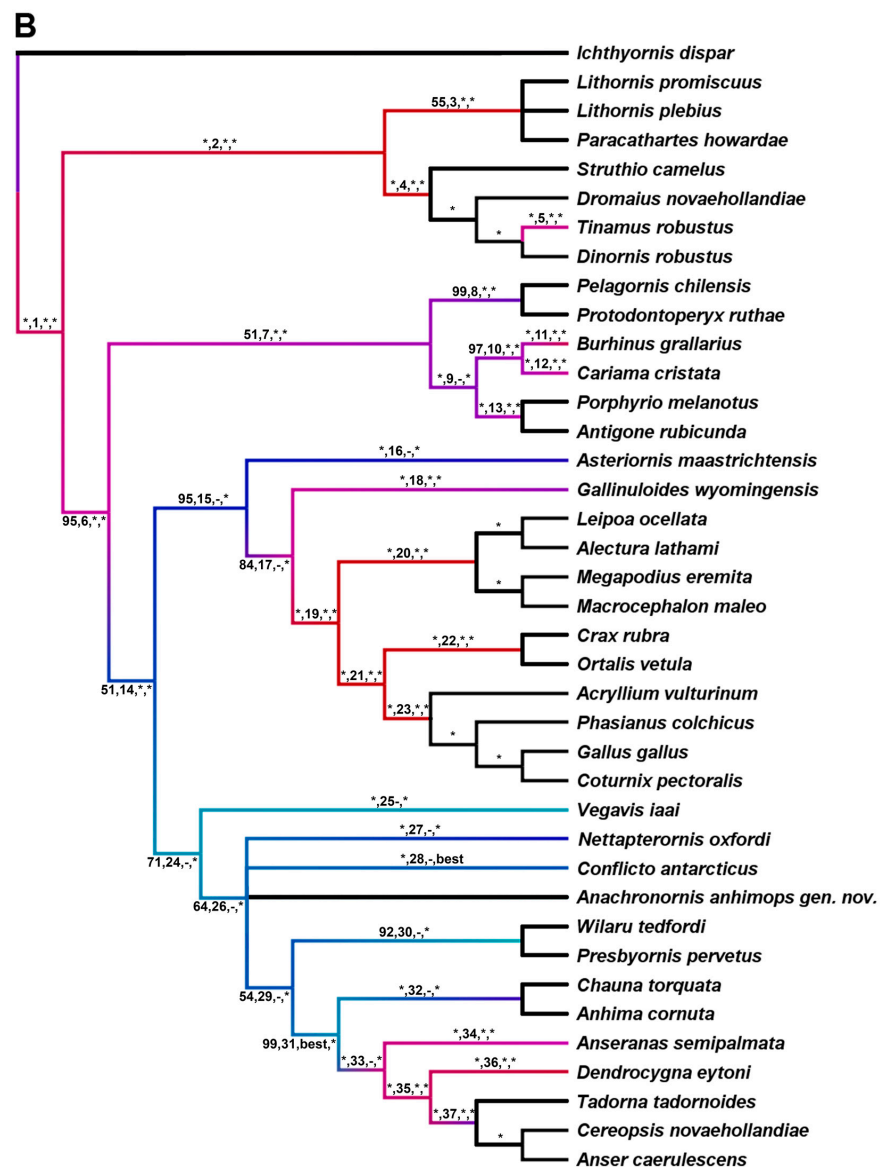


Figure 9. Cont.



**Figure 9.** Phylogeny reconstructions of dataset 7. Phylogenetically constrained maximum parsimony tree (A), and the phylogenetically constrained total-evidence (tip-dated) Bayesian tree (B). Graduated branch colors are proportional to *p* values determined by parsimony Kishino–Hasegawa (KH) test (blue, high *p*, i.e., not significantly different than “best”; red, low *p*, i.e., significantly different than “best”; black, not tested) wherein *Anachronornis* nov. gen. is moved from the position shown to each of the colored branches defined by constraint trees. Branch color in B is relative to the position of *Anachronornis* nov. gen. on tree 53, which was ranked “best” when 15 alternative backbone trees were included (tree 53: *Vegavis* sister to Neornithes, *Anachronornis* nov. gen. sister to Anhimidae plus Pan-Anseres; see Table S6, Supplementary Appendix G9 for details). Branch annotations separated by commas are as follows: (1) support value ((A) bootstrap; (B) posterior probability; “\*” indicates support of 100%; “-” indicates support below 50%), (2) constraint tree number (note: (A) and (B) differ), (3) result of parsimony KH (“-” indicates no significant difference from “best” (*p* > 0.05), “\*” indicates a significant difference from “best” (*p* < 0.05)), and (4) result of likelihood KH test, normal approximation, equal rates (“-” indicates no significant difference from “best” (*p* > 0.05), “\*” indicates a significant difference from “best” (*p* < 0.05)). See Supplemental Material, Table S6 (A) and Table S7 (B) and Appendices G9, G11, and G13–G15 for these and additional KH constraint trees and KH scores. Single labels on black branches represent bootstrap (A) or posterior probability (B).

Alternative trees that did not differ significantly from the MP tree were as much as 12 steps longer and demonstrated log likelihood ( $-\ln L$ ) differences up to 12.72239 (Table S6, Supplementary Appendix G9). All of these identified by parsimony KH placed *Anachronornis* nov. gen., *Vegavis*, and Anhimidae in basal positions of Pan-Anseriformes and/or *Anachronornis* nov. gen. sister to or within stem-Anseres. Additional trees identified by likelihood KH as not significantly different from the MP tree placed *Anachronornis* nov. gen. almost anywhere relative to *Vegavis*, Pan- or crown-Anseriformes, *Gallinuloides*, or Galloanseres, including *Asteriornis* but not pelagornithids.

#### 5.7.2. Fully Unconstrained Bayesian Tree

Fully unconstrained Bayesian analysis recovered *Anachronornis* nov. gen. in a polytomy with *Vegavis*, Anhimidae, and Pan-Anseres (PP = 91%; Figure S12; Supplementary Appendix G10). *Wilaru*, *Presbyornis*, *Conflicto*, and *Nettapterornis* formed a monophyletic group (PP = 52%) that was sister to crown-Anseres (PP = 59%). Pelagornithids were recovered as sister to Neoaves plus Pan-Anseriformes (PP = 88%). Palaeognathae were recovered as paraphyletic to Galliformes, *Asteriornis*, and *Gallinuloides*.

The fully unconstrained Bayesian tree, itself, was significantly different than “best” trees identified by likelihood KH ( $p < 0.01$ ) in all but the likelihood normal approximation with gamma rates (Supplementary Appendix G11). Alternative trees that did not differ significantly from the “best” as defined by parsimony and likelihood KH tests, respectively, included trees up to eight steps longer and log likelihood ( $-\ln L$ ) differences up to 13.78298. The fully unconstrained Bayesian tree differed from “best” by  $-\ln L$  7.54397 using the likelihood normal approximation with gamma rates.

Collectively, the trees identified by KH tests as not significantly different than “best” were those in which *Anachronornis* nov. gen., *Vegavis*, and Anhimidae were placed in basal positions of Pan-Anseriformes and/or *Anachronornis* nov. gen. was sister to or within stem-Anseres. However, in addition, likelihood KH tests also identified the placement of *Anachronornis* nov. gen. sister to crown-Anseres or to *Antigone* among Neoaves as “best” or not significantly different from “best”.

#### 5.7.3. Phylogenetically Unconstrained Total-Evidence Bayesian Tree

Phylogenetically unconstrained total-evidence (tip-dated) analysis recovered *Anachronornis* nov. gen. as sister to Pan-Anseriformes, not including *Vegavis* (PP = 66%, Figure S12; Supplementary Appendix G12). *Conflicto*, *Nettapterornis*, *Presbyornis*, and *Wilaru*, respectively, formed a paraphyletic grade to crown-Anseriformes (PP = 57–91%). *Vegavis* was recovered as sister to all of these, including *Anachronornis* nov. gen. (PP = 63%). Pan-Anseriformes, *Vegavis*, pelagornithids, and Neoaves formed a clade (PP = 56%) in a polytomy with Palaeognathae and Galliformes plus *Asteriornis* and *Gallinuloides* (PP = 52%).

The phylogenetically unconstrained total-evidence Bayesian tree was not recovered as “best” by any KH test, but it never differed significantly from “best” (Supplementary Appendix G13). Alternative trees that did not differ significantly from the total-evidence phylogenetically unconstrained Bayesian tree included trees up to 12 steps longer and  $-\ln L$  differences up to 12.51478 (parsimony and likelihood KH tests, respectively). All KH tests unanimously found the following trees as not significantly different than “best”: (1) trees uniting *Vegavis* with Pan-Anseriformes, (2) all stem-Anseres in more basal positions than Anhimidae, and (3) *Anachronornis* nov. gen. as basal among Pan-Anseriformes including *Vegavis* or (4) as sister to or among stem-Anseriformes or (5) sister to crown-Anseres, or (6) sister to Pan-Galliformes including *Asteriornis*. Parsimony KH identified even more distant positions of *Anachronornis* nov. gen. as not significantly different than “best”, including as sister to *Ichthyornis*, Neornithes, crown-Galliformes plus *Gallinuloides*, pelagornithids, or Neoaves. Similarly, likelihood KH found additional widespread positions of *Anachronornis* nov. gen. as not significantly different than “best”, including as sister to Palaeognathae, *Asteriornis*, *Anseranas*, and *Dendrocygna* plus Anatidae.

#### 5.7.4. Phylogenetically Constrained Total-Evidence Bayesian Tree

In total-evidence (tip-dated) analysis in which neotaxa and *Dinornis* were phylogenetically constrained (Figure 9; Supplementary Appendix G16), *Anachronornis* nov. gen. was recovered in a four-way polytomy (PP = 64%) with *Conflicto*, *Nettapterornis*, and crown-Anseriformes plus Presbyornithidae (PP = 54%), to which *Vegavis* was sister (PP = 71%). Pelagornithids were recovered as paraphyletic to Neoaves (PP = 51%), and *Asteriornis* and *Gallinuloides* were paraphyletic to Galliformes (PP = 84–95%).

The phylogenetically constrained total-evidence Bayesian tree shown in Figure 9B was not recovered as “best” by the parsimony KH test, but it did not differ significantly from it (Supplementary Appendix G14). Alternative trees that did not differ significantly from the Bayesian tree were as many as six steps longer or seven steps shorter. Parsimony KH found no significant difference between “best” and 27 alternative trees in which *Anachronornis* nov. gen. was sister to or nested within every higher group except crown-Anseres and at every level of the tree from Palaeognathae to Anhimidae. *Vegavis*, too, was consistently recovered as not significantly different than “best” when it was sister to or nested within various higher groups at every level of the tree from Neornithes to crown-Anseres. No significant difference was found by parsimony KH among trees in which *Vegavis*, stem-Anseres, Anhimidae, and crown-Anseres exchanged positions relative to one another. In contrast, all likelihood KH tests recovered *Anachronornis* nov. gen. as sister to Palaeognathae as “best” and all other trees as significantly different from it ( $p < 0.01$ ).

## 6. Discussion

### 6.1. Phylogenetic Analysis

We consider phylogenies in which *Anachronornis* nov. gen. was not recovered as sister to or within Pan-Anseriformes to be implausible (e.g., dataset 1) because it exhibits a combination of characters that are unique to Anseriformes, among neotaxa. These characters include the fusion of the zygomatic and orbital processes, resulting in a vacuous tympanic cavity, bicondylar quadrate with submeatic prominence or “pars quadratojugalis”, a large recurved retroarticular process, and large laterally positioned tuberosity for the insertion of the AME muscle.

Our chief phylogenetic conclusion is that *Anachronornis* nov. gen. is basal relative to crown-Anseriformes. However, its placement and support relative to paleotaxa are sensitive to the choice and inclusiveness of taxa and characters. Different datasets yielded mutually incongruent optimal positions of *Anachronornis* nov. gen. within crown-Anseriformes (Figures S9–S11; datasets 3–6), while others did not recover *Anachronornis* nov. gen. within crown-Anseriformes at all (datasets 1, 2, and 7). Adding to the uncertainty, BS and PP support values were low and KH tests showed that alternative constrained placements of *Anachronornis* nov. gen. were not significantly different from one another using any single dataset. We favor the results that accrued from dataset 7 because of its inclusiveness of relevant taxa and large number of characters.

Parsimony and/or likelihood KH tests found no significant difference from “best” among some if not many alternative placements of *Anachronornis* nov. gen. in all analyses of dataset 7 ( $p > 0.05$ ). Likelihood KH tests, involving equal vs. gamma distributed rates and normal approximation vs. bootstrap replicates, generally yielded different absolute  $p$  values but qualitatively similar rankings. Sometimes they did not. See Supplementary Appendices G9, G11 and G13–G15 for full details. The inclusion or exclusion of five updated characters for *Vegavis* [92] also affected the KH test results.

Loosely interpreted, alternative trees not rejected by KH tests are not significantly different than the “best” tree, but there are caveats. KH tests are not optimized phylogenetic reconstructions. Both are subject to the applicability of explicit and implicit methods, models, and assumptions that may skew results. This was manifest in the different results obtained by our phylogenetic analyses versus parsimony KH versus likelihood KH tests. Many “best” trees recovered by parsimony KH or by likelihood KH tests were not the same as the ones recovered by MP or Bayesian analyses, respectively. Both Bayesian phylogenetic



reconstruction and the KH test were originally designed for the analysis of nucleotide data, the coding and transformation properties of which are much better understood and readily modeled than those of morphological data. Whereas parsimony analysis employs the optimality criterion of tree length, parsimony KH is generally correlated with tree length, but not perfectly. On the other hand, the likelihood KH tests we used employed the Markov k model (Mkv), which does not accommodate the ordering of character state transformations. Other assumptions apply.

It is unsurprising that these methods of phylogenetic analysis were unable to resolve the relationships of fossils that may represent lineages close to the divergence of subsequently well-differentiated clades, but it is somewhat of an indictment of some datasets that provided seemingly strong support for incongruent phylogenies. The ambiguous relationships of *Anachronornis* nov. gen. suggest that it probably branched off very close to the divergence of the Anhimae and Anseres clades, regardless of which clade it is actually a member of, if either. This conclusion is, in fact, best supported by the most inclusive dataset, 7 [20,43], whether analyzed using phylogenetically constrained parsimony or Bayesian methods (backbone of neotaxa following Worthy et al. and Field et al. [20,43]). Bayesian analysis is alleged to be superior to parsimony in instances of relatively high homoplasy [118], but results are sensitive to the selection of priors. Among the Bayesian analyses we performed, we favored age-calibrated tip-dating used in our total-evidence analyses, consistent with the previous observations [43,119], because the monophyly of known clades, Palaeognathae, Neognathae, Galliformes, Anseriformes, and Neoaves, were each recovered even without imposing phylogenetic constraints (Figure S12). The fact that there are substantial numbers of putative apomorphies supporting alternate positions of *Anachronornis* nov. gen. as sister to Anseriformes, Anhimae, and Anseres, respectively, is further evidence in support of its true position very close to the divergence of the latter two (Supplemental Materials, Appendices A3, B2, C2, D2, F3, G6 and G7).

A new family is erected for *Anachronornis anhimops* nov. gen. et sp. because phylogenetic analyses do not unambiguously resolve whether it represents a stem lineage of Anhimidae or of Anseres or of Anseriformes. The familial level of distinction is consistent with the treatment of other stem-Anseriformes, with which *Anachronornis anhimops* nov. gen. et sp. shares distinctive differences from neotaxa of Anseriformes. Collectively, the London Clay specimens slightly more resemble modern screamers than does *Anachronornis* nov. gen. due to cranial characters and their stockier build. Nevertheless, a greater number of putative apomorphies of dataset 1 support the position of *Danielsavis* nov. gen. as sister to either Anseriformes or to Anseres than to Anhimidae (Supplemental Materials). Additionally, when treated as monophyletic, an equal number of unambiguous apomorphies of dataset 1 unite *Anachronornis* nov. gen. and *Danielsavis* nov. gen. with either Anhimidae or Anseres. The London Clay specimens are also more consistent with Anachronornithidae nov. fam. than with Anhimidae. Depending on their position relative to other Anseriformes, as many as 9 unambiguous and up to 32 total putative apomorphies of dataset 1 support the monophyly of *Anachronornis* nov. gen. and *Danielsavis* nov. gen., which suggests that they may be best included in the same family (Supplemental Materials, Appendix A3).

The differences between the North American and slightly younger European fossils could reflect an evolutionary trend in the acquisition of characters exhibited by modern screamers along an essentially direct lineage that is paraphyletic to crown-Anhimidae. If screamers were derived from more Anseres-like ancestors [2,15], then they would not necessarily have been relics in their time. Far more likely, the differences among these fossils simply exemplify diversity among stem-Anseriformes, with differential segregation and retention of primitive characters in extant clades that are not individually indicative of direct lines of ancestry or descent [120]. In either case, individual variation may be a source of misleading phylogenetic signals. For example, some of the characters used here to diagnose Anachronornithidae nov. fam. may be related to ontogeny in extant screamers (i.e., narrow supraorbital region) or other Anseriformes (i.e., unfused lacrimals).

Nevertheless, USNM 496700 shows no overt lack of cranial fusion definitively indicative of immaturity.

## 6.2. Character Distributions of the Datasets

Of course, the perceived number of apomorphies in support of any relationship is dependent on the selection of taxa compared and their positions in a reconstruction. The selection and definition of characters in a given dataset is generally tailored towards resolving the relationships of a particular taxon. For example, dataset 3 was focused on the position of *Presbyornis*. There were either 10 or no putative apomorphies supporting the sistership of *Anachronornis* nov. gen. with *Anseres* solely depending on whether *Presbyornis* was included within it (Supplemental Materials, Appendix C2). Thus, neither the number nor the consistency of putative apomorphies supporting the position of *Anachronornis* nov. gen. is directly comparable across datasets.

Since multiple putative apomorphies can be cited in support of most alternative reconstructions of *Anachronornis* nov. gen., defining those that most appropriately apply is a question of tree optimization. The principle of parsimony holds that the simplest explanation of character evolution should be favored, but the very existence of homoplasy is evidence that evolution is not always direct. We demonstrate using KH tests that alternate reconstructions from the optimal cannot be rejected. Moreover, in almost all datasets the fully optimized phylogenetically unconstrained trees should be rejected because they are incongruent with currently accepted phylogeny of neotaxa. Since all phylogenies merely represent evolutionary hypotheses, putative apomorphies in support of relationships in alternative phylogenies that cannot be rejected should be given full consideration. Failure to do so constitutes the incomplete presentation of results at best, or mere statements of opinion at worst.

We quantified uniquely and non-uniquely shared characters between *Anachronornis* nov. gen. and/or *Danielsavis* nov. gen. with one another and other taxa in an effort to determine whether the differences among the phylogenetic analyses of datasets 1–7 were influenced by the balance of cranial versus postcranial characters in the datasets for which the fossils could be scored (Supplementary Appendices A12, B5, C5, D5, F8 and G17).

There are two different reasons why cranial and postcranial characters might not contribute equally. The first is biological and has been a thesis of phylogenetic inference, i.e., that cranial characters are more stable and more reliable indicators of phylogeny. The second is a reflection of the dataset. There may be an imbalanced number of cranial and postcranial characters in any given dataset, either because they were not defined or because they might be missing in fossils. The latter is particularly relevant when comparing fossils to one another, because between the two there may be few if any that are not missing in one or the other. For example, there is no known hindlimb of *Nettapterornis*. Therefore, we considered the percentage of shared characters out of the total number of cranial or postcranial characters that are scorable in the pair of taxa being compared, in addition to the absolute number of shared cranial or postcranial characters.

We summarized uniquely and non-uniquely shared characters independently. The former are valuable as potential synapomorphies that are evidence of relatedness. Yet, they may not be recovered as apomorphies of a tree that is globally optimized for a preponderance of conflicting data (e.g., dataset 1, character 74). On the other hand, characters recovered as apomorphies may be shared non-uniquely. Non-uniquely shared characters more likely represent plesiomorphies or homoplasies that are ostensibly not valuable for inferring phylogeny, but still contribute to gestalt, which has historically influenced taxonomy. This is particularly evident in the optimal parsimony trees of datasets 1–3 that included neoavian outgroups.

There were few pairwise comparisons of taxa in any datasets in which the percentage of either cranial or postcranial characters exceeded the other by 20% and in which the characters of both taxa could be scored. This suggests that differences in phylogenetic results were derived from differences in defined characters, rather than whether the fossils

could be scored for those characters. The exceptions included comparisons of *Anachronornis* nov. gen. with *Burhinus* in datasets 1 and 7, with *Phoenicopterus* in dataset 3, and crown-Anseres in dataset 6. In all of these, the percentage of scorable shared postcranial characters exceeded the cranial characters by more than 20%. The disproportionate absolute number and percentage of postcranial characters shared by *Anachronornis* nov. gen. and *Burhinus* or *Phoenicopterus* are inferred to be primitive or homoplasious, but they may account for their attraction in phylogenetic analysis. In contrast, a disproportionate absolute number of characters of dataset 1 shared by *Anachronornis* nov. gen. and Anseres are cranial.

### 6.3. Neornithine Sympleiomorphies

O'Connor [105,106] interpreted large conspicuous lateral cavities of the thoracic vertebral bodies such as that exemplified by *Anachronornis* nov. gen. as impressions of pulmonary diverticula, although Mayr [108] disputed this interpretation, making a distinction between pneumatic foramina, pleurocoels, pulmonary diverticula, and lateral openings that are not traversed by air passages. While the associated morphologies are considerably varied in their extreme forms, it is clearly not possible to confidently distinguish the roles of the cavities or foramina of intermediate morphologies without the benefit of soft tissues to examine. The cavities in *Anachronornis* nov. gen. are suggestive of an early evolutionary stage of the development of the highly pneumatized vertebrae of extant screamers because the more constricted aperture of more caudal vertebrae progressively resembles pneumatic foramina, and because *Anachronornis* nov. gen. exhibits additional foramina in transverse processes of thoracic vertebrae that both closely resemble the cavities of vertebral bodies as well as the foramina of extant anhimids that are accepted as being pneumatic foramina. Although this character might appear to be a synapomorphy uniting *Anachronornis* nov. gen. with Anhimidae, the widespread occurrence of this character in numerous unrelated extant and extinct, including Mesozoic, birds (i.e., *Confuciusornis*, *Ichthyornis* Marsh, and various Enantiornithes [81,121,122]) suggests instead that the character is a sympleiomorphy of Neornithes. This character is exhibited by other related (e.g., *Presbyornis* and *Telmabates* [10] and *Nettapterornis* [55]) and unrelated early Paleogene birds [108]. Among living birds, it most closely resembles the condition of *Puffinus* (Procellariiformes), suggesting alternatively that it is homoplasious.

Other potential sympleiomorphies of Neornithes exhibited by *Anachronornis* nov. gen. include the rostrocaudally compressed mandibular process of the quadrate (i.e., absence of caudal condyle), costae with uncinat processes, sternum with an external spine and short cranially positioned costal margin, and long bowed femur. These traits are typical of Enantiornithes and other Mesozoic birds [123], as well as other early diverging Neornithes, the Lithornithiformes, Tinamiformes, and Galliformes.

### 6.4. Comparison to *Presbyornis*, *Nettapterornis*, and *Conflicto*

Inasmuch as *Anachronornis* nov. gen. differs significantly in bill morphology from *Presbyornis* and *Nettapterornis*, and from *Presbyornis* in limb proportions, they were clearly dissimilar in their feeding specializations and ecologies. Thus, whatever characters they do share are likely typical of early Anseriformes rather than convergent. *Anachronornis* nov. gen. is similar to *Presbyornis* and *Nettapterornis* (and *Conflicto* [15] (Figure 3)), in its extensive ventrally facing pseudotemporal fossa, short cranially directed postorbital process, and dorsoventrally broad retroarticular process (Figures S2 and S5). The squamosal region, including the ventrally facing pseudotemporal fossa and short cranially directed postorbital process, are of particular interest because the condition in *Anachronornis* nov. gen., *Presbyornis*, and *Conflicto*, resembles that of extant Anhimidae. This contrasts sharply with the narrow and rostrally elongate postorbital process of *Nettapterornis* and most extant Anseres. However, like anhimids, *Anachronornis* nov. gen. does not exhibit the dorsally extensive impressions of AME articularis and particularly depressor mandibulae muscles on the caudolateral surface of the neurocranium that are present in *Presbyornis*, *Conflicto*, *Nettapterornis*, and other Anseres.

Other traits shared among these fossils are lateral concavities of thoracic vertebrae, humerus with excavated tricipital and brachial fossae and broad pectoral crest, broadly bowed furcula that lacks a large hypocleideum and has pointed omal extremities, coracoid with long flared medial and lateral angles and bears a foramen of the supracoracoid nerve, broad pelvis with equally long preacetabular and postacetabular parts, and tibiotarsus with a cranially pronounced cranial cnemial crest and short fibular crest. The skeletons of *Anachronornis* nov. gen. and *Presbyornis* are poorly pneumatized, as is the Oligo-Miocene fossil screamer *Chaunoides* [34]. Thus, extensive skeletal pneumatization may be a relatively recently evolved autapomorphy of crown-screamers.

Differences of *Anachronornis* nov. gen. from the aforementioned include its more rounded neurocranium without ventrally pronounced exoccipitals. Impressions of the origin of the mandibular depressor muscles are faintly visible at best, whereas they are pronounced in *Presbyornis* and *Conflicto* and even deeper and wider in *Nettapterornis*. The occipital condyle is small and the foramen magnum is positioned centrally, i.e., with a relatively equal area of muscle insertions laterally as dorsally. The mandible has a shallow caudal fossa, the medial and lateral sternal angles of the coracoid are not as acute and its procoracoid process is positioned more sternad, the humerus possesses a smaller caput, larger dorsal tubercle, shorter bicipital crest, and neither the tricipital nor brachial fossae are as excavated, the head of the femur is much larger, and the tarsometatarsal trochleae are broader. The pelvic appendages of *Anachronornis* nov. gen., the Green River Formation and London Clay fossils referenced herein, and *Perplexicervix* are much shorter than those of the long-legged wader *Presbyornis*.

*Nettapterornis*, presbyornithids, and/or *Vegavis* have been described as similar to or even mistaken for Charadriiformes or Phoenicopteriformes [10,30]. *Anachronornis* nov. gen. shares similar postcranial attributes (Figures S6 and S7, Supplementary Appendices A12, B5, C5, D5, F8, and G17). There is no doubt that stem-Galloanseres pre-dated the Paleogene, and Phoenicopteriformes are members of a supraordinal clade (Phoenicopterimorphae or Columbea) that may have also diverged from other Neoaves pre-Paleogene [4,7]. It is far more questionable whether Charadriiformes had also diverged by this time, as they are not believed to be among the most basal lineages of Neoaves. Regardless, postcranial remains resembling Charadriiformes are relatively well-represented among isolated and fragmentary elements near the Cretaceous–Paleogene boundary [52]. *Anachronornis* nov. gen. and *Presbyornis* demonstrate that incomplete fossils of Anseriformes could mislead inference that crown-Charadriiformes were present in the Cretaceous even if they were not, or that crown-Charadriiformes were either sister or paraphyletic to clades that they are not. Charadriiform-like or phoenicopteriform-like postcranial characters may simply represent homoplasious adaptations to an aquatic lifestyle [30]. Crown-Charadriiformes also may have retained some such characters from very distantly related aquatic forebears.

*Anachronornis* nov. gen. exhibits galliform-like characters that distinctly differ from those of most Charadriiformes. These include the narrow supraorbital region, the pedicellate basipterygoid processes, the lack of the zygomatic process or its fusion with the postorbital processes, absence of occipital fontanelles, extremely narrow mandibular condyles of the quadrate, pronounced coronoid and retroarticular processes of the mandible, short generalized bill, and attributes of the femur, even though many differ in sufficient detail to warrant coding as separate states.

Fossil “mosaics” implicitly exhibit characters that are seemingly diagnostic of two or more diverged or even unrelated neotaxa, but which in fact are plesiomorphies that have been differentially retained and lost in the neotaxa. If all birds share a common ancestry, then their most recent common ancestor must have been somewhat intermediate between or shared characters with even the most disparate of modern birds. Over time, different groups lost different subsets of these primitive characters. Neither crown-Galliformes nor crown-Charadriiformes were ancestral to Anseriformes, but the forebears of Anseriformes presumably exhibited what now might be mistaken as apomorphies of all three. Similarly, some of the characters used to diagnose *Anachronornis* nov. gen. as anseriform could

eventually prove to be symplesiomorphies of a larger and even more ancient clade. This might also be true of the purportedly derived anseriform characters of *Vegavis*.

#### 6.5. Character Polarity of the Spatulate Bill in Anseriformes

Since phylogenomic analyses resolve a sistership of crown-Galliformes and Anseriformes, and of Anhimae and Anseres, respectively [4–7], then it logically follows that the spatulate bill of Anseres represents a derived state. This is contrary to Olson’s hypothesis that screamers evolved from Anseriformes with spatulate bills, and that ridges on the palate of *Chauna* represent vestigial lamellae [2] (Figure 5). Ericson [10] further noted similarities of *Anachronornis* nov. gen. to both anhimids and Anseres. Like Olson and Feduccia [2], he inferred that the intermediacy of these characters was evidence that the fowl-like bill of screamers evolved from the lamellate bill of Anseres. Neither author justified his interpretation of character state polarity. Yet, in both cases, there is no more reason to assume that these “duck-like” attributes are primitive or vestigial legacies than there is to assume that they represent early stages in the evolution of duck-like characteristics. The latter view is very much in keeping with the observation that, apart from its spatulate bill, there is little evidence that *Presbyornis* was capable of the rapid piston-like protraction and retraction of the mandible necessary for advanced filter feeding [124]. *Presbyornis* had what Zelenkov and Stidham described as a more galliform-like than Anseres-like jaw apparatus, and they concluded that *Presbyornis* documents a “slow and stepwise evolution of the complex morphological traits and emphasize(s) a mosaic nature of intermediate forms”. We refine this statement to say that *Presbyornis* and *Conflictio*, whose bill was not markedly spatulate like that of *Presbyornis*, had a somewhat more *Anachronornis*-like jaw apparatus. This suggests that collectively these birds document the gradual evolution of duck-like traits, not the reverse. By themselves, *Presbyornis*, *Nettapterornis*, and *Conflictio* can provide little insight on the character polarity of Anseriformes more basal than Pan-Anseres if they are themselves Pan-Anseres, i.e., that Anhimae and Anseres are sister clades and neither is paraphyletic to the other (this paper) [20]. In contrast, *Anachronornis* nov. gen. could provide insight on the morphology of more basal Anseriformes if it could be unambiguously shown to be sister either to all Anseriformes or to Anseres, as it is in some of our phylogenetic analyses. Unfortunately, this result is not robust to all analyses. Even if it were, then *Anachronornis* nov. gen. does not conclusively resolve whether the condition is either plesiomorphic or instead a homoplasious reversal in extant Anhimidae. Some analyses recovered Anhimidae in a more derived position than *Conflictio*, *Nettapterornis*, and Presbyornithidae among Anseriformes, implying paraphyly of stem-Anseres to Anhimidae [15,20] (Bayesian total-evidence analyses only). None of our analyses unambiguously support that result, but if it is correct then it is still possible that future analyses might recover *Anachronornis* nov. gen. higher within Anseriformes than stem-Anseres.

#### 6.6. Ecology of *Anachronornis* nov. gen.

Calcareous nodules, in which the holotype of *Anachronornis anhimops* nov. gen. et sp. was fossilized, characterize the more northerly wetter Clark’s Fork deposits of the Bighorn Basin. These represent wet temperate–subtropical forests, forested floodplains, and overbank deposits [125]. Although the presence of fine clastics (<1 mm) is not unusual in non-fossiliferous nodules from the area, their presence in the nodular matrix of the holotype of *Anachronornis anhimops* nov. gen. et sp. is atypical of calcareous nodules of the Clark’s Fork deposits from which fossil birds have been previously described [113,126]. The clastics are suggestive of a somewhat larger and more active depositional body of water, such as the edge of a stream, than is typical of fossiliferous nodules of the area that more likely formed in forested floodplains [127]. *Anachronornis* nov. gen. is also unusual in that it is the only probably aquatic or semi-aquatic bird yet discovered in calcareous nodules of this area. In contrast, while Lithornithiformes may have probed shorelines with their sensitive bills [126,128], they and all other birds yet known from the calcareous nodules are presumed to have been either arboreal or terrestrial [113,129,130]. Indeed, the identifiable

fossil vertebrates (i.e., sandcoleids, mammals, and a squamate lizard) associated with *Anachronornis anhimops* nov. gen. et sp. in the same nodule are arboreal and/or terrestrial.

The fragmentary nature of hindlimb elements of *Anachronornis* nov. gen. largely precludes inferences about its locomotory and foraging behavior based on limb proportions. Detailed morphometric analysis of the features of individual bones [131] has the potential to complement or even obviate inferences based on length ratios, but such an analysis is beyond the scope of this paper. Instead, the inferences below are gestalt comparisons made by reference to osteological specimens of modern birds of generally well-characterized behaviors. The risk, as with even the most statistically robust approaches, is that phylogenetic constraints and/or behavioral plasticity may obfuscate the true behaviors or breadth behaviors of species that are “exceptions” within their clades. Moreover, there is broad overlap in the morphospace of birds with significantly different locomotory or foraging behaviors that even structured statistical analyses may fail to discriminate [131].

Some details of the morphology of the hindlimb of *Anachronornis* nov. gen. are superficially similar to those of inhabitants of shallow wetlands, such as ibises (*Plegadis*) and stone-curlews (*Burhinus*). The carina of the sternum of *Anachronornis* nov. gen. is moderately shallow as in Anseres. The pectoral appendage is of unremarkable length. The brachium and antebrachium are equal in length to one another, and the manus and alar digits are relatively short. The relative lengths of the preacetabular and postacetabular portions of the pelvis are similar to most Charadriiformes and modern screamers, and are unlike foot-propelled swimmers (e.g., Anatidae) in which the postacetabular portion is longer, or waders (e.g., Ardeidae) in which the preacetabular portion is longer. The femur of *Anachronornis* nov. gen. is similar to those of Galliformes and *Presbyornis* because it is long, slender, and curved and its head is very large. However, none of its other appendicular elements are similarly long as they are in *Presbyornis*. In fact, although the lengths of the tibiotarsus and tarsometatarsus of *Anachronornis* nov. gen. are unknown, the pelvic limb of *Danielsavis* nov. gen. and other early Eocene screamer-like birds treated herein are fairly short, to the extent that they are known. The tibiotarsus of the GRF specimen is about equal in length to the humerus or antebrachium, and it is about one and a half times the length of the femur, tarsometatarsus, or third (middle) pedal digit. The cranial cnemial crest of the tibiotarsus of *Anachronornis* nov. gen. is large and pronounced cranially, as in active walkers of wetlands (e.g., *Burhinus*, *Jacana*, *Aramus*, *Gallinula*), not proximally, as in swimmers/divers (e.g., Anatidae), or short like those of sedentary waders (e.g., Ardeidae) or of terrestrial walkers (e.g., Galliformes). Trochlea II of the tarsometatarsus is deflected caudally, proximally short, and the intertrochlear notches are narrow, all of which are typical of generalist aquatic birds and exaggerated in foot-propelled swimmers and divers. Its pedal digits appear to have been more gracile than those of terrestrial and arboreal birds and foot-propelled swimmers.

Ibis-like or stone-curlew-like characters of the hindlimb may suggest that *Anachronornis* nov. gen. may have inhabited wetlands or shallow waters, but its method of feeding differed considerably from theirs. Its diet may have been similar to those of modern screamers, given the similarity of bill and cranial morphologies. Modern screamers forage on succulent floating vegetation [114]. However, characters of the jaw apparatus such as the shallow caudal fossa of the mandible, pronounced coronoid/angular process, and expanded occipital protuberances associated with the origin of the depressor mandibulae muscle imply jaw mechanics that were intermediate between those of Anhimae and Pan-Anseres. Regardless, it is doubtful that *Anachronornis* nov. gen. was an efficient dabbler, because the paucity of neurovascular foramina suggest that its bill was poorly innervated.

A lack of postcranial pneumaticity is characteristic of the extant diving Anseriformes, *Thalassornis*, *Oxyura*, *Aythya*, and *Bucephala* [105], as well as diving non-Anseriformes, whose thoracic vertebrae bear large cavities that closely resemble those of *Anachronornis* nov. gen. It is perhaps coincidental that the diet of *Thalassornis*, i.e., aquatic vegetation, is similar to that of screamers [132]. However, *Anachronornis* nov. gen. lacks overt specializations for either wing- or foot-propelled diving, such as flattened wing elements, greatly

elongated postacetabular pelvis, short femur, proximally exaggerated cranial cnemial crest, or extremely deflected second trochlea of the tarsometatarsus. The widespread distribution of cavities in the thoracic vertebrae of unrelated fossil birds suggests that these vertebral features and lack of postcranial pneumaticity in *Anachronornis* nov. gen. are more likely retained primitive characters [108] rather than specializations for diving.

#### 6.7. Postorbital and Zygomatic Processes

In a study of the development of soft anatomy and associated cranial bones, Zusi and Livezey [76] concluded that the zygomatic process is lacking in Anseriformes. Zweers [133] details a somewhat more complicated picture of the muscles and aponeuroses of the region. Zusi and Livezey's conclusion contrasts with an alternate interpretation that the postorbital process is fused with the zygomatic process to form a "sphenotemporal process", as described by Dzerzhinsky [104]. Before it was established that Galliformes and Anseriformes were sisters in the Galloanseres clade, it may have been an important distinction whether (1) the homology of the osseous structure extending from the zygomatic bone to fuse with the distal extremity of postorbital process in Galliformes represented the zygomatic process or the aponeurosis of the AME muscle or (2) whether or not the postorbital and zygomatic process was fused to the postorbital or lost in Anseriformes, because both the fusion of said processes or the loss of the zygomatic process could represent a synapomorphy in evidence of their sistership. We note what appears to be a persistent suture, ventrally facing, between what appears to be the zygomatic process and the laterosphenoid of *Anachronornis* nov. gen. and *Nettapterornis* and inconsistently among extant Anseriformes (Figure S2). It is also clear from the examination of immature specimens (Figure S3) and even the illustrations of Zusi and Livezey [76] that the squamosal bone itself is continuous with the ventral margin of the postorbital process in *Chauna* and *Anhima*. While we do not question that the ossified aponeurosis of the AME contributes to the ventrolateral margin of the squamosal in extant Anhimidae, we assert that whether the ventrorostral portion of the postorbital process comprises the body of the squamosal bone or instead by the zygomatic process is largely a question of interpretation or semantics, and of moot distinction. In either case, the AME muscle arises from it.

## 7. Conclusions

We describe a new family, genus, and species of Anseriformes (Anachronornithidae: *Anachronornis anhimops* nov. fam. nov. fam. et gen. et sp.) from the latest Paleocene/earliest Eocene of the Willwood Formation of Wyoming, as well as similar yet distinct specimens from the early Eocene of the Green River Formation of Wyoming and the from London Clay Formation that include one newly described (familia incertae sedis: *Danielsavis nazensis* nov. gen. et sp.) and one or more undescribed species. These birds all possess a superficially screamer-like skull, but they exhibit a mosaic of screamer-like and duck-like characters. Collectively, these fossils straddle the PETM, a brief period renowned for terrestrial mammal faunal turnover [134–137] for which there has been little attention given to birds.

Among the fossils newly described herein, the London Clay specimens are collectively more similar to crown-Anhimidae than is Anachronornithidae nov. fam. because the supraorbital region is broader, the mandible is uniformly dorsoventrally slender and decurved, the tubercle of the external head of the AME articularis is small and positioned dorsally and lacks crests that circumscribe a caudal fossa, the hepatic part of the sternum extends an unknown distance caudal to the carina and the carina is deep, the coracoid may possess a pneumatic foramen in the fossa of the sternocoracoideus muscle, the humerus is stouter, tarsometatarsal trochleae II and IV are subequally elevated and trochlea II is not strongly deflected caudally, and although the unguals of Anachronornithidae are unknown, the ungual of the ostensible digit I is long and relatively straight. Anachronornithidae, on the other hand, is more similar to Anseres than are the London Clay specimens with regard to all of the aforementioned characters. These differences could be interpreted alternatively to suggest that Anachronornithidae and the London Clay group are each

sister to Anseres and Anhimidae, respectively, that they are representative of a paraphyletic grade leading to either one or the other, or that they are sister to both. Our phylogenetic analyses suggest that these birds, together with presbyornithids, *Conflicto*, *Nettapterornis*, and possibly *Vegavis*, are parts of a much larger diversity and ever-increasing record of basal Anseriformes that collectively are sisters to crown-Anseriformes and close to the divergence of Anhimae and Anseres.

The pseudotemporal fossa and postorbital process of *Anachronornis* nov. gen. is remarkably similar to that of *Presbyornis*, which assuredly influenced their jaw mechanics; yet, *Anachronornis* nov. gen. is dissimilar to all sufficiently known early Paleogene Anseriformes in its screamer-like bill morphology, and hence feeding specialization. *Anachronornis* nov. gen. is similar to *Presbyornis* in some charadriiform-like aspects of postcranial anatomy, although it was clearly not as long-limbed, and it also exhibits a host of fowl-like characters. The fact that *Anachronornis* nov. gen. and *Presbyornis* are not ecologically similar suggests that the postcranial characters that they do share are plesiomorphies of Anseriformes, rather than convergently evolved. The wader-like proportions and the ecology used to diagnose Presbyornithidae [2,8] are autapomorphies, rather than primitive character states of either Anseriformes or Neoaves in general [30]. Moreover, because no members of the putative Vegaviidae are currently known to have possessed lamellate or spatulate bills [44], advanced filter feeding cannot be assumed to be present in even stem-Anseriformes by the Maastrichtian. The significance of this relates to whether the bill of screamers is a reversal to a more fowl-like state [2] and consequently whether crown-screamers diverged relatively late from more “typical” Anseriformes [15].

**Supplementary Materials:** The following supporting information can be downloaded at: <https://www.mdpi.com/article/10.3390/d15020233/s1>, Figure S1: Comparison of *Anatalavis rex* and *Nettapterornis oxfordi*; Figure S2: Details of the laterosphenoid and squamosal, postorbital and zygomatic processes; Figure S3: Skulls of *Anhima cornuta*; Figure S4: Quadrates of *Danielsavis nazensis* nov. gen. et sp. and other London Clay specimens; Figure S5: Comparison of skulls, mandibles, sterna, furculae, and pelves of select Anseriformes and outgroups; Figure S6: Comparison of pectoral elements of select Anseriformes and outgroups; Figure S7: Comparison of pelvic elements of select Anseriformes and outgroups; Figure S8: Phylogenetic trees of dataset 1; Figure S9: Phylogenetic trees of datasets 2 and 3; Figure S10: Phylogenetic trees of datasets 4 and 5; Figure S11: Phylogenetic trees of dataset 6; Figure S12: Fully unconstrained and phylogenetically unconstrained total-evidence (tip-dated) Bayesian phylogenies of dataset 7; Table S1: Measurements of vertebrae and pedal phalanges of *Anachronornis anhimops* nov. gen. et sp.; Table S2: Relative lengths of select bones among taxa; Table S3: Measurements of vertebrae and pedal phalanges of *Danielsavis nazensis* nov. gen. et sp.; Table S4: Measurements of vertebrae and phalanges of NMS.Z.2021.40.2; Table S5: Measurements of vertebrae and phalanges of NMS.Z.2021.40.3; Table S6: Kishino–Hasegawa test scores, dataset 7, to accompany Figure S9A; Table S7: Kishino–Hasegawa test scores, dataset 7, to accompany Figure S9B; Characters and scores of dataset 1; Apomorphies summarized by dataset. All Appendices are publicly available from: <https://doi.org/10.5061/dryad.8cz8w9gss>.

**Author Contributions:** Conceptualization, P.H.; methodology, P.H.; validation, P.H. and M.D.; formal analysis, P.H. and M.D.; investigation, P.H. and M.D.; writing—original draft preparation, P.H.; writing—review and editing, P.H., M.D. and D.C.; visualization, P.H., M.D. and D.C.; supervision, P.H.; project administration, P.H.; funding acquisition, P.H. All authors have read and agreed to the published version of the manuscript.

**Funding:** This research was funded in part by a gift from the estate of M.C.S. Daniels and Smithsonian Scholarly Studies Grant 1233S802 to S.L. Olson.

**Data Availability Statement:** See Supplementary Appendices in Supplementary Materials.



**Acknowledgments:** We are indebted to Sandra Chapman, Albert Chen, Santiago Claramunt, John D'Angelo, Torsten Eriksson, Fred Grady, Lance Grande, Andrew Kitchener, Susannah Maidment, Gerald Mayr, Sharon Messenger, Angela Milner, Juri A. Miyamae, Cécile Mourer-Chauviré, Storrs L. Olson, Brian Schmidt, Judith White, Niklas Wikström, Lawrence Witmer, Richard L. Zusi, Kristof Zyskowski, and an anonymous reviewer of an earlier version of this manuscript. Above all, we extend special thanks to Michael C. S. Daniels for generously providing funding, accommodations, access to his collection, photographs, measurements, commentary, and companionship.

**Conflicts of Interest:** The authors declare no conflict of interest.

## References

1. Livezey, B.C. A Phylogenetic Analysis of Basal Anseriformes, the Fossil *Presbyornis*, and the Interordinal Relationships of Waterfowl. *Zool. J. Linn. Soc.* **1997**, *121*, 361–428. [\[CrossRef\]](#)
2. Olson, S.L.; Feduccia, A. *Presbyornis* and the Origin of the Anseriformes (Aves: Charadriomorphae). *Smithson. Contrib. Zool.* **1980**, *323*, 1–24. [\[CrossRef\]](#)
3. Livezey, B.C.; Zusi, R.L. Higher-Order Phylogeny of Modern Birds (Theropoda, Aves: Neornithes) Based on Comparative Anatomy. II. Analysis and Discussion. *Zool. J. Linn. Soc.* **2007**, *149*, 1–95. [\[CrossRef\]](#) [\[PubMed\]](#)
4. Jarvis, E.D.; Mirarab, S.; Aberer, A.J.; Li, B.; Houde, P.; Li, C.; Ho, S.Y.W.; Faircloth, B.C.; Nabholz, B.; Howard, J.T.; et al. Whole-Genome Analyses Resolve Early Branches in the Tree of Life of Modern Birds. *Science* **2014**, *346*, 1320–1331. [\[CrossRef\]](#) [\[PubMed\]](#)
5. Claramunt, S.; Cracraft, J. A New Time Tree Reveals Earth History's Imprint on the Evolution of Modern Birds. *Sci. Adv.* **2015**, *1*, e1501005. [\[CrossRef\]](#)
6. Prum, R.O.; Berv, J.S.; Dornburg, A.; Field, D.J.; Townsend, J.P.; Lemmon, E.M.; Lemmon, A.R. A Comprehensive Phylogeny of Birds (Aves) Using Targeted next-Generation DNA Sequencing. *Nature* **2015**, *526*, 569–573. [\[CrossRef\]](#)
7. Kimball, R.T.; Oliveros, C.H.; Wang, N.; White, N.D.; Barker, F.K.; Field, D.J.; Ksepka, D.T.; Chesser, R.T.; Moyle, R.G.; Braun, M.J.; et al. A Phylogenomic Supertree of Birds. *Diversity* **2019**, *11*, 109. [\[CrossRef\]](#)
8. Olson, S.L. The Fossil Record of Birds. In *Avian Biology*; Farner, D.S., King, J., Parkes, K.C., Eds.; Academic Press: New York, NY, USA, 1985; pp. 79–238.
9. Feduccia, A. *The Origin and Evolution of Birds*; Yale University Press: New Haven, CT, USA, 1996.
10. Ericson, P.G.P. Systematic Relationships of the Palaeogene Family Presbyornithidae (Aves: Anseriformes). *Zool. J. Linn. Soc.* **1997**, *121*, 429–483. [\[CrossRef\]](#)
11. Waddell, P.J.; Cao, Y.; Hasegawa, M.; Mindell, D.P. Assessing the Cretaceous Superordinal Divergence Times within Birds and Placental Mammals by Using Whole Mitochondrial Protein Sequences and an Extended Statistical Framework. *Syst. Biol.* **1999**, *48*, 119–137. [\[CrossRef\]](#) [\[PubMed\]](#)
12. Dyke, G.J. The Fossil Waterfowl (Aves: Anseriformes) from the Eocene of England. *Am. Mus. Novit.* **2001**, *3354*, 1–15. [\[CrossRef\]](#)
13. Kurochkin, E.N.; Dyke, G.J.; Karhu, A.A. A New Presbyornithid Bird (Aves, Anseriformes) from the Late Cretaceous of Southern Mongolia. *Am. Mus. Novit.* **2002**, *3386*, 1–11. [\[CrossRef\]](#)
14. Clarke, J.A.; Tambussi, C.P.; Noriega, J.I.; Erickson, G.M.; Ketchum, R.A. Definitive Fossil Evidence for the Extant Avian Radiation in the Cretaceous. *Nature* **2005**, *433*, 305–308. [\[CrossRef\]](#)
15. Tambussi, C.P.; Degrange, F.J.; De Mendoza, R.S.; Sferco, E.; Santillana, S. A Stem Anseriform from the Early Palaeocene of Antarctica Provides New Key Evidence in the Early Evolution of Waterfowl. *Zool. J. Linn. Soc.* **2019**, *186*, 673–700. [\[CrossRef\]](#)
16. Parham, J.F.; Donoghue, P.C.J.; Bell, C.J.; Calway, T.D.; Head, J.J.; Holroyd, P.A.; Inoue, J.G.; Irmis, R.B.; Joyce, W.G.; Ksepka, D.T.; et al. Best Practices for Justifying Fossil Calibrations. *Syst. Biol.* **2012**, *61*, 346–359. [\[CrossRef\]](#) [\[PubMed\]](#)
17. Hope, S. The Mesozoic Radiation of Neornithes. In *Mesozoic Birds: Above the Heads of Dinosaurs*; Chiappe, L.M., Witmer, L.M., Eds.; University of California Press: Berkeley, CA, USA, 2002; pp. 339–388.
18. Ericson, P.G.P.; Parsons, T.J.; Johansson, U.S. Morphological and Molecular Support for the Nonmonophyly of the Galloanserae. In Proceedings of the Proceedings of the International Symposium in Honor of John, H. Ostrom; Gauthier, J., Gall, J.E., Eds.; Yale University Press: New Haven, CT, USA, 2001; pp. 159–168.
19. Elzanowski, A.; Stidham, T.A. Morphology of the Quadrate in the Eocene Anseriform *Presbyornis* and Extant Galloanserine Birds. *J. Morphol.* **2010**, *271*, 305–323. [\[CrossRef\]](#)
20. Field, D.J.; Benito, J.; Chen, A.; Jagt, J.W.M.; Ksepka, D.T. Late Cretaceous Neornithine from Europe Illuminates the Origins of Crown Birds. *Nature* **2020**, *579*, 397–401. [\[CrossRef\]](#)
21. Mlíkovský, J. *Cenozoic Birds of the World, Part 1: Europe*; Ninox Press: Prauge, Czech Republic, 2002.
22. Ericson, P.G.P. Systematic Revision, Skeletal Anatomy, and Paleocology of the New World Early Tertiary Presbyornithidae (Aves: Anseriformes). *PaleoBios* **2000**, *20*, 1–23.
23. Dyke, G.J.; Van Tuinen, M. The Evolutionary Radiation of Modern Birds (Neornithes): Reconciling Molecules, Morphology and the Fossil Record. *Zool. J. Linn. Soc.* **2004**, *141*, 153–177. [\[CrossRef\]](#)
24. Mayr, G. The Paleogene Fossil Record of Birds in Europe. *Biol. Rev.* **2005**, *80*, 515. [\[CrossRef\]](#) [\[PubMed\]](#)

25. Mayr, G. Phylogenetic Affinities and Morphology of the Late Eocene Anseriform Bird *Romainvillia Stehlini* Lebedinsky, 1927. *Neues Jahrb. Für Geol. Und Paläontologie-Abh.* **2008**, *248*, 365–380. [[CrossRef](#)]
26. Mayr, G. Paleogene fossil birds. In *Fascinating Life Sciences*, 2nd ed.; Springer International Publishing: Cham, Switzerland, 2022; ISBN 978-3-030-87644-9.
27. Kurochkin, E.N.; Dyke, G.J. A Large Collection of *Presbyornis* (Aves, Anseriformes, Presbyornithidae) from the Late Paleocene and Early Eocene of Mongolia. *Geol. J.* **2010**, *45*, 375–387. [[CrossRef](#)]
28. Mayr, G.; De Pietri, V.L. A Goose-Sized Anseriform Bird from the Late Oligocene of France: The Youngest Record and Largest Species of Romainvilliinae. *Paläontol. Z.* **2013**, *87*, 423–430. [[CrossRef](#)]
29. Stidham, T.A.; Ni, X.-J. Large Anseriform (Aves: Anatidae: Romainvilliinae?) Fossils from the Late Eocene of Xinjiang, China. *Vertebr. Palasiatica* **2014**, *52*, 98–111.
30. De Pietri, V.L.; Scofield, R.P.; Zelenkov, N.; Boles, W.E.; Worthy, T.H. The Unexpected Survival of an Ancient Lineage of Anseriform Birds into the Neogene of Australia: The Youngest Record of Presbyornithidae. *R. Soc. Open Sci.* **2016**, *3*, 150635. [[CrossRef](#)]
31. Worthy, T.H.; Lee, M.S.Y. Affinities of Miocene Waterfowl (Anatidae: *Manuherikia*, *Dunstanetta*, and *Miotadorna*) from the St Bathans Fauna, New Zealand. *Palaeontology* **2008**, *51*, 677–708. [[CrossRef](#)]
32. Zelenkov, N.V. Cenozoic Evolution of Eurasian Anatids (Aves: Anatidae s. l.). *Biol. Bull. Rev.* **2020**, *10*, 417–426. [[CrossRef](#)]
33. Zelenkov, N.V. A Revision of the Palaeocene–Eocene Mongolian Presbyornithidae (Aves: Anseriformes). *Paleontol. J.* **2021**, *55*, 323–330. [[CrossRef](#)]
34. Alvarenga, H.M.F. A Fossil Screamer (Anseriformes: Anhimidae) from the Middle Tertiary of Southeastern Brazil. *Smithson. Contrib. Zool.* **1999**, *89*, 223–230.
35. Elzanowski, A.; Boles, W.E. Australia’s Oldest Anseriform Fossil: A Quadrate from the Early Eocene Tingamarra Fauna. *Palaeontology* **2012**, *55*, 903–911. [[CrossRef](#)]
36. Zelenkov, N.V. A Swan-Sized Anseriform Bird from the Late Paleocene of Mongolia. *J. Vertebr. Paleontol.* **2018**, *38*, e1531879. [[CrossRef](#)]
37. Mayr, G. A New Avian Species with Tubercle-Bearing Cervical Vertebrae from the Middle Eocene of Messel (Germany). *Rec. Aust. Mus.* **2010**, *62*, 21–28. [[CrossRef](#)]
38. Zelenkov, N.V.; Martynovich, N.V. A rich bird fauna from the Miocene locality Tagay (Olkhon Island, Baikal Lake). *Arch. Menzbier. Ornithol. Soc.* **2013**, *2*, 73–93.
39. Noriega, J.I.; Tambussi, C.P. A Late Cretaceous Presbyornithidae (Aves: Anseriformes) from Vega Island, Antarctic Peninsula: Paleo-Biogeographic Implications. *Ameghiniana* **1995**, *32*, 57–61.
40. Clarke, J.A.; Norell, M.A. New Avialan Remains and a Review of the Known Avifauna from the Late Cretaceous Nemegt Formation of Mongolia. *Am. Mus. Novit.* **2004**, *3447*, 1–12. [[CrossRef](#)]
41. Novas, F.; Agnolin, F.; Rozadilla, S.; Aranciaga-Rolando, A.; Brissón-Eli, F.; Motta, M.; Cerroni, M.; Ezcurra, M.; Martinelli, A.; D’Angelo, J.; et al. Paleontological Discoveries in the Chorrillo Formation (Upper Campanian-Lower Maastrichtian, Upper Cretaceous), Santa Cruz Province, Patagonia, Argentina. *MACN* **2019**, *21*, 217–293. [[CrossRef](#)]
42. Agnolín, F.L.; Egli, F.B.; Chatterjee, S.; Alexis, J.; Marsa, G.; Novas, F.E. Vegaviidae, a New Clade of Southern Diving Birds That Survived the K/T Boundary. *Sci. Nat.* **2017**, *104*, 87. [[CrossRef](#)]
43. Worthy, T.H.; Degrange, F.J.; Handley, W.D.; Lee, M.S.Y. The Evolution of Giant Flightless Birds and Novel Phylogenetic Relationships for Extinct Fowl (Aves, Galloanseres). *R. Soc. Open Sci.* **2017**, *4*, 170975. [[CrossRef](#)]
44. Mayr, G.; De Pietri, V.L.; Scofield, R.P.; Worthy, T.H. On the Taxonomic Composition and Phylogenetic Affinities of the Recently Proposed Clade Vegaviidae Agnolín et al., 2017–Neornithine Birds from the Upper Cretaceous of the Southern Hemisphere. *Cretac. Res.* **2018**, *86*, 178–185. [[CrossRef](#)]
45. McLachlan, S.M.S.; Kaiser, G.W.; Longrich, N.R. *Maaqi cascadiensis*: A Large, Marine Diving Bird (Avialae: Ornithurae) from the Upper Cretaceous of British Columbia, Canada. *PLoS ONE* **2017**, *12*, e0189473. [[CrossRef](#)]
46. Clarke, J.A.; Chatterjee, S.; Li, Z.; Riede, T.; Agnolin, F.; Goller, F.; Isasi, M.P.; Martinioni, D.R.; Mussel, F.J.; Novas, F.E. Fossil Evidence of the Avian Vocal Organ from the Mesozoic. *Nature* **2016**, *538*, 502–505. [[CrossRef](#)]
47. Mayr, G. A Partial Skeleton of a New Fossil Loon (Aves, Gaviiformes) from the Early Oligocene of Germany with Preserved Stomach Content. *J. Ornithol.* **2004**, *145*, 281–286. [[CrossRef](#)]
48. Cracraft, J. Phylogenetic Relationships and Monophyly of Loons, Grebes, and Hesperonithiformes Birds, with Comments on the Early History of Birds. *Syst. Biol.* **1982**, *31*, 35–56. [[CrossRef](#)]
49. Bourdon, E. Osteological Evidence for Sister Group Relationship between Pseudo-Toothed Birds (Aves: Odontopterygiformes) and Waterfowls (Anseriformes). *Naturwissenschaften* **2005**, *92*, 586–591. [[CrossRef](#)] [[PubMed](#)]
50. Wetmore, A. Fossil Birds from the Green River Deposits of Eastern Utah. *Ann. Carnegie Mus.* **1926**, *16*, 391–402. [[CrossRef](#)]
51. Feduccia, A.; McGrew, P.O. A Flamingo-like Wader from the Eocene of Wyoming. *Contrib. Geol.* **1974**, *13*, 49–61.
52. Olson, S.L.; Parris, D.C. The Cretaceous Birds of New Jersey. *Smithson. Contrib. Zool.* **1987**, *63*, 1–22. [[CrossRef](#)]
53. Olson, S.L. A Giant *Presbyornis* (Aves: Anseriformes) and Other Birds from the Paleocene Aquia Formation of Maryland and Virginia. *Proc. Biol. Soc. Wash* **1994**, *107*, 429–435.
54. Boles, W.E.; Finch, M.A.; Hofheins, R.H.; Walters, M.; Rich, T.H. A Fossil Stone-Curlew (Aves: Burhinidae) from the Late Oligocene/Early Miocene of South Australia. In Proceedings of the 8th International Meeting of the Society of Avian Paleontology and Evolution, Wien, Austria, 11–16 June 2012; pp. 43–62.

55. Olson, S.L. The Anseriform Relationships of *Anatalavis* Olson and Parris (Anseranatidae), with a New Species from the Lower Eocene London Clay. *Smithson. Contrib. Zool.* **1999**, *89*, 231–243.
56. Shufeldt, R.W. Fossil Birds in the Marsh Collection of Yale University. *Trans. Conn. Acad. Arts Sci.* **1915**, *19*, 1–110.
57. Mourer-Chauviré, C. [Review of] Cenozoic Birds of the World, Part 1: Europe by Jiri Mlíkovský, 2002. *Auk* **2004**, *121*, 623–627. [[CrossRef](#)]
58. Worthy, T.H.; Scanlon, J.D. An Oligo-Miocene Magpie Goose (Aves: Anseranatidae) from Riversleigh, Northwestern Queensland, Australia. *J. Vertebr. Paleontol.* **2009**, *29*, 205–211. [[CrossRef](#)]
59. Zelenkov, N. The Oldest Diving Anseriform Bird from the Late Eocene of Kazakhstan and the Evolution of Aquatic Adaptations in the Intertarsal Joint of Waterfowl. *Acta Palaeontol. Pol.* **2020**, *65*, 733–742. [[CrossRef](#)]
60. Mourer-Chauviré, C.; Berthet, D.; Hungueney, M. The Late Oligocene Birds of the Créchy Quarry (Allier, France), with a Description of Two New Genera (Aves: Pelecaniformes: Phalacrocoracidae, and Anseriformes: Anseranatidae). *Senckenberg. Lethaea* **2004**, *84*, 303–315. [[CrossRef](#)]
61. Mayr, G.; Smith, R. Ducks, Rails, and Limicoline Waders (Aves: Anseriformes, Gruiformes, Charadriiformes) from the Lowermost Oligocene of Belgium. *Geobios* **2001**, *34*, 547–561. [[CrossRef](#)]
62. Milne-Edwards, A. Sur La Distribution Géologique des Oiseaux Fossiles et Description de Quelques Espèces Nouvelles. *C. R. Séances Sci. Acad. Sci.* **1863**, *56*, 1219–1222.
63. Milne-Edwards, A. *Recherches Anatomiques et Paléontologiques Pour Servir à l'Histoire Des Oiseaux Fossiles de La France*; Victor Masson: Paris, France, 1867.
64. Mayr, G.; De Pietri, V.L.; Love, L.; Mannering, A.; Scofield, R.P. Oldest, Smallest and Phylogenetically Most Basal Pelagornithid, from the Early Paleocene of New Zealand, Sheds Light on the Evolutionary History of the Largest Flying Birds. *Pap. Palaeontol.* **2021**, *7*, 217–233. [[CrossRef](#)]
65. Benito, J.; Kuo, P.-C.; Widrig, K.E.; Jagt, J.W.M.; Field, D.J. Cretaceous Ornithurine Supports a Neognathous Crown Bird Ancestor. *Nature* **2022**, *612*, 100–105. [[CrossRef](#)]
66. Andors, A.V. Reappraisal of the Eocene Groundbird *Diatryma* (Aves: Anserimorphae). *Nat. His. Mus. Los Angeles Sci. Ser.* **1992**, *36*, 109–125.
67. Angst, D.; Lécuyer, C.; Amiot, R.; Buffetaut, E.; Fourel, F.; Martineau, F.; Legendre, S.; Abourachid, A.; Herrel, A. Isotopic and Anatomical Evidence of an Herbivorous Diet in the Early Tertiary Giant Bird *Gastornis*. Implications for the Structure of Paleocene Terrestrial Ecosystems. *Naturwissenschaften* **2014**, *101*, 313–322. [[CrossRef](#)]
68. Andors, A.V. Giant Groundbirds of North America (Aves, Diatrymidae). Ph.D. Thesis, Columbia University, New York, NY, USA, 1988.
69. Angst, D. Successeurs des Dinosaures? Paléobiologie et Paléoécologie d'un oiseau géant terrestre du Paléogène. Ph.D. Thesis, Université Claude Bernard-Lyon 1, Lyon, France, 2014.
70. Buffetaut, E. The Giant Bird *Gastornis* in Asia: A Revision of *Zhongyuanus Xichuanensis* Hou, 1980, from the Early Eocene of China. *Paleontol. J.* **2013**, *47*, 1302–1307. [[CrossRef](#)]
71. Murray, P.F.; Vickers-Rich, P. *Magnificent Mihirungs: The Colossal Flightless Birds of the Australian Dreamtime*; Indiana University Press: Bloomington, IN, USA, 2004.
72. Mayr, G.; Smith, T. Bony-Toothed Birds (Aves: Pelagornithidae) from the Middle Eocene of Belgium. *Palaeontology* **2010**, *53*, 365–376. [[CrossRef](#)]
73. Mayr, G.; Rubilar-Rogers, D. Osteology of a New Giant Bony-Toothed Bird from the Miocene of Chile, with a Revision of the Taxonomy of Neogene Pelagornithidae. *J. Vertebr. Paleontol.* **2010**, *30*, 1313–1330. [[CrossRef](#)]
74. Mayr, G. Cenozoic Mystery Birds—on the Phylogenetic Affinities of Bony-toothed Birds (Pelagornithidae). *Zool. Scr.* **2011**, *40*, 448–467. [[CrossRef](#)]
75. Baumel, J.J.; Witmer, L.M. Osteologica. In *Handbook of Avian Anatomy: Nomina Anatomica Avium*; King, A.S., Breazile, J.E., Evans, H.E., Vanden Berge, J.C., Eds.; Publications of the Nuttall Ornithological Club: Cambridge, MA, USA, 1993; pp. 45–132.
76. Zusi, R.L.; Livezey, B.C. Homology and Phylogenetic Implications of Some Enigmatic Cranial Features in Galliform and Anseriform Birds. *Ann. Carnegie Mus.* **2000**, *69*, 157–193. [[CrossRef](#)]
77. Livezey, B.C.; Zusi, R.L. Phylogeny of Neornithes. *Bull. Carnegie Mus. Nat. Hist.* **2006**, *37*, 1–544. [[CrossRef](#)]
78. Howard, H. *The Avifauna of Emryville Shellmound*; University of California Press: Berkeley, CA, USA, 1929; Volume 32.
79. Bock, W.J. Secondary Articulation of the Avian Mandible. *Auk* **1960**, *77*, 19–55. [[CrossRef](#)]
80. Ballmann, P. Les Oiseaux Miocènes de La Grive-Saint-Alban (Isère). *Geobios* **1969**, *2*, 157–204. [[CrossRef](#)]
81. Dyke, G.J.; Gulas, B.E. The Fossil Galliform Bird *Paraortygoides* from the Lower Eocene of the United Kingdom. *Am. Mus. Novit.* **2002**, *3360*, 1–14. [[CrossRef](#)]
82. Bourdon, E.; De Ricqlès, A.; Cubo, J. A New Transantarctic Relationship: Morphological Evidence for a Rheidae-Dromaiidae-Casuariidae Clade (Aves, Palaeognathae, Ratitae). *Zool. J. Linn. Soc.* **2009**, *156*, 641–663. [[CrossRef](#)]
83. Worthy, T.; Scofield, R. Twenty-First Century Advances in Knowledge of the Biology of Moa (Aves: Dinornithiformes): A New Morphological Analysis and Moa Diagnoses Revised. *N. Z. J. Zool.* **2012**, *39*, 87–153. [[CrossRef](#)]
84. Zinoviev, A.V. Notes on Pelvic and Hindlimb Myology and Syndesmology of *Emeus Crassus* and *Dinornis Robustus* (Aves: Dinornithiformes). In Proceedings of the 8th International Meeting of the Society of Avian Paleontology and Evolution, Wien, Austria, 11–16 June 2012; pp. 253–278.

85. Ellerby, D.J.; Marsh, R.L. The Energetic Costs of Trunk and Distal-Limb Loading during Walking and Running in Guinea Fowl *Numida Meleagris*. *J Exp Biol* **2006**, *209*, 2064–2075. [[CrossRef](#)] [[PubMed](#)]
86. Lamas, L.P.; Main, R.P.; Hutchinson, J.R. Ontogenetic Scaling Patterns and Functional Anatomy of the Pelvic Limb Musculature in Emus (*Dromaius Novaehollandiae*). *PeerJ* **2014**, *2*, e716. [[CrossRef](#)]
87. Clifton, G.T.; Carr, J.A.; Biewener, A.A. Comparative Hindlimb Myology of Foot-Propelled Swimming Birds. *J. Anat.* **2018**, *232*, 105–123. [[CrossRef](#)] [[PubMed](#)]
88. Li, Z.; Clarke, J.A.; Eliason, C.M.; Stidham, T.A.; Deng, T.; Zhou, Z. Vocal Specialization through Tracheal Elongation in an Extinct Miocene Pheasant from China. *Sci. Rep.* **2018**, *8*, 8099. [[CrossRef](#)]
89. Swofford, D.L. Phylogenetic Analysis Using Parsimony (\* and Other Methods). Available online: <https://paup.phylosolutions.com> (accessed on 27 January 2022).
90. Livezey, B.C. A Phylogenetic Analysis of Recent Anseriform Genera Using Morphological Characters. *Auk* **1986**, *103*, 737–754. [[CrossRef](#)]
91. Livezey, B.C. Erratum—A Phylogenetic Analysis of Basal Anseriformes, the Fossil *Presbyornis*, and the Interordinal Relationships of Waterfowl. *Zool. J. Linn. Soc.* **1998**, *124*, 397–398. [[CrossRef](#)]
92. Acosta Hospitaleche, C.; Worthy, T.H. New Data on the *Vegavis Iaii* Holotype from the Maastrichtian of Antarctica. *Cretac. Res.* **2021**, *124*, 104818. [[CrossRef](#)]
93. Smith, M.E.; Chamberlain, K.R.; Singer, B.S.; Carroll, A.R. Eocene Clocks Agree: Coeval <sup>40</sup>Ar/<sup>39</sup>Ar, U-Pb, and Astronomical Ages from the Green River Formation. *Geology* **2010**, *38*, 527–530. [[CrossRef](#)]
94. Allentoft, M.E.; Heller, R.; Oskam, C.L.; Lorenzen, E.D.; Hale, M.L.; Gilbert, M.T.P.; Jacomb, C.; Holdaway, R.N.; Bunce, M. Extinct New Zealand Megafauna Were Not in Decline before Human Colonization. *Proc. Natl. Acad. Sci. USA* **2014**, *111*, 4922–4927. [[CrossRef](#)]
95. Solórzano, A.; Rincón, A.D. The Earliest Record (Early Miocene) of a Bony-Toothed Bird from South America and a Reexamination of Venezuelan Pelagornithids. *J. Vertebr. Paleontol.* **2015**, *35*, e995188. [[CrossRef](#)]
96. Collinson, M.E.; Adams, N.F.; Manchester, S.R.; Stull, G.W.; Herrera, F.; Smith, S.Y.; Andrew, M.J.; Kenrick, P.; Sykes, D. X-Ray Micro-Computed Tomography (Micro-CT) of Pyrite-Permineralized Fruits and Seeds from the London Clay Formation (Ypresian) Conserved in Silicone Oil: A Critical Evaluation. *Botany* **2016**, *94*, 697–711. [[CrossRef](#)]
97. Benito, J.; Chen, A.; Wilson, L.E.; Bhullar, B.-A.S.; Burnham, D.; Field, D.J. 40 New Specimens of *Ichthyornis* Provide Unprecedented Insight into the Postcranial Morphology of Crownward Stem Group Birds. *PeerJ* **2022**, *10*, e13919. [[CrossRef](#)]
98. Welch, J.L.; Foreman, B.Z.; Malone, D.; Craddock, J. Provenance of Early Paleogene Strata in the Bighorn Basin (Wyoming, USA): Implications for Laramide Tectonism and Basin-Scale Stratigraphic Patterns. In *Tectonic Evolution of the Sevier-Laramide Hinterland, Thrust Belt, and Foreland, and Postorogenic Slab Rollback (180–20 Ma)*; GSA Special Papers: Boulder, CO, USA, 2022; Volume 555, ISBN 978-0-8137-9555-3.
99. Ronquist, F.; Teslenko, M.; van der Mark, P.; Ayres, D.L.; Darling, A.; Höhna, S.; Larget, B.; Liu, L.; Suchard, M.A.; Huelsenbeck, J.P. MrBayes 3.2: Efficient Bayesian Phylogenetic Inference and Model Choice Across a Large Model Space. *Syst. Biol.* **2012**, *61*, 539–542. [[CrossRef](#)]
100. Rambaut, A.; Drummond, A.J.; Xie, D.; Baele, G.; Suchard, M.A. Posterior Summarisation in Bayesian Phylogenetics Using Tracer 1.7.2. *Syst. Biol.* **2018**, *67*, 901–904. [[CrossRef](#)] [[PubMed](#)]
101. Reddy, S.; Kimball, R.T.; Pandey, A.; Hosner, P.A.; Braun, M.J.; Hackett, S.J.; Han, K.-L.; Harshman, J.; Huddleston, C.J.; Kingston, S.; et al. Why Do Phylogenomic Data Sets Yield Conflicting Trees? Data Type Influences the Avian Tree of Life More than Taxon Sampling. *Syst. Biol.* **2017**, *66*, 857–879. [[CrossRef](#)]
102. Burleigh, J.G.; Kimball, R.T.; Braun, E.L. Building the Avian Tree of Life Using a Large-Scale, Sparse Supermatrix. *Mol. Phylogenet. Evol.* **2015**, *84*, 53–63. [[CrossRef](#)]
103. Goldman, N.; Anderson, J.P.; Rodrigo, A.G. Likelihood-Based Tests of Topologies in Phylogenetics. *Syst. Biol.* **2000**, *49*, 652–670. [[CrossRef](#)]
104. Dzerzhinsky, F.Y. Evidence for Common Ancestry of the Galliformes and Anseriformes. *Cour. Forsch. Senckenb.* **1995**, *181*, 325–336.
105. O'Connor, P.M. Pulmonary Pneumaticity in the Postcranial Skeleton of Extant Aves: A Case Study Examining Anseriformes. *J. Morphol.* **2004**, *261*, 141–161. [[CrossRef](#)] [[PubMed](#)]
106. O'Connor, P.M. Postcranial Pneumaticity: An Evaluation of Soft-Tissue Influences on the Postcranial Skeleton and the Reconstruction of Pulmonary Anatomy in Archosaurs. *J. Morphol.* **2006**, *267*, 1199–1226. [[CrossRef](#)] [[PubMed](#)]
107. De Mendoza, R.S.; Gómez, R.O.; Tambussi, C.P. The Lacrimal/Ectethmoid Region of Waterfowl (Aves, Anseriformes): Phylogenetic Signal and Major Evolutionary Patterns. *J. Morphol.* **2020**, *281*, 1486–1500. [[CrossRef](#)]
108. Mayr, G. On the Occurrence of Lateral Openings and Fossae (Pleurocoels) in the Thoracic Vertebrae of Neornithine Birds and Their Functional Significance. *VZ* **2021**, *71*, 453–463. [[CrossRef](#)]
109. Secord, R.; Gingerich, P.D.; Smith, M.E.; Clyde, W.C.; Wilf, P.; Singer, B.S. Geochronology and Mammalian Biostratigraphy of Middle and Upper Paleocene Continental Strata, Bighorn Basin, Wyoming. *Am. J. Sci.* **2006**, *306*, 211–245. [[CrossRef](#)]
110. Secord, R. The Tiffanian Land-Mammal Age (Middle and Late Paleocene) in the Northern Bighorn Basin, Wyoming. *Uni. Mich. Pap. Paleo.* **2008**, *35*, 1–192.

111. Bowen, G.J.; Maibauer, B.J.; Kraus, M.J.; Röhl, U.; Westerhold, T.; Steimke, A.; Gingerich, P.D.; Wing, S.L.; Clyde, W.C. Two Massive, Rapid Releases of Carbon during the Onset of the Palaeocene–Eocene Thermal Maximum. *Nat. Geosci.* **2014**, *8*, 44–47. [[CrossRef](#)]
112. Field, D.J.; Lynner, C.; Brown, C.; Darroch, S.A.F. Skeletal Correlates for Body Mass estimation in Modern and Fossil Flying Birds. *PLoS ONE* **2013**, *8*, e82000. [[CrossRef](#)] [[PubMed](#)]
113. Houde, P.; Olson, S.L. A Radiation of Coly-like Birds from the Eocene of North America (Aves: Sandcoleiformes, New Order). *Nat. Hist. Mus. Los Angeles Cty. Sci. Ser.* **1992**, *36*, 137–160.
114. Van Tyne, J.; Berger, A.J. *Fundamentals of Ornithology*; Dover Publications: New York, NY, USA, 1971.
115. Campbell, B.; Lack, E. *A Dictionary of Birds*; British Ornithologist's Union, Buteo Books: Vermillion, SD, USA, 1985; ISBN 0-931130-12-3.
116. Buchheim, H.P.; Biaggi, R.E.; Cushman, R.A. Stratigraphy and Interbasinal Correlations Between Fossil and the Green River Basin, Wyoming. In *Stratigraphy and Paleolimnology of the Green River Formation, Western USA*; Smith, M.E., Carroll, A.R., Eds.; Syntheses in Limnogeology; Springer: Dordrecht, The Netherlands, 2015; Volume 1, pp. 127–151; ISBN 978-94-017-9905-8.
117. Grande, L. Birds. In *The Lost World of Fossil Lake*; University of Chicago Press: Chicago, IL, USA, 2013; pp. 215–257.
118. Puttick, M.N.; O'Reilly, J.E.; Pisani, D.; Donoghue, P.C.J. Probabilistic Methods Outperform Parsimony in the Phylogenetic Analysis of Data Simulated without a Probabilistic Model. *Palaeontology* **2019**, *62*, 1–17. [[CrossRef](#)]
119. King, B. Bayesian Tip-Dated Phylogenetics in Paleontology: Topological Effects and Stratigraphic Fit. *Syst. Biol.* **2021**, *70*, 283–294. [[CrossRef](#)]
120. Feng, S.; Bai, M.; Rivas-González, I.; Li, C.; Liu, S.; Tong, Y.; Yang, H.; Chen, G.; Xie, D.; Sears, K.E.; et al. Incomplete Lineage Sorting and Phenotypic Evolution in Marsupials. *Cell* **2022**, *185*, 1646–1660.e18. [[CrossRef](#)]
121. Marsh, O.C. *Odontornithes: Monograph on the Extinct Toothed Birds of North America*; United States Geological Exploration of the Fortieth Parallel; Government Printing Office: Washington, DC, USA, 1880.
122. Sanz, J.L.; Chiappe, L.M.; Buscalioni, A.D. The Osteology of *Concornis Lacustris* (Aves: Enantiornithes) from the Lower Cretaceous of Spain and a Reexamination of Its Phylogenetic Relationships. *Am. Mus. Novit.* **1995**, *3133*, 1–23.
123. Chiappe, L.M. Late Cretaceous Birds of Southern South America: Anatomy and Systematics of Enantiornithes and *Patagopteryx deferrariisi*. *Mün. Geo. Abh.* **1996**, *30*, 203–244.
124. Zelenkov, N.V.; Stidham, T.A. Possible Filter-Feeding in the Extinct *Presbyornis* and the Evolution of Anseriformes (Aves). *Zool. Z.* **2018**, *97*, 943–956. [[CrossRef](#)]
125. Rose, K.D. The Clarkforkian Land Mammal Age. *Uni. Mich. Papers in Paleo.* **1981**, *26*, 1–197.
126. Houde, P. Paleognathous Birds from the Early Tertiary of the Northern Hemisphere. In *Publications of the Nuttall Ornithological Club*; Paynter, R.A., Jr., Ed.; Nuttall Ornithological Club: Cambridge, MA, USA, 1988.
127. Bowen, G.J.; Bloch, J.I. Petrography and geochemistry of floodplain limestones from the Clarks Fork Basin, Wyoming, USA: Carbonate deposition and fossil accumulation on a Paleocene-Eocene floodplain. *J. Sediment. Res.* **2002**, *72*, 46–58. [[CrossRef](#)]
128. du Toit, C.J.; Chinsamy, A.; Cunningham, S.J. Cretaceous Origins of the Vibrotactile Bill-Tip Organ in Birds. *Proc. R. Soc. B* **2020**, *287*, 20202322. [[CrossRef](#)] [[PubMed](#)]
129. Mayr, G.; Gingerich, P.D.; Smith, T. *Calcardea Junnei* Gingerich, 1987 from the Late Paleocene of North America Is Not a Heron, but Resembles the Early Eocene Indian Taxon *Vastanavis* Mayr et al., 2007. *J. Paleontol.* **2019**, *93*, 359–367. [[CrossRef](#)]
130. Mayr, G.; Gingerich, P.D.; Smith, T. Skeleton of a New Owl from the Early Eocene of North America (Aves, Strigiformes) with an Accipitrid-like Foot Morphology. *J. Vertebr. Paleontol.* **2020**, *40*, e1769116. [[CrossRef](#)]
131. Degrange, F.J. Hind Limb Morphometry of Terror Birds (Aves, Cariamiformes, Phorusrhacidae): Functional Implications for Substrate Preferences and Locomotor Lifestyle. *Earth Env. Sci. Trans. R. Soc. Edinb.* **2017**, *106*, 257–276. [[CrossRef](#)]
132. IUCN Red List 2022-2 White Backed Duck. Available online: <https://www.iucnredlist.org/species/22679785/92830036#habitat-ecology> (accessed on 23 January 2023).
133. Zweers, G.A. Structure, movement, and myography of the feeding apparatus of the mallard (*Anas platyrhynchos* L.) A study in functional anatomy. *Neth. J. Zool.* **1973**, *24*, 323–467. [[CrossRef](#)]
134. Clyde, W.C.; Gingerich, P.D. Mammalian Community Response to the Latest Paleocene Thermal Maximum: An Isotaphonomic Study in the Northern Bighorn Basin, Wyoming. *Geology* **1998**, *26*, 1011. [[CrossRef](#)]
135. Woodburne, M.O.; Gunnell, G.F.; Stucky, R.K. Climate Directly Influences Eocene Mammal Faunal Dynamics in North America. *Proc. Natl. Acad. Sci. USA* **2009**, *106*, 13399–13403. [[CrossRef](#)] [[PubMed](#)]
136. Hooker, J.J.; Collinson, M.E. Mammalian Faunal Turnover across the Paleocene-Eocene Boundary in NW Europe: The Roles of Displacement, Community Evolution and Environment. *Austrian J. Earth Sci.* **2012**, *105*, 17–28.
137. Widlansky, S.J.; Secord, R.; Snell, K.E.; Chew, A.E.; Clyde, W.C. Carbon Isotope Stratigraphy and Mammal Turnover during Post-PETM Hyperthermals. *Clim. Past* **2022**, *18*, 681–712. [[CrossRef](#)]

**Disclaimer/Publisher's Note:** The statements, opinions and data contained in all publications are solely those of the individual author(s) and contributor(s) and not of MDPI and/or the editor(s). MDPI and/or the editor(s) disclaim responsibility for any injury to people or property resulting from any ideas, methods, instructions or products referred to in the content.